The Synthesis and Properties of Polycyclic Aromatic Thiophenes and Related Heterocycles Occurring in Coal-derived Products

Raymond N. Castle [1], Marvin L. Tedjamulia, Yoshinori Tominaga [2], Ram Pratap [3], Michiharu Sugiura [4] and Hirotaka Kudo*

Department of Chemistry, University of South Florida, Tampa, FL 33620 USA

Milton L. Lee, Masatomo Iwao [5] and Robert D. Thompson [6]

Department of Chemistry, Brigham Young University, Provo, UT 84602 USA

Gary E. Martin [a], Robert T. Gampe, Jr. [a], M. J. Musmar [a] and M. Robert Willcott, III [b]

Departments of Medicinal Chemistry [a] and Chemistry [b], University of Houston Houston, TX 77004 USA

Stanford L. Smith and W. John Layton

Department of Chemistry, University of Kentucky, Lexington, KY 40507 USA

Ralph E. Hurd and LeRoy F. Johnson

Nicolet Magnetics Corporation, 255 Fourier Avenue, Fremont, CA 94539 USA

Vol. VIII. R.N. Castle ed. 1984.

As the supplies of petroleum diminish, it will become necessary to search for other sources of liquid fuels. Because of the relatively large coal reserves available world wide, this appears to be the logical source of additional quantities of liquid fuels.

Recently, much attention has been focussed on coal liquification and as recently as September, 1982, the Division of Fuel Chemistry of the American Chemical Society sponsored a Symposium on Coal Liquification [7].

In contrast with petroleum, the components of coal, coal liquids and other coal-derived products are primarily aromatic in nature and as a result present considerably greater health hazards when produced and handled on a large scale. There have been many different structures proposed for coal. They all have many common features. In slide 1 is

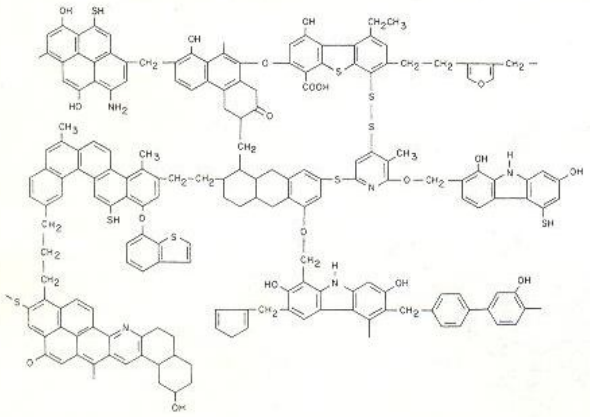

shown one recently proposed structure [8] in which one can observe the benzo[*b*]thiophene moiety, the dibenzothiophene ring as well as aromatic mercapto groups and disulfide linkages. Thus it appeared of interest to examine the heterocyclic components of coal liquids with emphasis on the sulfur heterocycles. Lee, Willey, Castle and White [9] have reported a method for the separation and identification of sulfur heterocycles in coal-derived products. As a result, a great many isomeric polycyclic thiophenes have been identified by gc/ms and the molecular weight of the several isomers determined. One is then able to classify the components. However, unequivocal assignment of structure is not possible by the gc/ms technique alone, therefore the synthesis of standard polycyclic thiophenes by unequivocal methods is required. Thus we have undertaken the synthesis of all isomers of various classes of polycyclic thiophenes with specific molecular weights and some of the methyl and ethyl derivatives in order to make available these pure standard compounds for gc/ms study and thus allow positive identification of individual component compounds in coal liquids and shale oils and at the same time provide pure samples for mutagenic, carcinogenic and teratogenic screening. In this vein, we have limited the synthesis of standard compounds to [*b*]-fused polycyclic thiophenes because [*c*]-fused polycyclic thiophenes are less stable and we pedict that the [*c*]-fused isomers would not survive the drastic conditions necessary for the conversion of coal to liquid products.

Phenanthro[*b*]thiophenes [10].

1-Naphthalenecarboxaldehyde (**1**), when allowed to react with diethyl 3-thenylphosphonate (**2**) [sodium hydride, dry dimethoxyethane, 2 hours at room temperature (typical Wadsworth-Emmons [11] conditions)] gave 1-(3-thienyl)-2-(1-naphthyl)ethene (**3**) in 76% yield. Photocyclization

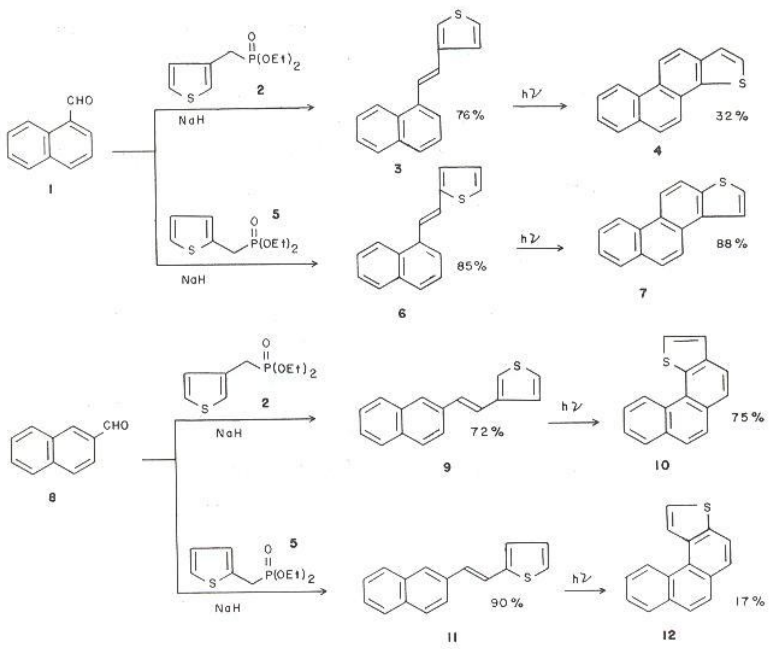

of **3** [I_2, O_2, cyclohexane, 450 watt medium pressure Hanovia mercury lamp] produced phenanthro[1,2-*b*]thiophene (**4**) in 32% yield. Reaction of **1** with diethyl 2-thenylphosphonate (**5**) gave 1-(2-thienyl)-2-(1-naphthyl)ethene (**6**) in 85% yield which upon photocyclization produced phenanthro[2,1-*b*]thiophene (**7**) in 88% yield. Likewise the Wadsworth-Emmons reaction of 2-naphthalenecarboxaldehyde (**8**) with **2** gave 1-(3-thienyl)-2-(2-naphthyl)ethene (**9**) in 72% yield which was photocyclized into phenanthro-[4,3-*b*]thiophene (**10**) [12-13] while **8** and **5** gave 1-(2-thienyl)-2-(2-naphthyl)ethene (**11**, 90% yield). Photocyclization of **11** allowed the isolation of phenanthro[3,4-*b*]thiophene (**12**) in only 17% yield. Phenanthro[3,4-*b*]thiophene (**12**) is approximately as mutagenic as benzo[*a*]pyrene in the Ames test against TA98 and TA100 strains [14].

The synthesis of phenanthro[2,3-*b*]thiophene (**19**) was accomplished in five steps. 2-(3-Thienyl)-5,5-dimethyl-2-oxazoline (**13**) was readily lithiated (*n*-butyllithium) and allowed to react with 2-naphthalenecarboxaldehyde to give alcohol **14** which when cleaved under acidic conditions spontaneously lactonized into 3-(2-naphthyl)thieno[2,3-*c*]-furan-1-one (**15**) in 56% yield. Reduction of **15** with hydrogen (Pd/C) gave 2-naphthylmethyl-3-thiophenecarboxylic acid (**16**) in 72% yield. Cyclization of **16** with acetic anhydride (zinc chloride) gave 11-acetoxyphenanthro[2,3-*b*]-thiophene (81% yield) which when deacetoxylated with zinc gave phenanthro[2,3-*b*]thiophene (**19**) in a disappointingly low yield of 3%. Alternately, the carboxylic acid **16** was reduced with lithium aluminum hydride (LAH) to the primary alcohol which was oxidized to 2-(2-naphthylmeth-

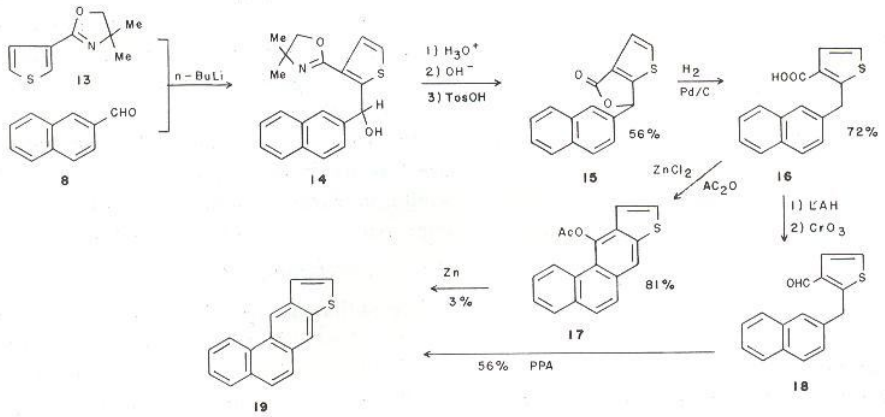

yl)-3-thiophenecarboxaldehyde (**18**) with the chromium trioxide-pyridine complex and then cyclized with polyphosphoric acid (PPA) into phenanthro[2,3-*b*]thiophene (**19**) [15] with a yield of 56% from **16**. In like manner the oxazoline **13** and 1-naphthalenecarboxaldehyde (**1**) gave the alcohol **20** (84% yield) which spontaneously lactonized upon treatment with acid to give the lactone **21** (38% yield) which was reduced (hydrogen, Pd/C) to give 2-(1-naphthylmethyl)-3-thiophenecarboxylic acid (**22**) in 62% yield. Reduction of **22** (LAH) followed by oxidation of the primary alcohol (chromium trioxide-pyridine complex) gave 2-(1-naphthylmethyl)-3-thiophenecarboxaldehyde (**23**) which upon PPA cyclization produced phenanthro[3,2-*b*]-thiophene (**24**) in 57% yield from the carboxylic acid **22**.

Phenanthro[9,10-*b*]thiophene (**27**) [16] was synthesized by allowing 9-bromophenanthrene (**25**) to react with magnesium to form the Grignard reagent which when treated with the acetal of 2-oxoethyl disulfide gave 9-phenanthrylthioethanal diethyl acetal (**26**). Cyclization (PPA) of **26** produced phenanthro[9,10-*b*]thiophene (**27**) in 25% yield from **25**.

Anthra[*b*]thiophenes [17].

Anthra[2,3-*b*]thiophene (**34**) [18] was obtained in five steps from naphthalene-2,3-dicarboxylic acid anhydride (**28**) and thiophene (**29**) *via* a Friedel-Crafts reaction (aluminum chloride) giving the ketoacid **30** (32% yield) which was smoothly reduced to 3-(2-thenyl)-2-naphthalenecarboxylic acid (**31**) with zinc and ammonium hydroxide in 82% yield. Reduction of **31** (LAH) gave the primary alcohol **32** which upon oxidation (chromium trioxide-pyridine complex) produced the aldehyde **33** which upon PPA cyclization produced anthra[2,3-*b*]thiophene (**34**) in 51% yield from **31**.

Anthra[2,1-*b*]thiophene (**40**) [18] was synthesized in four steps. A Diels-Alder reaction between 1,4-naphthoquinone (**35**) and 2-vinylthiophene (**36**) produced 4,5,6,11-tetrahydroanthra[2,1-*b*]thiophene-6,11-dione (**27**) (22% yield). The 4,5-double bond was introduced by allowing **37** to re-

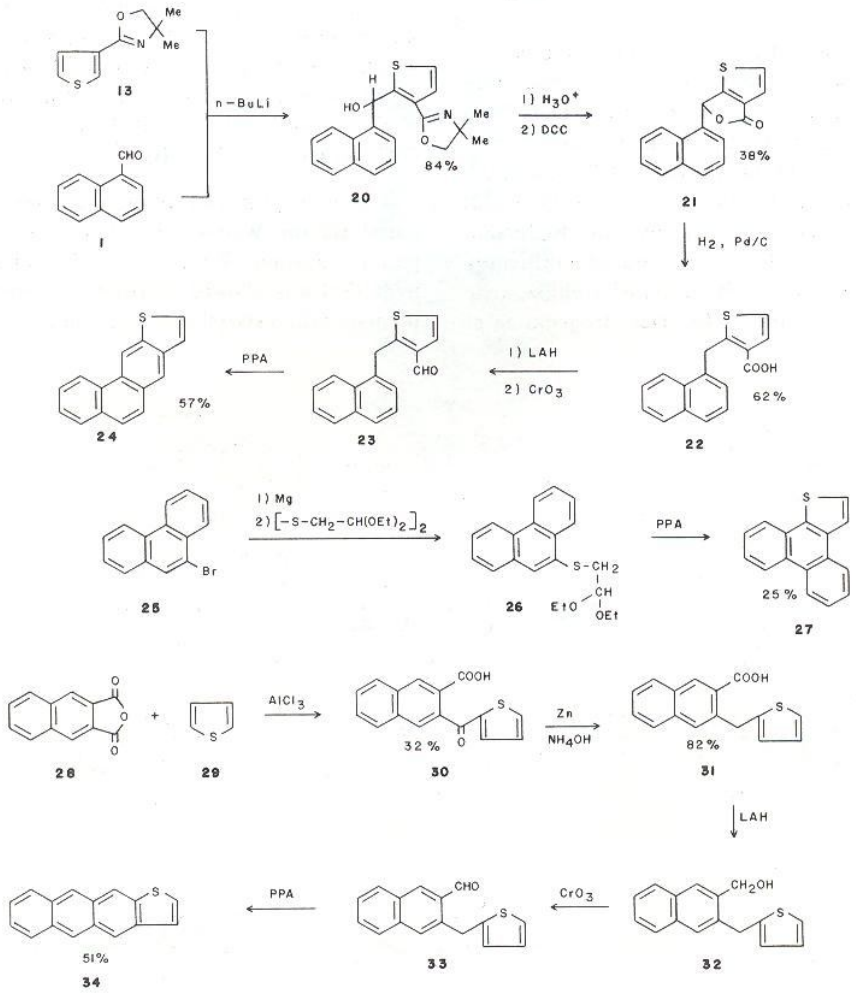

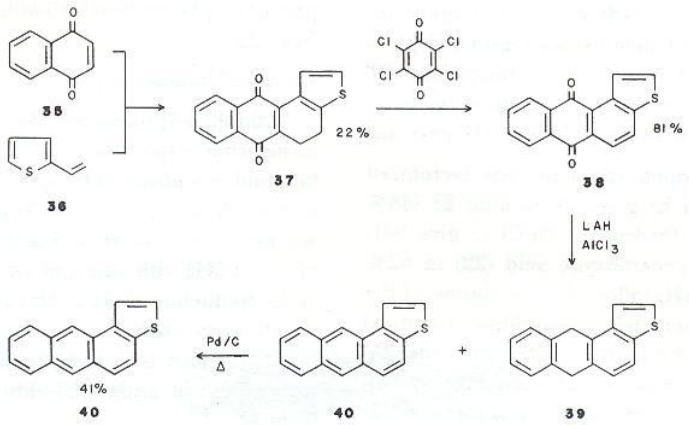

act with *p*-chloranil producing anthra[2,1-*b*]thiophene-6,11-dione (**38**) in 81% yield. Reduction (LAH and aluminum chloride) gave a difficultly separable mixture of 6,11-dihydroanthra[2,1-*b*]thiophene (**39**) and anthra[2,1-*b*]thiophene (**40**). By dehydrogenating the mixture of **39** and **40** (Pd/C) a yield of 41% of anthra[2,1-*b*]thiophene (**40**) was obtained from **38**.

Anthra[1,2-*b*]thiophene (**45**) [18] was synthesized *via* the same sequence of reactions described for the preparation of **40**. Thus **35** was allowed to undergo a Diels-Alder reaction with 3-vinylthiophene (**41**) to give 4,5,6,11-tetrahydroanthra[1,2-*b*]thiophene-6,11-dione (**42**) in 44% yield which was converted into anthra[1,2-*b*]thiophene-6,11-dione (**43**) (85% yield) when treated with *p*-chloranil. Reduction (LAH and aluminum chloride) again produced a difficultly separable mixture of 6,11-dihydroanthra[1,2-*b*]thiophene (**44**) and anthra[1,2-*b*]thiophene (**45**). Dehydrogenation of the mixture of **44** and **45** (Pd/C) gave **45** in 37% yield from **43**.

Benzo[*b*]naphtho[*d*]thiophenes [17].

Benzo[*b*]naphtho[2,3-*d*]thiophene (**50**) was prepared as described by Mayer *et al.* [19]. The lactone **46** (whose detailed synthesis will be described later (from **87, 57** → **88**) was reduced (Pd/C) to *o*-(2-benzo[*b*]thenyl)benzoic acid (**47**) which with LAH gave the alcohol **48**. When **48** was oxidized (chromium trioxide-pyridine complex) the aldehyde **49** was obtained which upon PPA cyclization gave **50** [19] in 58% overall yield from **46**.

Benzo[*b*]naphtho[2,1-*d*]thiophene (**56**) [20,21] was prepared *via* the Wadsworth-Emmons reaction followed by photocyclization. When benzo[*b*]thiophene-3-carboxaldehyde (**51**) was allowed to react with diethyl benzylphosphonate (**52**) 3-styrylbenzo[*b*]thiophene (**55**) was obtained

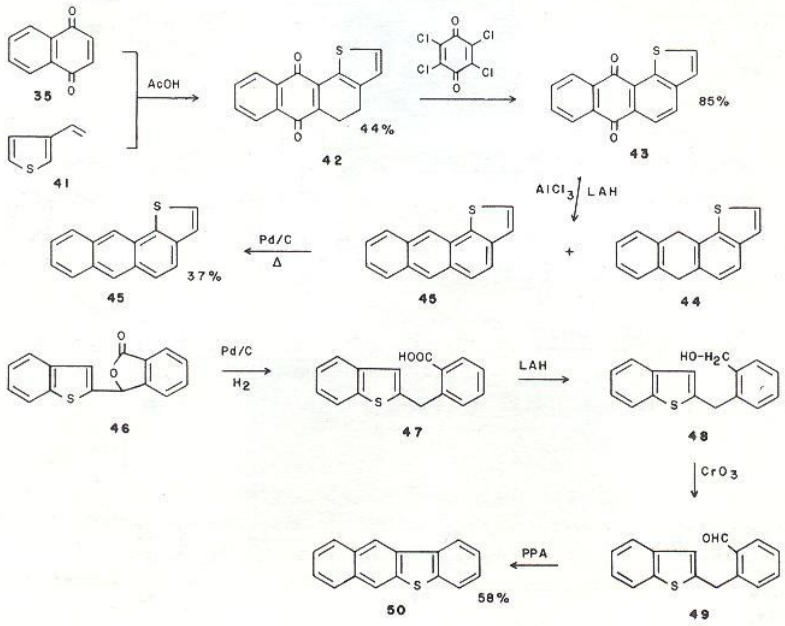

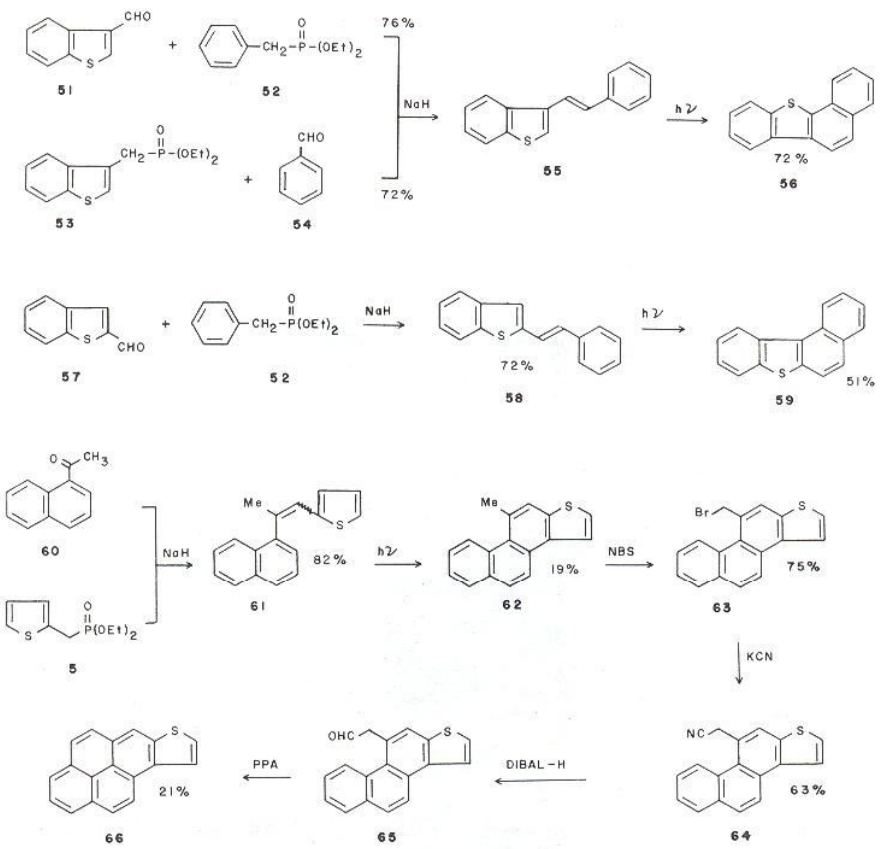

in 76% yield, while the Wadsworth-Emmons reaction of diethyl 3-benzo[*b*]thenylphosphonate (**53**) and benzaldehyde (**54**) gave **55** in 72% yield. Photocyclization of **55** produced benzo[*b*]naphtho[2,1-*d*]thiophene (**56**) in 72% yield.

In like manner benzo[*b*]naphtho[1,2-*d*]thiophene (**59**) [21,22] was obtained from benzo[*b*]thiophene-2-carboxaldehyde (**57**) and **52** (Wadsworth-Emmons) with the intermediate 2-styrylbenzo[*b*]thiophene (**58**) (72% yield) which gave **59** in 51% yield upon photocyclization.

Pyreno[*b*]thiophenes [23].

Pyreno[2,1-*b*]thiophene (**66**) was synthesized in six steps beginning with the Wadsworth-Emmons reaction of 1-acetylnaphthalene (**60**) and **5** which gave 1-(2-thienyl)-2-(1-naphthyl)propene (**61**) (82% yield) which upon photocyclization gave 10-methylphenanthro[2,1-*b*]thiophene (**62**) (19%). Compound **62** reacted smoothly *via* the Wohl-Ziegler reaction (NBS) to give 10-bromomethylphenanthro[2,1-*b*]thiophene (**63**) in 75% yield. When **63** was treated with potassium cyanide, 10-cyanomethylphenanthro-[2,1-*b*]thiophene (**64**) (63%) was obtained which was converted into the aldehyde **65** upon treatment of **64** with diisobutyl aluminum hydride (DIBAL-H). Cyclization of **65** (PPA) gave pyreno[2,1-*b*]thiophene (**66**) in 21% yield from the nitrile **64**. Compound **66** can be regarded as a thiophene isostere of benzo[*a*]pyrene.

Pyreno[4,5-*b*]thiophene (**72**) was obtained in five steps. Pyrene (**67**) was reduced with sodium in amyl alcohol [24] and 1,2,3,6,7,8-hexahydropyrene was obtained which was brominated [25] to give 4-bromo-1,2,3,6,7,8-hexahydropyrene (**69**). Compound **69** was readily aromatized (*p*-chloranil) into 4-bromopyrene (**70**) [25]. Lithiation of **70** (phenyllithium) followed by reaction with the acetal of 2-oxoethyl disulfide produced the acetal of 4-pyrenylthioethanal (**71**) which was cyclized into pyreno[4,5-*b*]thiophene (**72**) with PPA. Compound **72** is a benzo[*e*]pyrene isostere.

Pyreno[1,2-*b*]thiophene was prepared as previously reported by Pandya and Tilak [26].

Phenaleno[1,9-*bc*]thiophene [27].

Phenaleno[1,9-*bc*]thiophene (**79**) has been synthesized in six steps. The Wadsworth-Emmons reaction of **52** and 4-methyl-2-thiophenecarboxaldehyde (**73**) gave 5-methyl-2-styrylthiophene (**74**) in 87% yield. Photocyclization of **74** gave 1-methylnaphtho[2,1-*b*]thiophene (**75**) (41% yield), which with NBS gave 1-bromomethylnaphtho[2,1-*b*]thio-

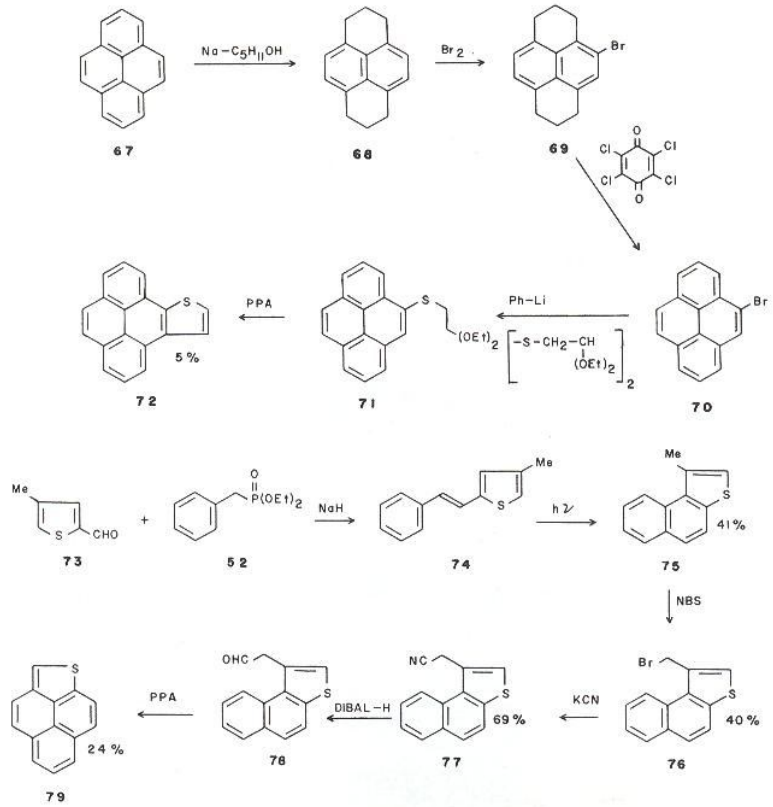

phene (**76**) (40% yield). Reaction of potassium cyanide and **76** produced 1-cyanomethylnaphtho[2,1-*b*]thiophene (**77**) (69% yield) which with DIBAL-H gave the aldehyde **78**. Cyclization of **78** with PPA produced phenyleno[1,9-*bc*]-thiophene (**79**) in 24% yield.

Benzo[2,3]phenanthro[4,5-*bcd*]thiophene (**86**) [28].

The benzo[*a*]pyrene isostere, benzo[2,3]phenanthro-[4,5-*bcd*]thiophene (**86**) has been prepared in six steps. By allowing 3-acetylbenzo[*b*]thiophene to react with diethyl benzylphosphonate (**52**) (Wadsworth-Emmons conditions), a yield of 80% of 2-(3-benzo[*b*]thienyl)-1-phenylpropene was obtained which was readily photocyclized into 6-methylbenzo[*b*]naphtho[2,1-*d*]thiophene (**82**) in 73% yield which when treated with NBS gave 6-bromomethylbenzo-[*b*]naphtho[2,1-*d*]thiophene (**83**) (78% yield). Compound **83** was allowed to react with potassium cyanide giving 6-cyanomethylbenzo[*b*]naphtho[2,1-*d*]thiophene (**84**) (85% yield) which in turn was allowed to react with DIBAL-H producing the aldehyde **85** which was then cyclized (PPA) into benzo[2,3]phenanthro[4,5-*bcd*]thiophene (**86**) in 42% yield from **84**. Karcher *et al.* has isolated **86** from coal derived products and reported the high mutagenicity in the Ames test. We have confirmed that **86** is approximately as mutagenic as benzo[*a*]pyrene [30].

Chryseno[4,5-*bcd*]thiophene (**96**) [28].

Nine steps were required for the synthesis of chryseno-[4,5-*bcd*]thiophene (**96**) an isostere of benzo[*a*]pyrene. Lithiation of 2-phenyl-4,4-dimethyl-2-oxazoline (**87**) followed by treatment of the lithio derivative with 2-benzo[*b*]thiophenecarboxaldehyde (**57**) gave the alcohol **88** (62% yield) which when treated with acid opened the oxazoline ring to give the carboxylic acid which spontaneously lactonized into **89** (89% yield) which was readily reduced (Pd/C, acetic acid) to give the carboxylic acid **90** in 87% yield. Reaction of **90** with methyllithium gave the ketone **91** which was cyclized (PPA) to give 11-methylbenzo[*b*]-naphtho[2,3-*d*]thiophene (**92**) in 43% yield. A Wohl-Ziegler reaction (NBS) on **92** gave 11-bromomethylbenzo[*b*]-naphtho[2,3-*d*]thiophene (**93**) (76% yield) which upon treatment with potassium cyanide produced 11-cyanomethylbenzo[*b*]naphtho[2,3-*d*]thiophene (**94**) in 72% yield. Treatment of **94** with DIBAL-H gave the aldehyde **95** which cyclized with PPA into **96** in 32% yield from **94**. Compound **96** is another isostere of benzo[*a*]pyrene which has been mentioned by Karcher *et al.* [29].

Triphenyleno[*b*]thiophenes [31].

Triphenyleno[1,2-*b*]thiophene (**99**) was prepared in two steps from phenanthrene-9-carboxaldehyde (**97**) when **97**

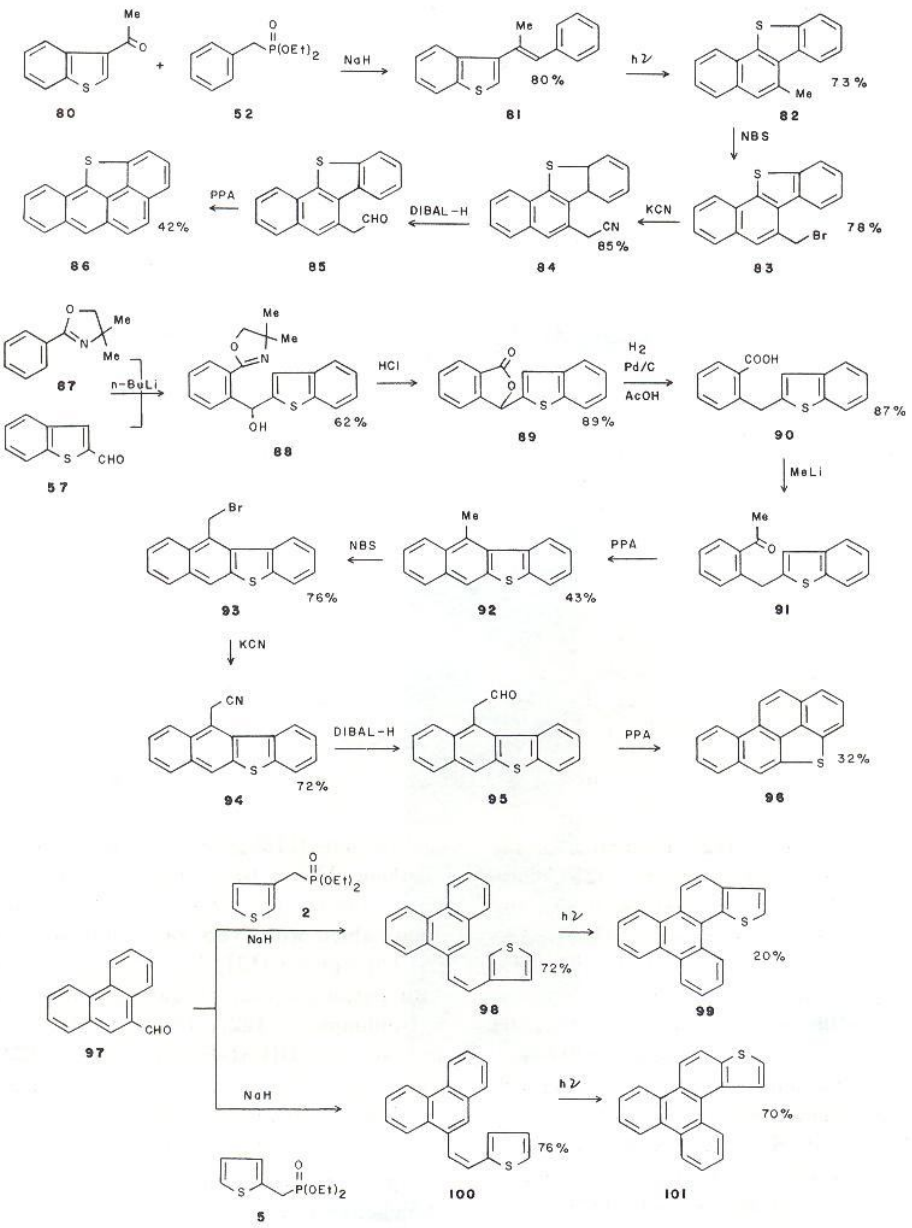

was allowed to undergo the Wadsworth-Emmons reaction with **2** to yield 3-(9-phenanthrylethenyl)thiophene (**98**) (72% yield) which when photocyclized gave **99** in 20% yield. Likewise the reaction of **97** and **5** gave 2-(9-phenanthrylethenyl)thiophene (**100**) (76% yield) which upon photocyclization produced triphenyleno[2,1-*b*]thiophene (**101**) in 70% yield.

Four steps were required for the synthesis of triphenyleno[2,3-*b*]thiophene (**105**) previously reported by another method by Nicolaides [32]. 9-Phenanthrenecarboxaldehyde (**97**) was allowed to react with the lithio derivative of 2-(3-thienyl)-4,4-dimethyl-2-oxazoline (**13**) to give the alcohol **102** which upon acidification and lactonization gave **103** (21% yield) which was converted to the carboxylic acid **104** in 33% yield. Reduction (LAH) to the alcohol, oxidation (chromium trioxide-pyridine complex) followed by PPA cyclization of the aldehyde produced **105** (11% yield).

Benzo[1,2]phenaleno[*bc*]thiophenes [33].

Seven steps were required for the synthesis of benzo-

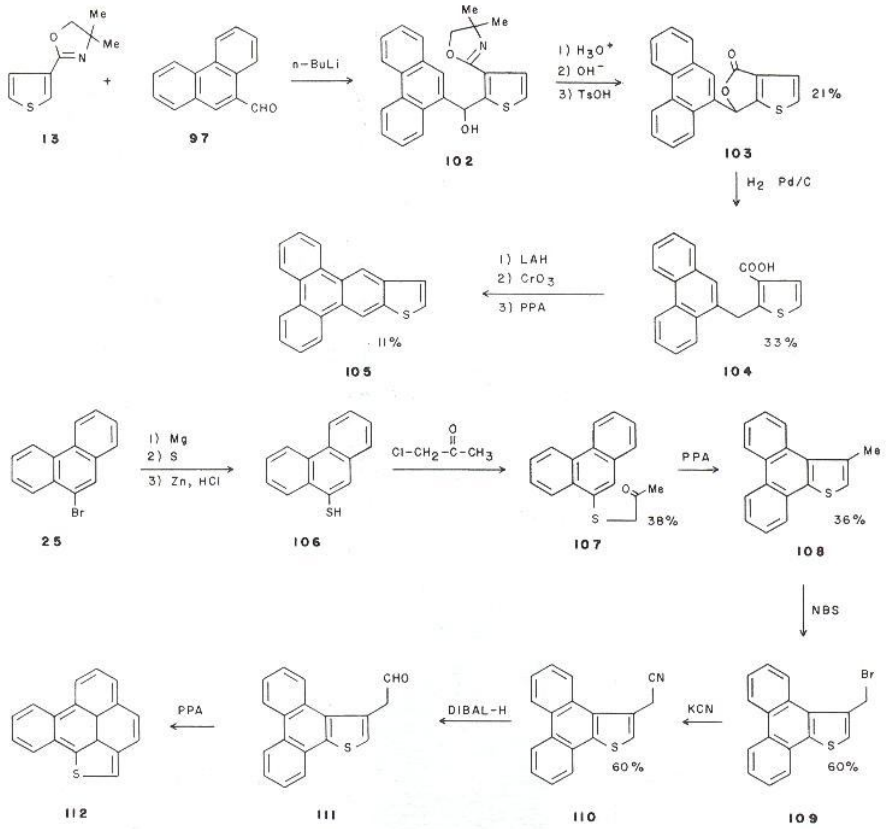

[1,2]phenaleno[3,4-*bc*]thiophene (**112**). Formation of the Grignard reagent from 9-bromophenanthrene (**25**) followed by reaction with sulfur then treatment with zinc and hydrochloric acid gave 9-phenanthrenethiol (**106**) which with chloroacetone produced the ketosulfide **107** (38% yield) which upon cyclization (PPA) gave 3-methylphenanthro[9,10-*b*]thiophene (**108**) in 36% yield. Reaction of **108** with NBS gave 3-bromomethylphenanthro[9,10-*b*]thiophene (**109**) (60% yield) which when allowed to react with potassium cyanide gave 3-cyanomethylphenanthro[9,10-*b*]-thiophene (**110**) (60% yield). Reaction of **110** with DIBAL-H gave the aldehyde **111** which upon PPA cyclization produced benzo[1,2]phenaleno[3,4-*bc*]thiophene (**112**).

Benzo[1,2]phenaleno[4,3-*bc*]thiophene (**117**) was obtained in three steps. Phenacyl bromide (**113**) reacted with 2-naphthalenethiol in base to give the ketosulfide **115** which upon PPA cyclization gave 1-phenylnaphtho[2,1-*b*]-thiophene (**116**) in 75% yield. Photocyclization of **116** gave benzo[1,2]phenaleno[4,3-*bc*]thiophene (**117**) in 5% yield.

Benzo[4,5]phenaleno[*bc*]thiophenes [34].

The synthesis of benzo[4,5]phenaleno[1,9-*bc*]thiophene was accomplished in six steps. Reaction of 4-methyl-2-thiophenecarboxaldehyde (**73**) with diethyl 1-naphthylmethylphosphonate (**118**) gave 1-(4-methyl-2-thienyl)-2-(1-naphthyl)ethene (**119**) in 68% yield which upon photocyclization gave 3-methylphenanthro[2,1-*b*]thiophene (**120**) 84% yield) which with NBS gave 3-bromomethylphenanthro-[2,1-*b*]thiophene (**121**) in 69% yield. Treatment of **121** with potassium cyanide gave 3-cyanomethylphenanthro-[2,1-*b*]thiophene (**122**) (71% yield). When **122** was allowed to react with DIBAL-H, the aldehyde **123** was obtained which was cyclized with PPA into benzo[4,5]phenaleno-[1,9-*bc*]thiophene (**124**) in 24% yield. This compound is a thiophene isostere of benzo[*a*]pyrene.

Eight steps were required for the synthesis of benzo-[4,5]phenaleno[9,1-*bc*]thiophene (**133**). A Diels-Alder reaction between 4-methyl-2-vinylthiophene (**125**) and 1,4-naphthoquinone (**35**) gave 1-methyl-4,5,6,11-tetrahydroanthra[2,1-*b*]thiophene-6,11-dione (**126**) which was dehydrogenated in the 4,5 position with *p*-chloranil to give 1-methylanthra[2,1-*b*]thiophene-6,11-dione (**127**) (62% yield). Deoxygenation (LAH, aluminum chloride) gave a mixture of **128** and **129** which when heated (Pd/C) gave 1-methylanthra[2,1-*b*]thiophene (**129**) in 66% yield from **127**. Bromination (NBS, benzene) of **129** gave **130** which upon treatment with potassium cyanide produced 1-cyanomethylanthra[2,1-*b*]thiophene (**131**) in 62% yield from **129**. Reaction of **131** with DIBAL-H produced the aldehyde **132**

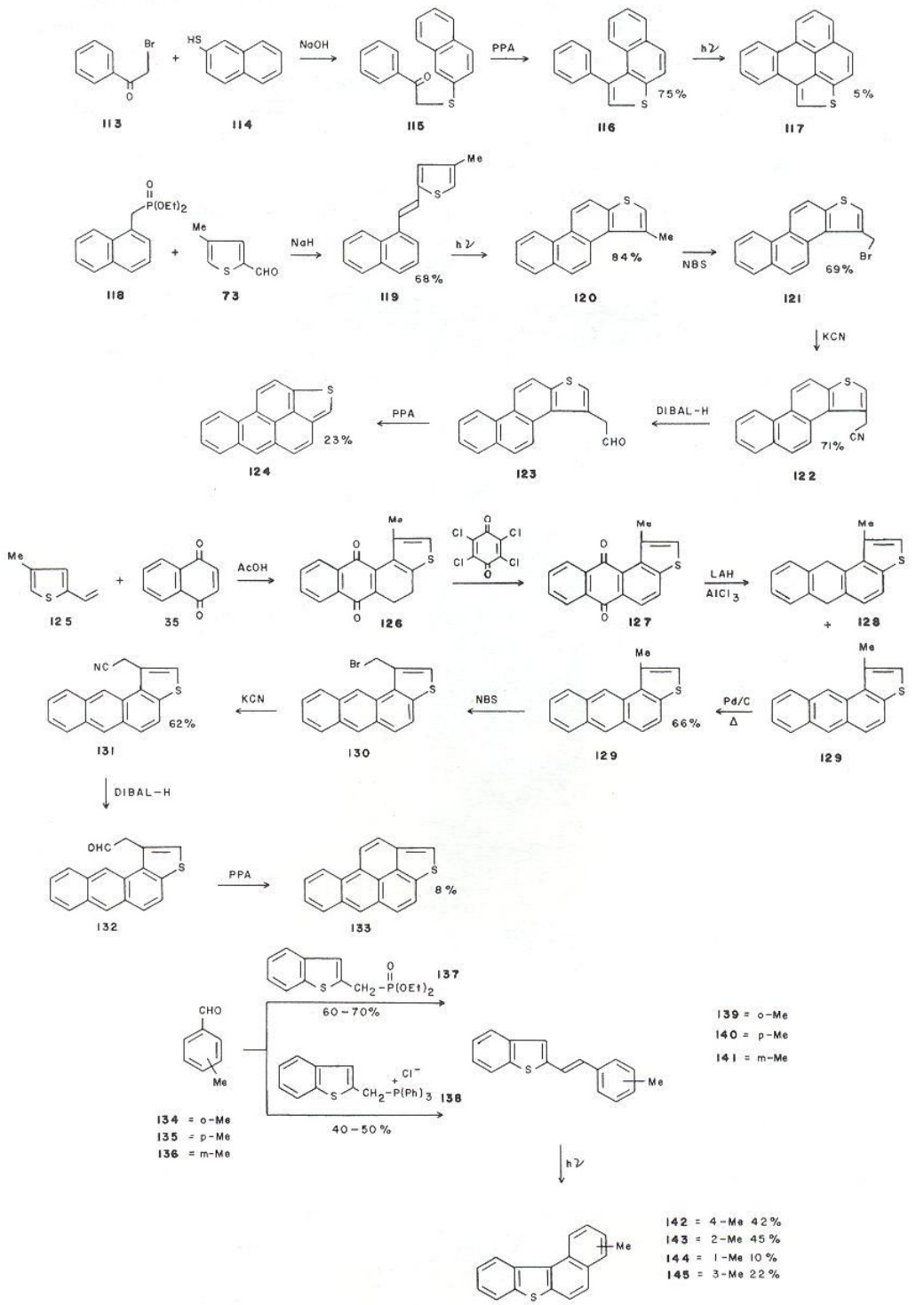

which upon cyclization (PPA) gave benzo[4,5]phenaleno-[9,1-*bc*]thiophene (**133**) in only 5% yield from **131**. Thus the synthesis of all of the thiophene isosteres of benzo[*a*]pyrene has been accomplished.

Monomethyl Isomers of Benzo[*b*]naphtho[1,2-*d*]thiophene [34].

The Wadsworth-Emmons reaction of *o*- (**134**), *p*- (**135**) or *m*-methylbenzaldehydes (**136**) with diethyl 2-benzo[*b*]then-

ylphosphonate (**137**) gave the corresponding *o*- (**139**), *p*- (**140**) or *m*-methylstyrylbenzo[*b*]thiophene (**141**) in 60-70% yields. The Wittig reaction of **134, 135** or **136** with **138** gave **139, 140** or **141** in lower yields (40-50%) under less favorable conditions. Photocyclization of **139** or **140** gave 4-methylbenzo[*b*]naphtho[1,2-*d*]thiophene (**142**) (42% yield) or 2-methylbenzo[*b*]naphtho[1,2-*d*]thiophene (**143**) in 45% yield. Photocyclization of **141** gave a separable mixture of 1-methylbenzo[*b*]naphtho[1,2-*d*]thiophene (**144**) (10%) and 3-methylbenzo[*b*]naphtho[1,2-*d*]thiophene (**145**) (22%).

In like manner, **146, 147** or **148** with **52** gave 5-methyl-2-styrylbenzo[*b*]thiophene (**149**) (81% yield), 6-methyl-2-styrylbenzo[*b*]thiophene (**150**) (72% yield) or 7-methyl-2-styrylbenzo[*b*]thiophene (**151**) (80% yield). Photocyclization of **149, 150** or **151** gave 10-methylbenzo[*b*]naphtho-[1,2-*d*]thiophene (**152**) (45% yield), 9-methylbenzo[*b*]naphtho[1,2-*d*]thiophene (**153**) (45% yield) or 8-methylbenzo-[*b*]naphtho[1,2-*d*]thiophene (**154**) (40% yield).

For the synthesis of the 11-methyl isomer, 3-(*o*-methylphenyl)propenoic acid was cyclized with thionyl chloride to give 3-chloro-4-methylbenzo[*b*]thiophene-2-carboxoyl chloride (**156**) (51% yield) which upon treatment with LAH gave the alcohol **157** (75% yield). Oxidation (chromium trioxide-pyridine complex) gave 3-chloro-4-methylbenzo-[*b*]thiophene-2-carboxaldehyde (**158**) (78% yield) which with diethyl benzylphosphonate gave 3-chloro-4-methyl-2-styrylbenzo[*b*]thiophene (**159**) (48% yield) which was photocyclized with elimination of hydrogen and chlorine into **160** (34% yield).

The Wadsworth-Emmons reaction of **137** and acetophenone (**161**) gave the adduct **162** (52% yield) which upon photocyclization gave 5-methylbenzo[*b*]naphtho-[1,2-*d*]thiophene (**163**) in 52% yield.

Monomethyl Isomers of Benzo[*b*]naphtho[2,1-*d*]thiophene [35].

The Wadsworth-Emmons reaction of the requisite alde-

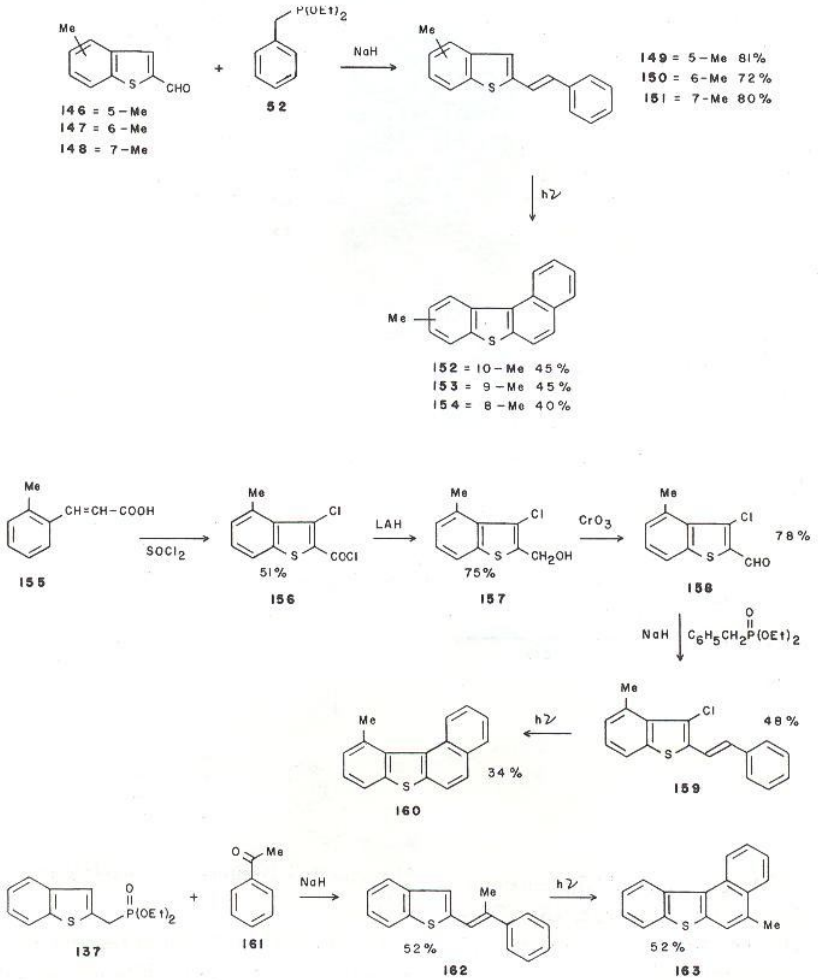

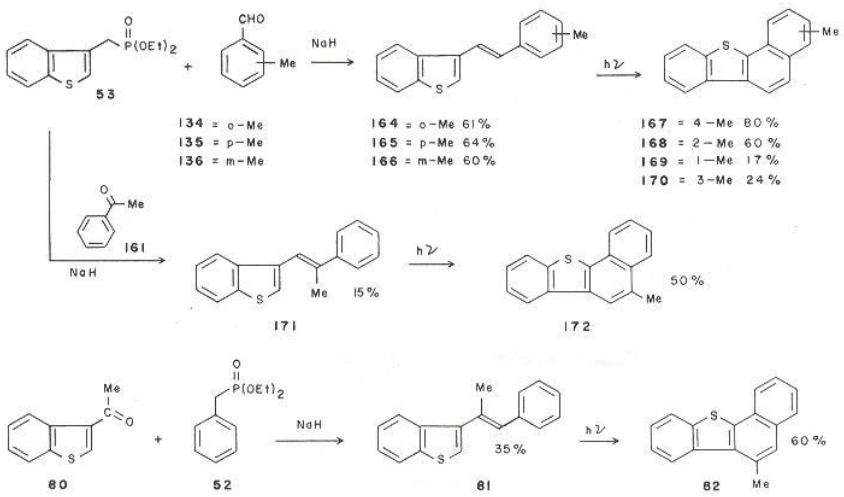

hydes **134, 135** or **136** with the phosphonate ester **53** gave the required styryl compounds **164** (61%), **165** (64%) and **166** (60%) respectively. Photocyclization of **164, 165** or **166** gave respectively 4-methylbenzo[*b*]naphtho[2,1-*d*]-thiophene (**167**) (80% yield), 2-methylbenzo[*b*]naphtho-[2,1-*d*]thiophene (**168**) (60% yield) and from **166** the two separable products, namely, 1-methylbenzo[*b*]-naphtho[2,1-*d*]thiophene (**169**) (17% yield) and 3-methylbenzo[*b*]naphtho[2,1-*d*]thiophene (**170**) (24% yield). Acetophenone (**161**) and **53** gave the required alkene **171** (15%) which upon photocyclization gave 5-methylbenzo[*b*]naphtho[2,1-*d*]thiophene (**172**) in 50% yield. Diethyl benzylphosphonate (**52**) and 3-acetylbenzo[*b*]thiophene (**80**) gave the alkene **81** (35% yield) which photocyclized into 6-methylbenzo[*b*]naphtho[2,1-*d*]thiophene (**82**) in 60% yield, previously prepared by another route.

The 7-, 8-, 9-, and 10-methylbenzo[*b*]naphtho[2,1-*d*]thiophenes (**189, 188, 190** and **187**) respectively were prepared in six steps. The *o*- (**173**), *p*- (**174**), or *m*-methylbenzenethiols (**175**) condensed with ethyl 4-chloro-2-oxobutanoate in pyridine to give the ester ketosulfides **176, 177** or **178** respectively which upon PPA cyclization gave the requisite esters **179, 180, 181** and **182** (the latter two isomers from the *m*-isomer **178**). The esters **179, 180, 181** or **182** were hydrolyzed to the carboxylic acids **183** (45%), **184** (30%), **185** (19%) and **186** (15%), all yields for the three step sequence. Compounds **183, 184, 185** and **186** condense with benzaldehyde to give the required substituted propenoic acids **195** (36%), **196** (51%), **197** (42%) and **198** (32%) respectively. Photocyclization of **195, 196, 197** or **198** gave the cyclized carboxylic acids **191, 192, 193** or **194** respectively. Copper (quinoline) decarboxylation of **191, 192, 193** or **194** gave the following, respectively: 10-methylbenzo[*b*]naphtho[2,1-*d*]thiophene (**187**) (60% yield); 8-methylbenzo[*b*]naphtho[2,1-*d*]thiophene (**188**) (52% yield); 7-methylbenzo[*b*]naphtho[2,1-*d*]thiophene

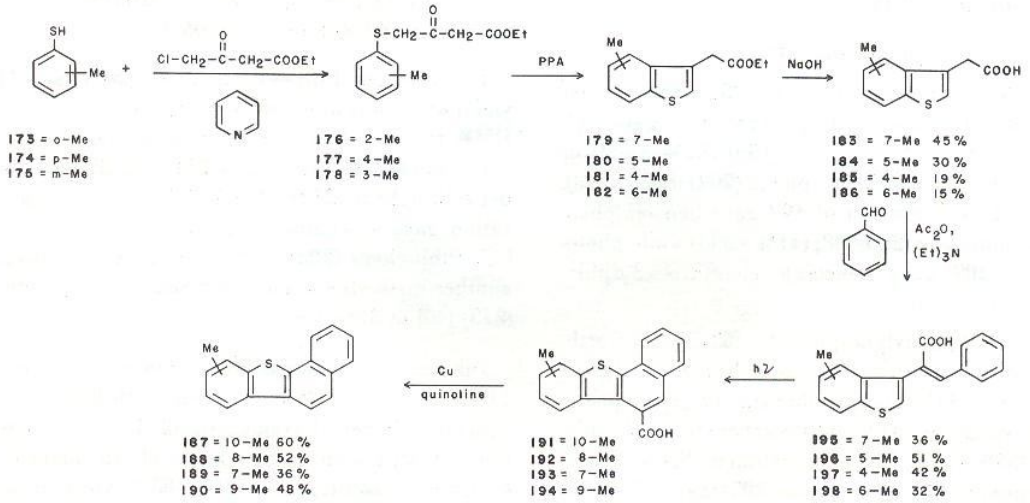

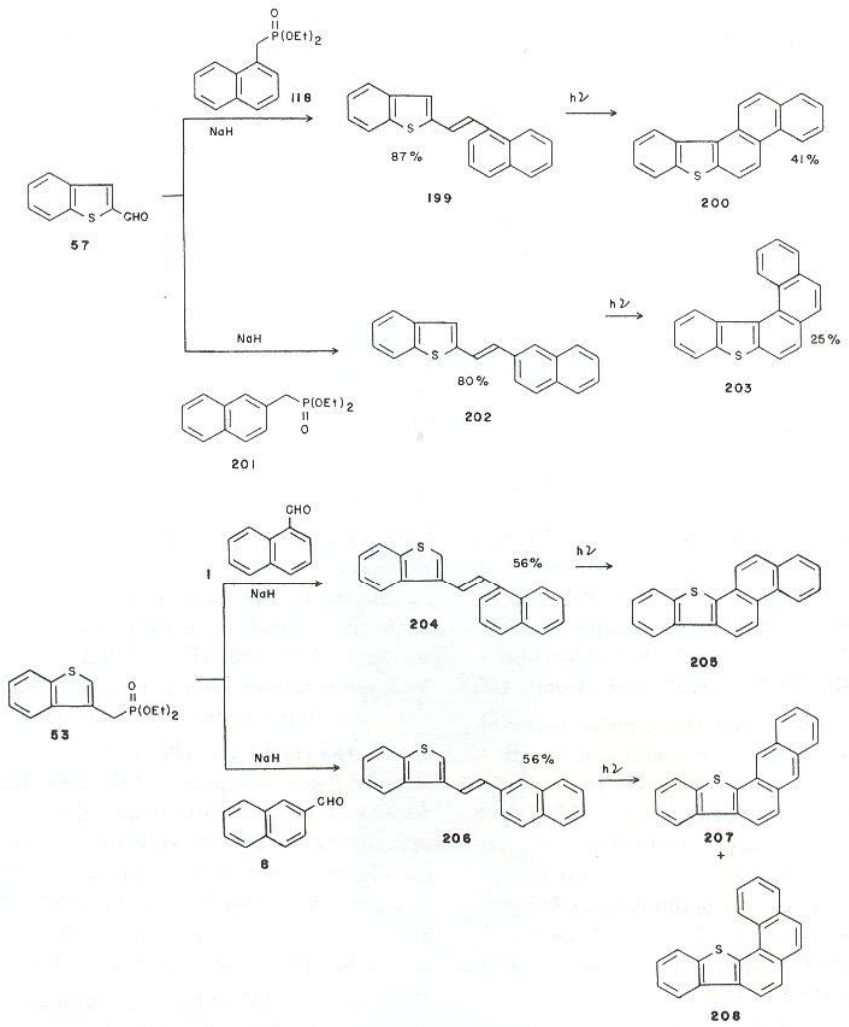

(**189**) (36% yield); and 9-methylbenzo[*b*]naphtho[2,1-*d*]-thiophene (**190**) (48% yield).

Benzo[*b*]phenanthro[*d*]thiophenes [36,37].

2-Benzo[*b*]thiophenecarboxaldehyde (**57**) with either 1-naphthyl- or 2-naphthyl diethylphosphonates gave 2-(1-naphthylethenyl)benzo[*b*]thiophene (**199**) (87% yield) or 2-(2-naphthylethenyl)benzo[*b*]thiophene (**202**) (80% yield), respectively. Photocyclization of **199** gave benzo[*b*]phenanthro[1,2-*d*]thiophene (**200**) [38] (41% yield) while photocyclization of **202** gave benzo[*b*]phenanthro[4,3-*d*]thiophene (**203**) (25% yield).

Diethyl benzo[*b*]thenylphosphonate (**53**) (Wadsworth-Emmons conditions) with 1- (**1**) or 2-naphthalenecarboxaldehyde (**8**) gave 3-(1-naphthylethenyl)benzo[*b*]thiophene (**204**) (56% yield) or 3-(2-naphthylethenyl)benzo[*b*]thiophene (**206**) (56% yield). Photocyclization of **204** produced benzo[*b*]phenanthro[2,1-*d*]thiophene (**205**) [39] (10% yield) while photocyclization of **206** gave two compounds, namely anthra[1,2-*b*]benzo[*d*]thiophene (**207**) [39] and benzo[*b*]-phenanthro[3,4-*d*]thiophene (**206**) [39].

Bromination of dibenzothiophene (**209**) gave **210** (89% yield) which was lithiated (*n*-butyllithium) and treated with DMF to yield 2-dibenzothiophenecarboxaldehyde (**211**) (85% yield). The reaction of **211** with **52** gave 2-styryldibenzothiophene (**212**) (86% yield) which upon photocyclization gave a separable mixture of benzo[*b*]phenanthro-[4,3-*d*]thiophene (**203**) (50% yield, previously prepared by another method) and benzo[*b*]phenanthro[2,3-*d*]thiophene (**213**) [40] in 37% yield.

Dibenzothiophene was lithiated (*n*-butyllithium) and the 4-lithio derivative allowed to react with DMF to give 4-dibenzothiophenecarboxaldehyde (**214**) (86% yield) which when treated with diethyl benzylphosphonate (**52**) gave 4-styryldibenzothiophene (**215**) (85% yield) which upon

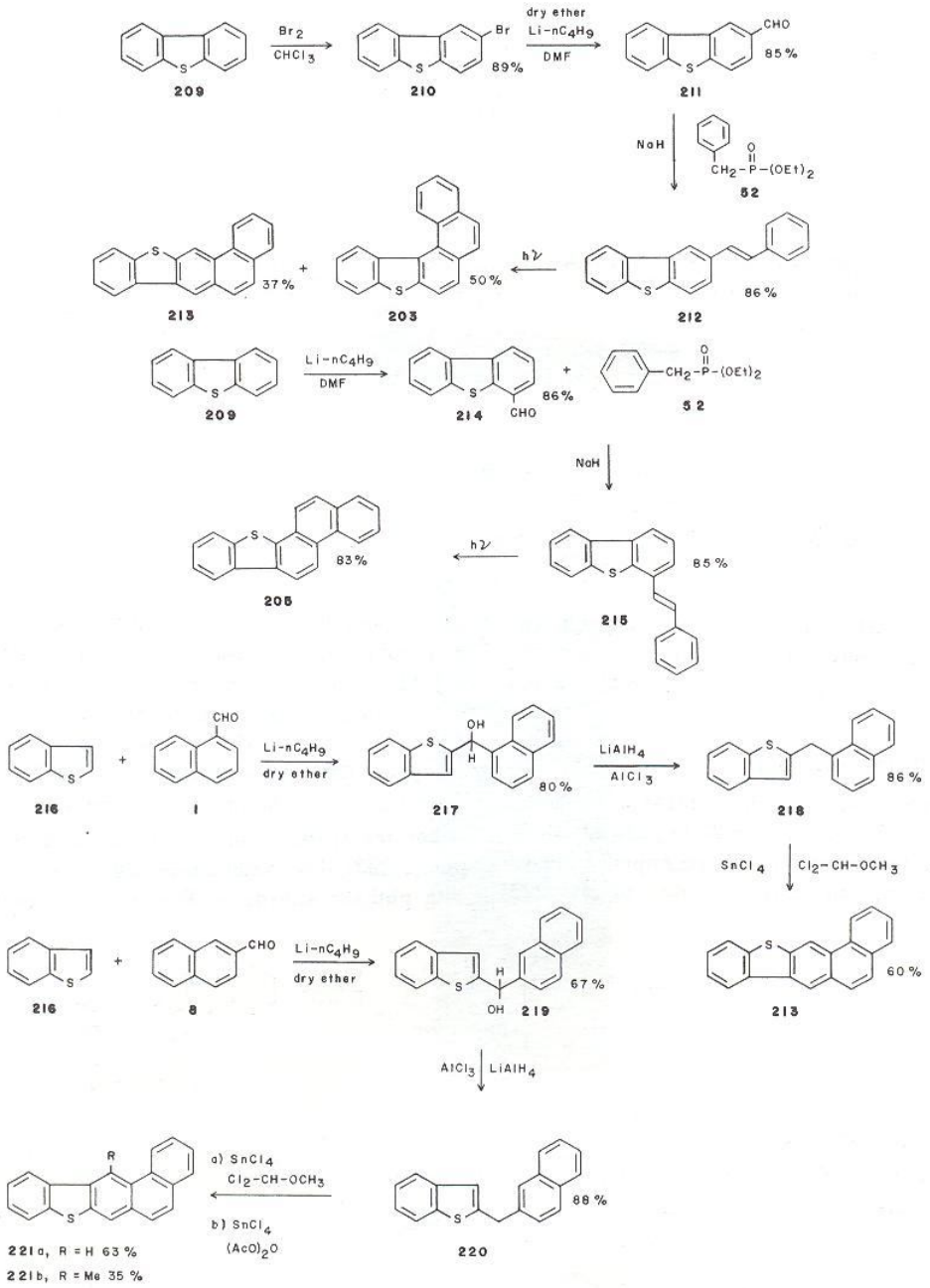

photocyclization produced benzo[*b*]phenanthro[2,1-*d*]thiophene (**205**) in 83% yield which has also been prepared *via* the Wadsworth-Emmons reaction followed by photocylization from different starting materials (**53** + **1** → **204** → **205**).

Lithiation of benzo[*b*]thiophene (**216**) followed by treatment of the 2-lithio derivative with 1-naphthalenecarboxaldehyde gave the alcohol **217** (80% yield) which was reduced (LAH and aluminum chloride) to 2-(1-naphthylmethyl)benzo[*b*]thiophene (**218**) (86% yield). Treatment of **218** with dichloromethyl methyl ether and stannic chloride gave **213** (60%) previously prepared by us *via* another route. Likewise **216**, when lithiated, with 2-naphthalenecarboxaldehyde (**8**) reacted to give the alcohol **219** (67% yield) which was reduced (LAH and aluminum chloride) to produce 2-(2-naphthylmethyl)benzo[*b*]thiophene (**220**) (88% yield). Cyclization of **220** with dichloromethyl methyl ether and stannic chloride produced benzo[*b*]phenanth-

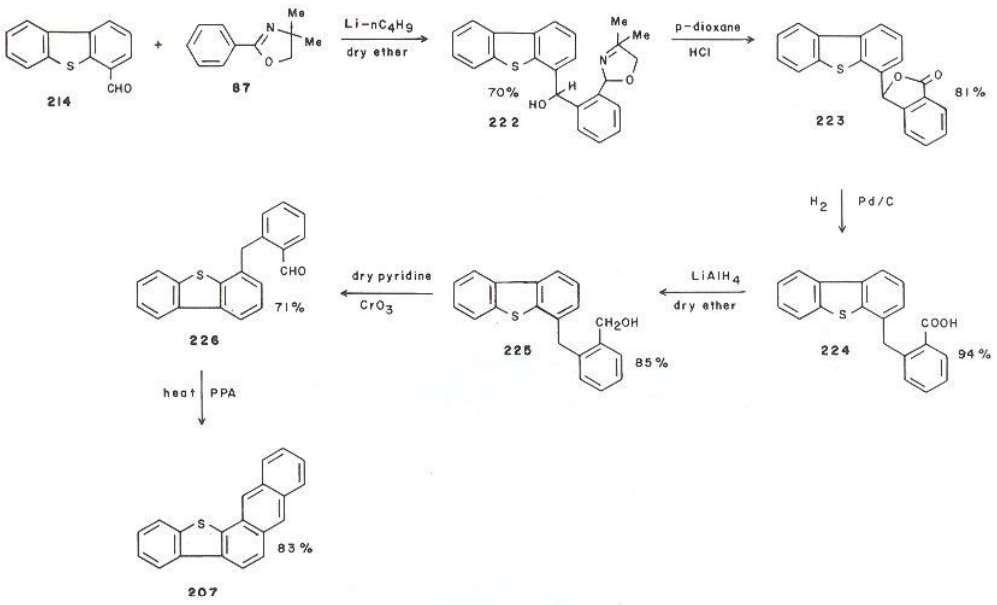

ro[3,2-*d*]thiophene (**221a**) in 63% yield. When **220** was cyclized with acetic anhydride and stannic chloride 13-methylbenzo[*b*]phenanthro[3,2-*d*]thiophene (**221b**) was obtained in 35% yield.

Anthra[*b*]benzo[*d*]thiophenes [37].

4-Dibenzothiophenecarboxaldehyde (**214**) was allowed to react with the lithio derivative of **87** to yield **222** (70% yield) which upon treatment wtih acid ring-opened the oxazoline ring and spontaneously lactonized to give **223** (81% yield). Reduction (Pd/C) of **223** gave the carboxylic acid **224** (94% yield) which was reduced (LAH) to the alcohol **225** (85% yield). Oxidation (chromium trioxide-pyridine complex) of **225** gave the aldehyde **226** (71% yield) which was cyclized (PPA) to give anthra[1,2-*b*]benzo[*d*]-thiophene (**207**) (83% yield). Compound **207** was also obtained as one of the products of photocyclization of **206**.

For the synthesis of the remaining anthra[2,3-*b*]thiophene (**233**), dibenzothiophene (**209**) was allowed to react with phthalic anhydride (Friedel-Crafts reaction, alumi-

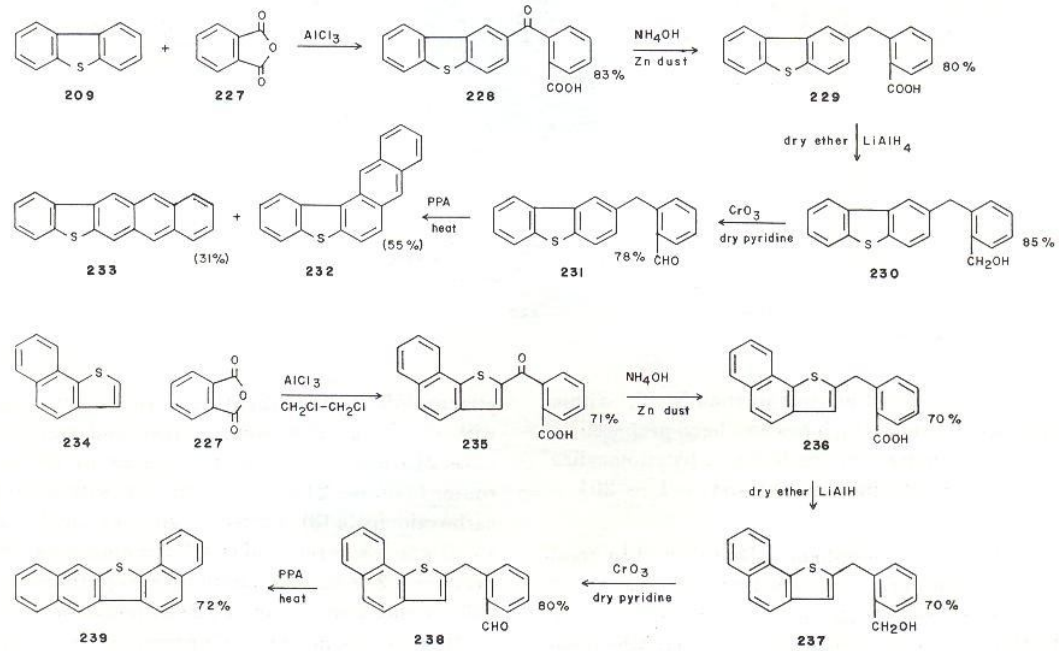

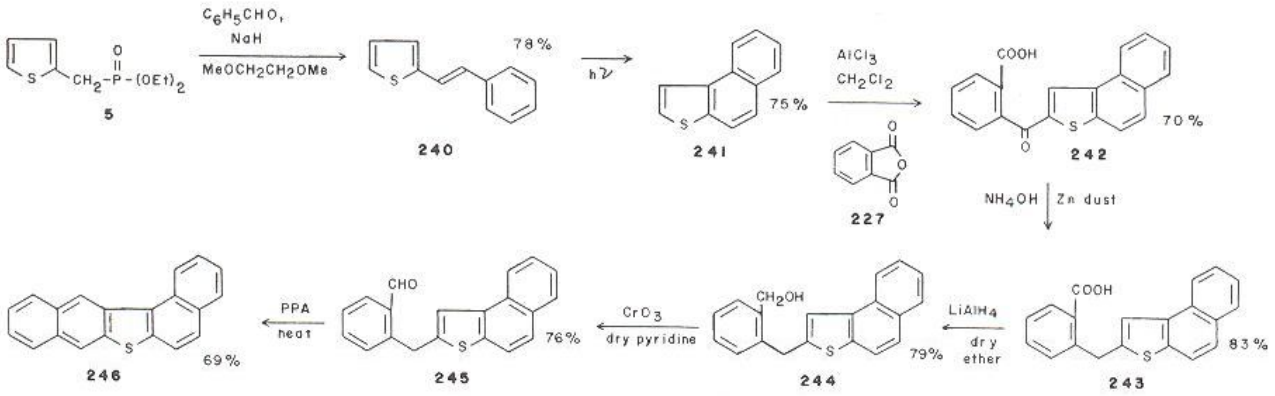

num chloride) to give the ketoacid **228** (83% yield) which was reduced (zinc and ammonium hydroxide) to the acid **229** (80% yield). Reduction of **229** (LAH) to the alcohol **230** (85% yield) followed by oxidation of **230** (chromium trioxide-pyridine complex) produced the aldehyde **231** (78% yield) which with PPA gave a separable mixture consisting of anthra[2,1-*b*]benzo[*d*]thiophene (**232**) in 55% yield and anthra[2,3-*b*]benzo[*d*]thiophene (**233**) [19,41] in 31% yield.

Dinaphthothiophenes [42].

Naphtho[1,2-*b*]thiophene (**234**) reacted smoothly with phthalic anhydride (**227**) (Friedel-Crafts, aluminum chloride) to give the ketoacid **235** (71% yield) which upon reduction (zinc, ammonium hydroxide) gave the carboxylic acid **236** (70% yield). Reduction of **236** (LAH) produced the alcohol **237** (70% yield) which was oxidized (chromium trioxide-pyridine complex) to yield the aldehyde **238** (78% yield). Cyclization (PPA) gave dinaphtho[1,2-*b*:2′,3′-*d*]thiophene (**239**) in 72% yield.

2-Styrylthiophene (**240**) was obtained from diethyl 2-thenylphosponate (**5**) and benzaldehyde in 79% yield. Photocyclization of **240** gave naphtho[2,1-*b*]thiophene (**241**) (75% yield) which *via* a Friedel-Crafts reaction with **227** produced the ketoacid **242** (70% yield). Reduction (zinc, ammonium hydroxide) of **242** gave the carboxylic acid **243** (83% yield) which with LAH gave the alcohol **244** (79% yield). Oxidation of **244** (chromium trioxide-pyridine complex) produced the aldehyde **245** (76% yield) which upon cyclization (PPA) gave dinaphtho[2,1-*b*:2′,3′-*d*]thiophene (**246**) [43] (69% yield).

Ethyl 2-naphtho[1,2-*b*]thiophenecarboxylate (**247**) was reduced (LAH) to yield the alcohol **248** (90% yield) which upon oxidation (chromium trioxide-pyridine complex) gave the aldehyde **249** (76% yield). With diethyl benzylphosphonate, **249** produced 2-styrylnaphtho[1,2-*b*]thiophene (**250**) (75% yield) which upon photocyclization gave dinaphtho[1,2-*b*:1′,2′-*d*]thiophene (**251**) [44].

3-(1-Naphthyl)-2-mercaptopropenoic acid (**252**) was cyclized (iodine, *p*-dioxane) and 2-naphtho[2,1-*b*]thiophenecarboxylic acid (**253**) (82% yield) was obtained. Reduction of **253** (LAH) yielded the alcohol **254** (89%) which with chromium trioxide-pyridine complex produced the aldehyde **255** (78% yield). Diethyl benzylphosphonate and **255** (Wadsworth-Emmons) gave 2-styrylnaphtho[2,1-*b*]thiophene (**256**) (72% yield) which upon photocyclization yielded dinaphtho[2,1-*b*:1′,2′-*d*]thiophene (**257**) [44] in 45% yield.

1-Naphthalenamine (**258**) was diazotized and treated with potassium ethyl xanthate to give the xanthate **259** (85%) which with LAH gave 1-naphthalenethiol (**260**) (90%). Bromoacetone with **260** gave the ketosulfide which was cyclized (PPA) to give 3-methylnaphtho[1,2-*b*]thiophene (**261**) (71% yield). Oxidation (selenium dioxide) of **261** gave the aldehyde **262** (75%) which with diethyl benzylphosphonate produced 3-styrylnaphtho[1,2-*b*]thiophene (**263**) (74% yield). Photocyclization of **263** produced dinaphtho[1,2-*b*:2′,1′-*d*]thiophene (**264**) [45] in 76% yield.

Naphtho[2,3-*b*]thiophene (**238**) reacted with **227** (aluminum chloride) to yield the ketoacid **266** (80%) which was reduced (zinc, ammonium hydroxide) to the carboxylic acid **267** (84% yield). Reduction of **267** (LAH) gave the alcohol **268** (84% yield) which was oxidized (chromium trioxide-pyridine complex) to the aldehyde **269** (82% yield) which was cyclized (PPA) to give dinaphtho[2,3-*b*:2′,3′-*d*]-thiophene (**270**).

Phenanthro[4,5-*bcd*]thiophene and the Monomethyl Derivatives [46].

Phenanthro[4,5-*bcd*]thiophene (**302**) and some of the monomethyl derivatives have been shown to occur in coal liquids and shale oils [47], thus in order to provide **302** and the monomethyl derivatives for biological testing and unequivocal identification, these compounds were synthesized in eight steps. The sequence of reactions are outlined in Scheme 34.

Benzo[*b*]thiophene (**216**), 5-methyl- (**271**), 6-methyl- (**272**) and 7-methylbenzo[*b*]thiophene (**273**) were each individually lithiated (*n*-butyllithium) and the lithio derivatives were allowed to react with allyl bromide giving the allyl derivatives **274**, **275**, **276**, **277** (yields, 72-85%). These

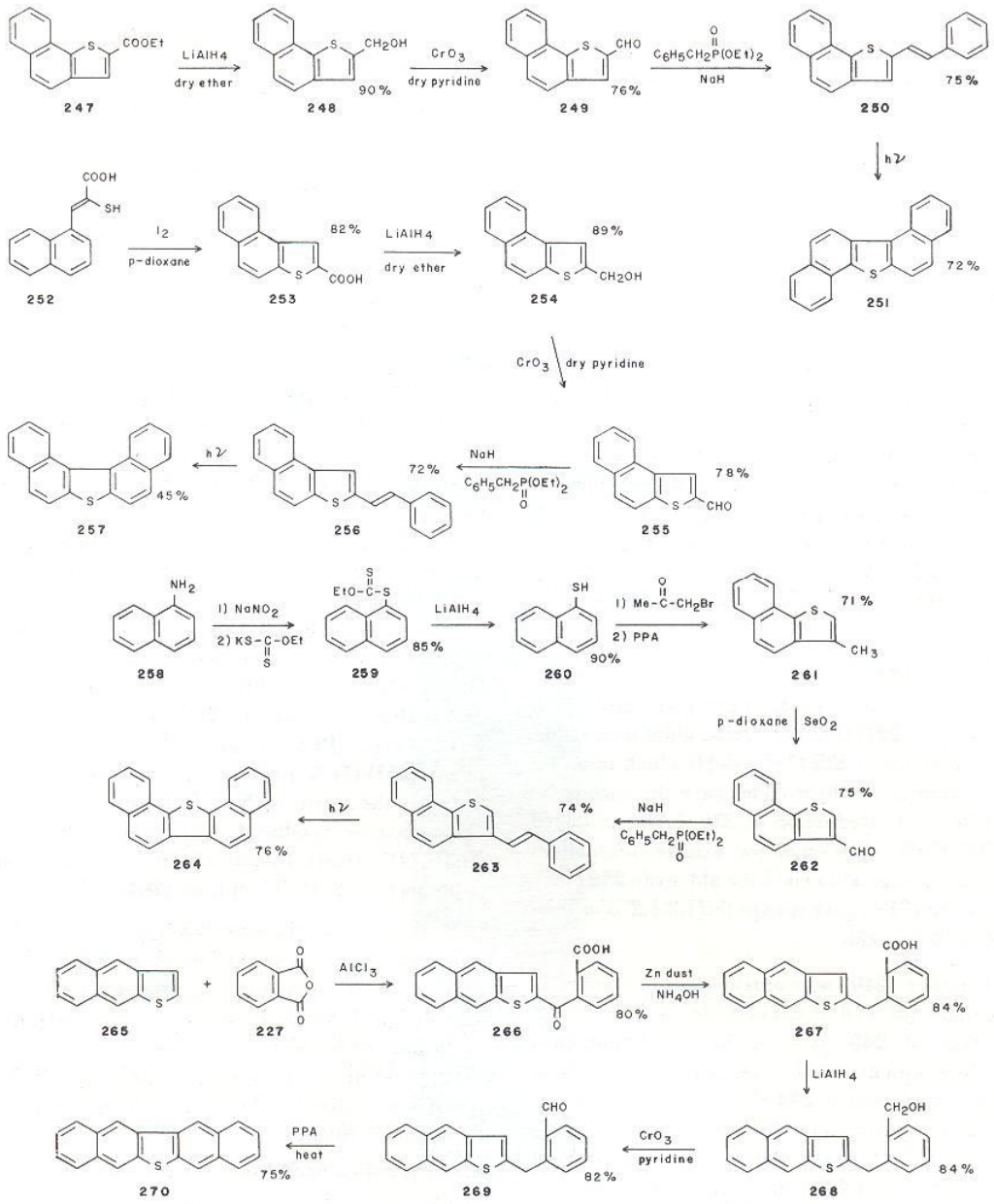

latter compounds were cyclized (ethyl dichloroethoxyacetate) into the esters **278, 279, 280, 281** (73-79% yields). These esters were hydrolyzed to the carboxylic acids **282, 283, 284, 285** (87-94% yields) which upon reduction (LAH) gave the alcohols **286, 287, 288, 289** (90-94% yields). These alcohols were converted into the chlorides **290, 291, 292, 293** (77-88% yields) with thionyl chloride. These benzylic chlorides were allowed to react with potassium cyanide to give the 1-cyanomethyl compounds **294, 295, 296, 297** (86-92% yields) which with DIBAL-H produced the aldehydes **298, 299, 300, 301** in 55-64% yields. Cyclization (PPA) of **298** gave phenanthro[4,5-*bcd*]thiophene (**302**) [48,49]. Cyclization (PPA) of **299, 300, 301** gave 1-methylphenanthro[4,5-*bcd*]thiophene (**303**); 2-methylphenanthro[4,5-*bcd*]thiophene (**304**); and 3-methylphenanthro[4,5-*bcd*]thiophene (**305**) respectively. The yield of **302, 303, 304** and **305** from the aldehyde precursors were 41-47%.

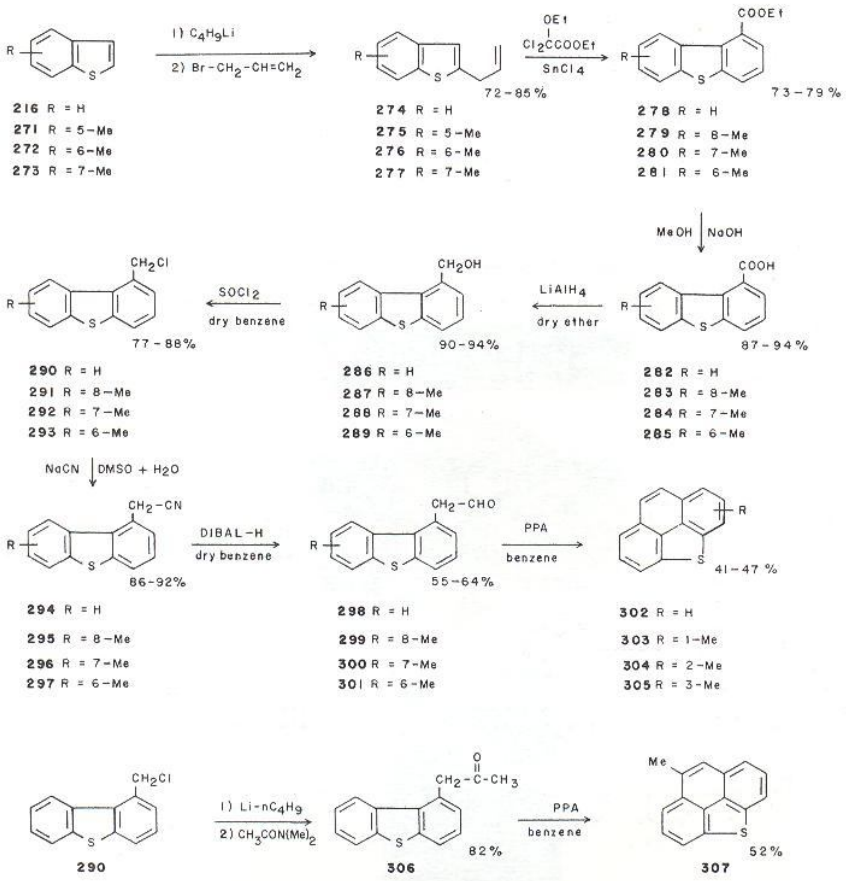

1-Chloromethyldibenzothiophene (**290**) was lithiated (*n*-butyllithium) and then treated with DMF to give the ketone **306** (82% yield) which was cyclized (PPA) into 8-methylphenanthro[4,5-*bcd*]thiophene (**307**) in 52% yield.

Dimethyldibenzothiophenes [50].

The synthesis of all sixteen dimethyldibenzothiophenes has been accomplished by unequivocal routes.

2-Bromo-4-methylcyclohexanone (**308**) when treated with *o*-methyl- (**173**), *p*-methyl- (**174**) or *m*-methylbenzenethiol (**175**) gave the sulfides **309, 310** or **311**, respectively (~80% yield). Upon cyclization (PPA) **309** gave the 3,6-dimethyl isomer **312; 310** gave the 3,8-dimethyl isomer **313**, and **311** gave a mixture of the 3,7- **314** and 3,9-dimethyl **315** isomers (average yields, 65%). Selenium aromatization of **312** gave 3,6-dimethyldibenzothiophene (**316**); **313** gave 2,7-dimethyldibenzothiophene (**217**); **314** gave 3,7-dimethyldibenzothiophene (**318**); and **315** gave 1,7-dimethyldibenzothiophene (**319**). The yields averaged 65%.

4- (**320**), 5- (**271**), 6- (**272**) and 7-methylbenzo[*b*]thiophene (**273**) were lithiated (*n*-butyllithium), then allowed to react with allyl bromide. The 2-allyl isomers **321, 275, 276** and **277** were obtained (72-85% yields) which upon cyclization (ethyl dichloroethoxyacetate) gave the esters **322, 279, 280, 281** in 75-80% yields. The corresponding esters were hydrolyzed (87-94% yields) then reduced (LAH (90-94% yields) to alcohols **323, 287, 288, 289**. These alcohols were converted into the benzylic chlorides (thionyl chloride) (77-88% yields) and reductively dechlorinated (LAH) (80-94% yields) to give 1,9-dimethyldibenzothiophene (**324**); 1,8-dimethyldibenzothiophene (**325**), 1,7-dimethyldibenzothiophene (**319**) and 1,6-dimethyldibenzothiophene (**326**) respectively.

3-Methylcyclohexanone (**327**) gave a mixture of 2-bromo-5-methylcyclohexanone (**328**) and 2-bromo-3-methylcyclohexanone (**329**). When 4-methylbenzenethiol (**174**) was allowed to react with the mixture of **328** and **329** the sulfides **330** and **331** were obtained. They were cyclized (PPA) to a mixture of **332** and **333** which upon selenium aromatization gave the chromatographically separable 2,6-dimethyldibenzothiophene (**334**) (31% yield) and 2,8-dimethyldibenzothiophene (**335**) (34% yield). Reaction of

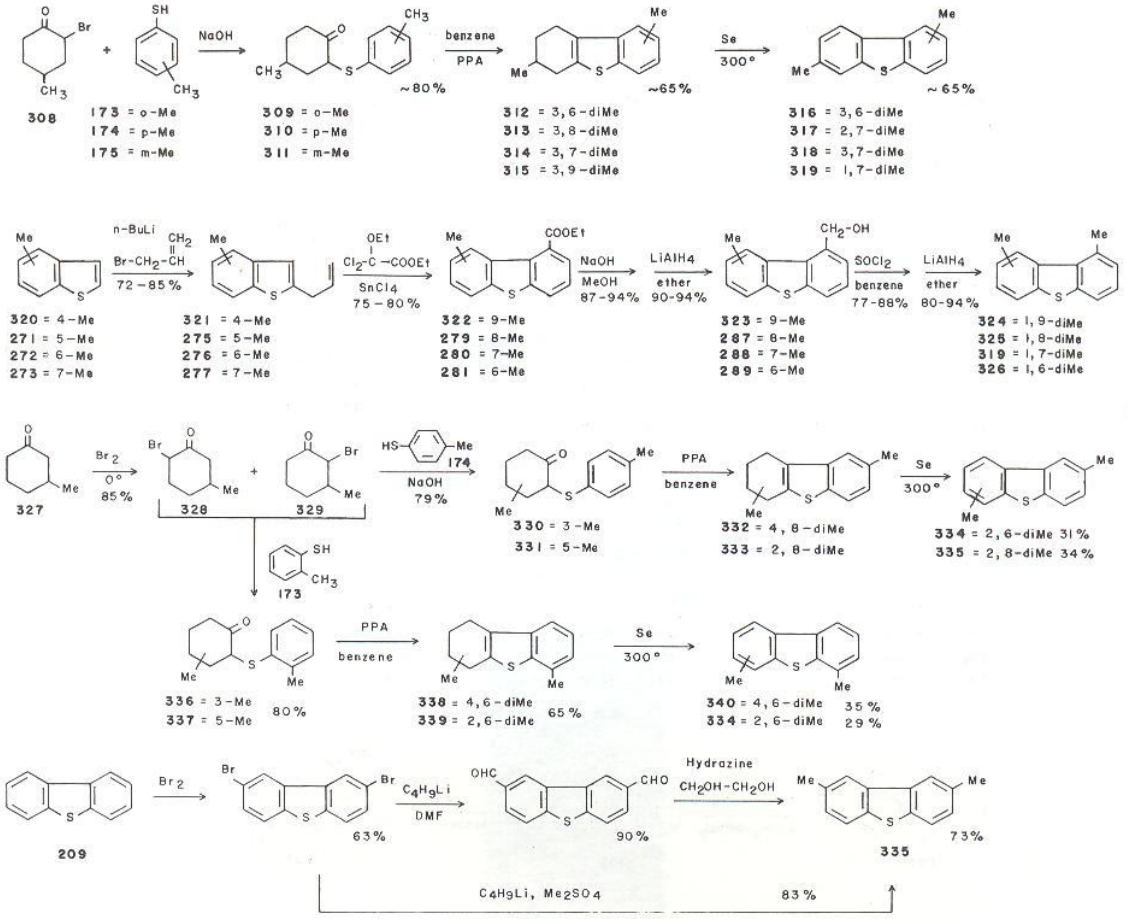

2-methylbenzenethiol (**173**) with the mixture of **328** and **329** gave a mixture of sulfides **336** and **337** (80%) which upon cyclization (PPA) produced a mixture of **338** and **339** in 65% yield. Selenium aromatization of **338** or **339** gave the chromatographically separable 4,6-dimethyldibenzothiophene (**340**) (35% yield) or 2,6-dimethyldibenzothiophene (**334**) (29%, yield) respectively.

Bromination of dibenzothiophene (**209**) gave 2,8-dibromodibenzothiophene (63%) which was lithiated (*n*-butyllithium) followed by DMF gave 2,8-dibenzothiophenedicarboxaldehyde (90% yield) which upon reduction (hydrazine in ethylene glycol) gave 2,8-dimethyldibenzothiophene (**335**) in 73% yield. Furthermore, lithiation of 2,8-dibromodibenzothiophene followed by treatment of the dilithio compound with dimethyl sulfate gave 3,8-dimethyldibenzothiophene (**335**) in 73% yield.

The following dimethylanilines 2,3- (**341**), 2,4- (**342**), 2,5- (**343**), 3,5 (**344**) or 3,4- (**345**) were diazotized giving the intermediate diazonium cations (**346, 347, 348, 349, 350**) which with potassium ethyl xanthate gave the following ethyl dimethylphenylxanthates: 2,3- (**351**), 2,4- (**352**), 2,5- (**353**) 3,5- (**354**) and 3,4- (**355**) in yields of 94-98% from the anilines. Reduction of the xanthates (LAH) gave the following dimethylbenzenethiols: 2,3- (**356**), 2,4- (**357**), 2,5- (**358**), 3,5- (**359**) and 3,4- (**360**) in 92-95% yields. Reaction of the anions of the dimethylbenzenethiols with 2-bromocyclohexanone (**361**) gave the following ketosulfides: 2,3- (**362**), 2,4- (**363**), 2,5- (**364**), 3,5- (**365**) or 3,4- (**366**) in 79-82% yields. Cyclization of the ketosulfides **362, 363, 364** or **365** gave the dimethyltetrahydrodibenzothiophenes **367, 368, 369** or **370**, respectively, in yields of 63-69%. However, PPA cyclization of 2-(3,4-dimethylphenylthio)cyclohexanone gave a mixture of two products, namely the 8,9- (**371**) and the 7,8-dimethyl-1,2,3,4-tetrahydrodibenzothiophene (**372**) which were not separated at this stage. Selenium dehydrogenation of **367, 368, 369** or **370** gave 3,4-dimethyldibenzothiophene (**373**), 2,4-dimethyldibenzothiophene (**374**), 1,4-dimethyldibenzothiophene (**375**) or 1,3-dimethyldibenzothiophene (**376**) in 70-74% yields. Selenium dehydrogenation of the mixture of **371** and **372** gave a chromatographically separable mix-

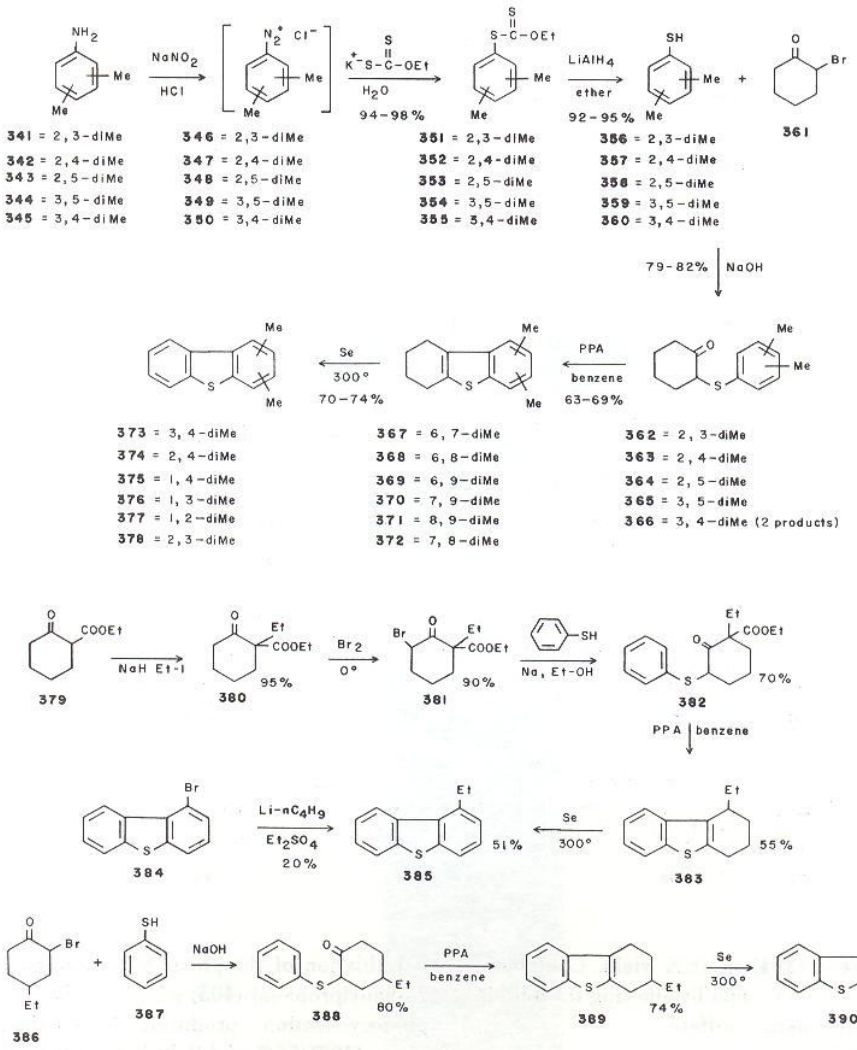

ture of 1,2-dimethyldibenzothiophene (**377**) and 2,3-dimethyldibenzothiophene (**378**). Thus this completes the synthesis of all sixteen isomers of the dimethyldibenzothiophenes.

Monoethyldibenzothiophenes [50].

Ethyl 2-oxocyclohexanecarboxylate (**379**) was ethylated (ethyl iodide, sodium hydride) to give ethyl 1-ethyl-2-oxocyclohexanecarboxylate (**380**) in 95% yield. Bromination of **380** gave ethyl 3-bromo-1-ethyl-2-oxocyclohexanecarboxylate (**381**) in 90% yield. Treatment of **381** with the anion of benzenethiol gave ethyl 1-ethyl-2-oxo-3-phenylthiocyclohexanecarboxylate (**382**) (70% yield). Cyclization (PPA) gave 1-ethyl-1,2,3,4-tetrahydrodibenzothiophene (**383**) (55% yield). Selenium dehydrogenation of **383** gave 1-ethyldibenzothiophene (**385**) (51% yield) which was also obtained by lithiation (*n*-butyllithium) of 1-bromodibenzothiophene (**384**) and allowing the 1-lithio derivative to react with diethyl sulfate (20% yield). In like manner 2-bromo-4-ethylcyclohexanone (**386**) was treated with the benzenethiol anion to give the ketosulfide **388** (80% yield) which with PPA, cyclized to give **389** (74% yield) which upon selenium dehydrogenation gave 3-ethyldibenzothiophene (**390**) (67% yield).

Bromination of dibenzothiophene (**209**) gave 2-bromodibenzothiophene (**210**) which upon lithiation (*n*-butyllithium) followed by treatment with *N,N*-dimethylacetamide gave 2-acetyldibenzothiophene (**391**) (77% yield) which upon reduction (hydrazine) gave 2-ethyldibenzothiophene (**392**) (70% yield). Compound **392** was also obtained from the lithio derivative of **210** by treatment with diethyl sulfate (82% yield). Lithiation of dibenzothiophene (**209**) (*n*-butyllithium) gave the 4-lithio derivative which upon treatment with *N,N*-dimethylacetamide gave 4-acetyldibenzothiophene (**393**) (80% yield) which with hydrazine gave

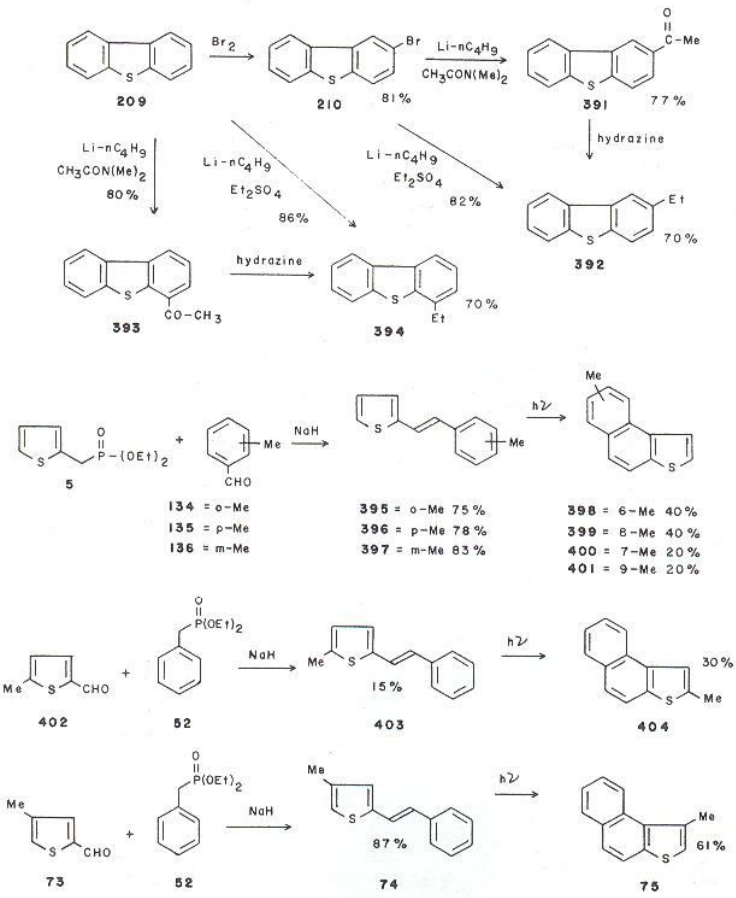

4-ethyldibenzothiophene (**394**) in 70% yield. Compound **394** was also obtained in 86% yield by allowing the 4-lithio derivative to react with diethyl sulfate.

Monomethylnaphtho[2,1-*b*]thiophenes [51].

Treatment of the *o*- (**134**), *p*- (**135**) or *m*-methylbenzaldehyde (**136**) with diethyl 2-thenylphosphonate (**5**) (Wadsworth-Emmons) gave *o*- (**395**) (75%), *p*- (**396**) (78%) or 2-(*m*-methylstyryl)thiophene (**397**) (83%). Photocyclization of **395** or **396** gave 6-methylnaphtho[2,1-*b*]thiophene (**398**) (40%) or 8-methylnaphtho[2,1-*b*]thiophene (**399**) (40%), respectively. Photocyclization of **397** gave a separable mixture of 7-methylnaphtho[2,1-*b*]thiophene (**400**) (20%) and 9-methylnaphtho[2,1-*b*]thiophene (**401**) (20% yield). 5-Methyl-2-thiophenecarboxaldehyde (**402**) when treated with diethyl benzylphosphonate (**51**) gave 5-methyl-2-styrylthiophene (**403**) in 15% yield which upon photocyclization gave 2-methylnaphtho[2,1-*b*]thiophene (**404**) in 30% yield. Likewise 4-methyl-2-thiophenecarboxaldehyde (**73**) and **52** gave 4-methyl-2-styrylthiophene (**74**) (87% yield) which upon photocyclization produced 1-methylnaphtho-[2,1-*b*]thiophene (**75**) in 81% yield.

Lithiation of thiophene (**29**) followed by reaction with 2-phenylpropanal (**405**) gave the alkene **407** which upon photocyclization produced 5-methylnaphtho[2,1-*b*]thiophene (**407**) (56% yield). In like manner the 2-lithio derivative of thiophene (**29**) with phenylacetone gave the alkene **409** (68% yield) which upon photocyclization gave 4-methylnaphtho[2,1-*b*]thiophene (**410**) in 38% yield.

Monomethylbenzo[*b*]naphtho[2,3-*d*]thiophenes [52].

Treatment of 3-bromo-2-decalone (**411**) in pyridine with *o*-methyl- (**173**) or *p*-methylbenzenethiol (**174**) gave the intermediate ketosulfides which upon cyclization (PPA) gave the 4-methyl- (**412**) or the 2-methyl derivative (**413**). The same reaction of **411** and *m*-methylbenzenethiol gave the intermediate ketosulfide which upon cyclization (PPA) gave a mixture of the 1-methyl **414** and the 3-methyl isomer **415**. Selenium dehydrogenation of **412**, **413**, **414** or **415** gave respectively, 4-methylbenzo[*b*]naphtho[2,3-*d*]-thiophene (**416**) (18% yield), 2-methylbenzo[*b*]naphtho-[2,3-*d*]thiophene (**417**) (12%), or 1-methylbenzo[*b*]naphtho[2,3-*d*]thiophene (**419**) (10% yield).

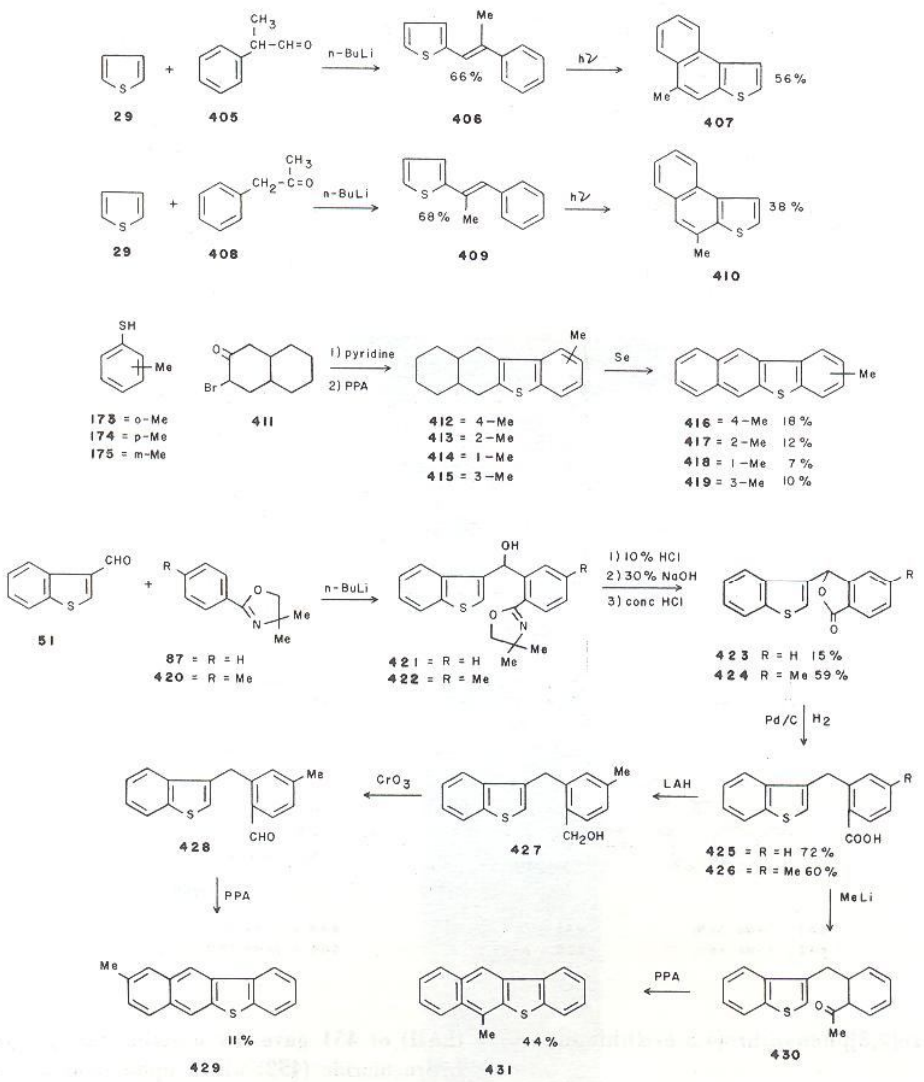

3-Benzo[*b*]thiophenecarboxaldehyde (**51**) was allowed to react with the lithio derivatives of either **87** or **420** and the alcohols **421** or **422** were obtained respectively. Acid cleavage of **421** or **422** followed by spontaneous lactonization gave **423** (15% yield) or **424** (59% yield) both of which were reduced (Pd/C) to give the carboxylic acids **425** (72% yield) or **426** (60% yield). When the carboxyl group of **426** was reduced (LAH), the alcohol **427** was obtained which upon oxidation (chromium trioxide-pyridine complex) was converted into the aldehyde **428**. Cyclization (PPA) of **428** gave 9-methylbenzo[*b*]naphtho[2,3-*d*]thiophene (**429**) (11% yield from **426**). The reaction of **425** with methyllithium gave the ketone **430** which was readily cyclized (PPA) into 6-methylbenzo[*b*]naphtho[2,3-*d*]thiophene (**431**) (44% yield from **425**).

The 2-lithio derivative of benzo[*b*]thiophene (**216**) upon reaction with *o*-methylbenzaldehyde (**134**) gave the alcohol **432** which when reduced (LAH, aluminum chloride) gave 2-(*o*-methylbenzyl)benzo[*b*]thiophene (**433**) in 66% yield. Cyclization of **433** (dichloromethyl methyl ether, stannic chloride) produced 7-methylbenzo[*b*]naphtho[2,3-*d*]thiophene (**434**) in 35% yield. Likewise lithiation of 3-bromobenzo[*b*]thiophene (**435**) followed by reaction of the 3-lithio derivative with *o*-methylbenzaldehyde (**134**) gave the alcohol **436** which upon reduction (LAH, aluminum chloride) produced 3-(*o*-methylbenzyl)benzo[*b*]thiophene (**437**) in 60% yield which upon cyclization (dichloromethyl methyl ether, stannic chloride) gave 10-methylbenzo[*b*]naphtho[2,3-*d*]thiophene (**438**) in 15% yield.

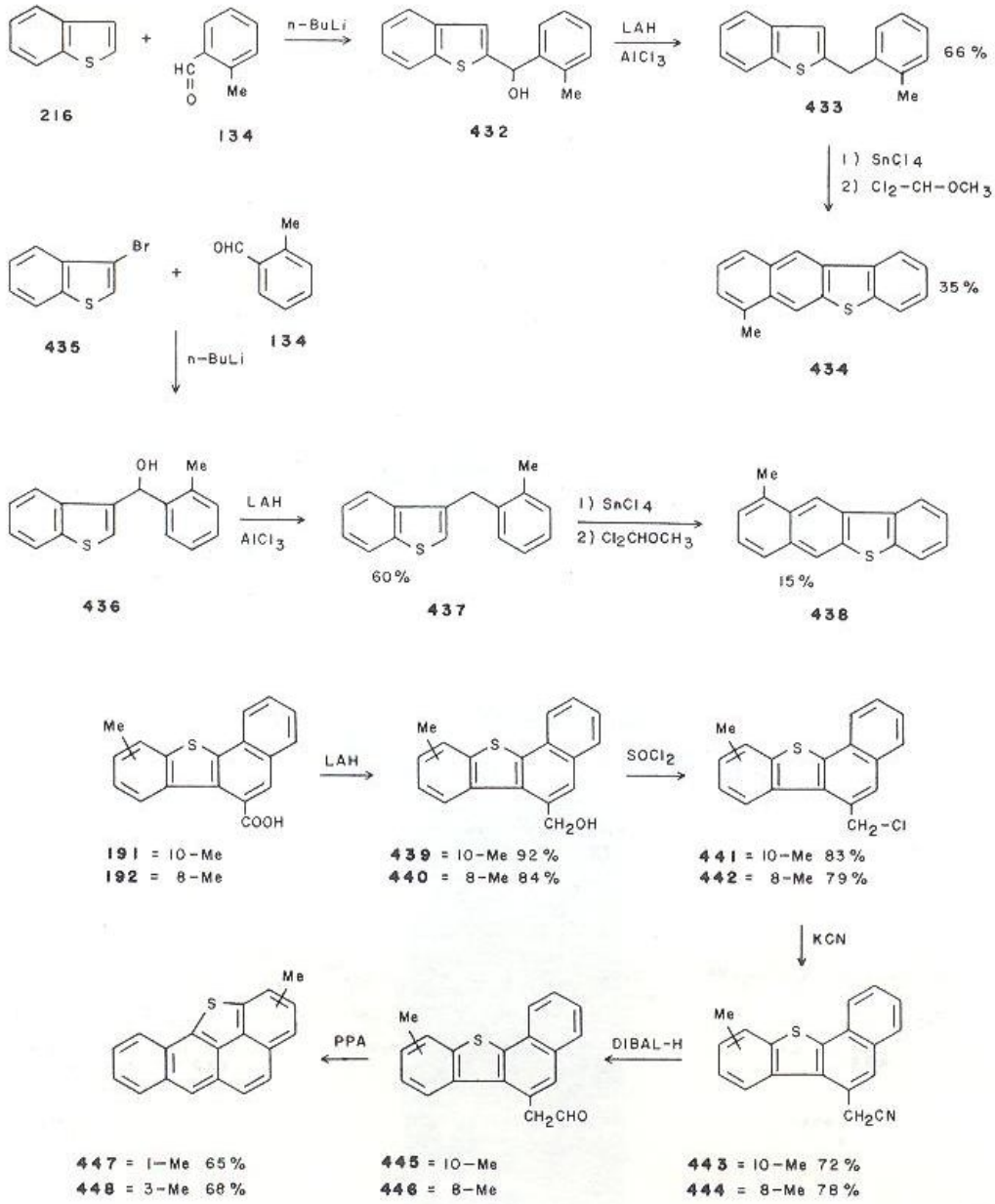

Monomethylbenzo[2,3]phenanthro[4,5-*bcd*]thiophenes [53].

10-Methyl- (**191**) or 8-methylbenzo[*b*]naphtho[2,1-*d*]thiophene-6-carboxylic acid (**192**) gave the corresponding alcohols **439** (92% yield) or **440** (84% yield). The alcohols **439** or **440** each were chlorinated (thionyl chloride) to give **441** (83% yield) or **442** (79% yield). The chloro compounds **441** and **442** each reacted with potassium cyanide to give the nitriles **443** (72% yield) and **444** (78% yield). Nitriles **443** or **444** with DIBAL-H gave the aldehydes **445** or **446** which were individually cyclized (PPA) into 1-methylbenzo[2,3]phenanthro[4,5-*bcd*]thiophene (**447**) (65% yield) or 3-methylbenzo[2,3]phenanthro[4,5-*bcd*]thiophene (**448**) in 68% yield.

Condensation of benzaldehyde (**54**) with 3-cyanomethylbenzo[*b*]thiophene (**449**) gave the cyanoalkene **450** (92% yield) which when photocyclized gave 6-cyanobenzo[*b*]naphtho[2,1-*d*]thiophene (**451**) (90% yield). Reduction (LAH) of **451** gave the unstable amine, isolated as the hydrochloride (**452**) which upon treatment with sodium nitrite gave the alcohol **453** (68% yield). Conversion of **453** to the chloride **454** (81% yield) was accomplished by thionyl chloride. Compound **454** was lithiated (*n*-butyllithium) and the lithio derivative was allowed to react with *N,N*-dimethylacetamide to give the ketone **454** which was cyclized (PPA) into 4-methylbenzo[2,3]phenanthro[4,5-*bcd*]thiophene (**456**) in 67% yield.

Treatment of the nitrile **451** with methyllithium gave the ketone **457** (72% yield) which upon reduction (LAH) produced the alcohol **458** (85% yield). Chlorination of **458** (thionyl chloride) gave **459** (82% yield) which reacted with potassium cyanide to give the nitrile **460** (70% yield). Reaction of the nitrile **460** with DIBAL-H produced the aldehyde **461** which was cyclized (PPA) into 5-methylbenzo[2,3]phenanthro[4,5-*bcd*]thiophene (**462**) in 62% yield.

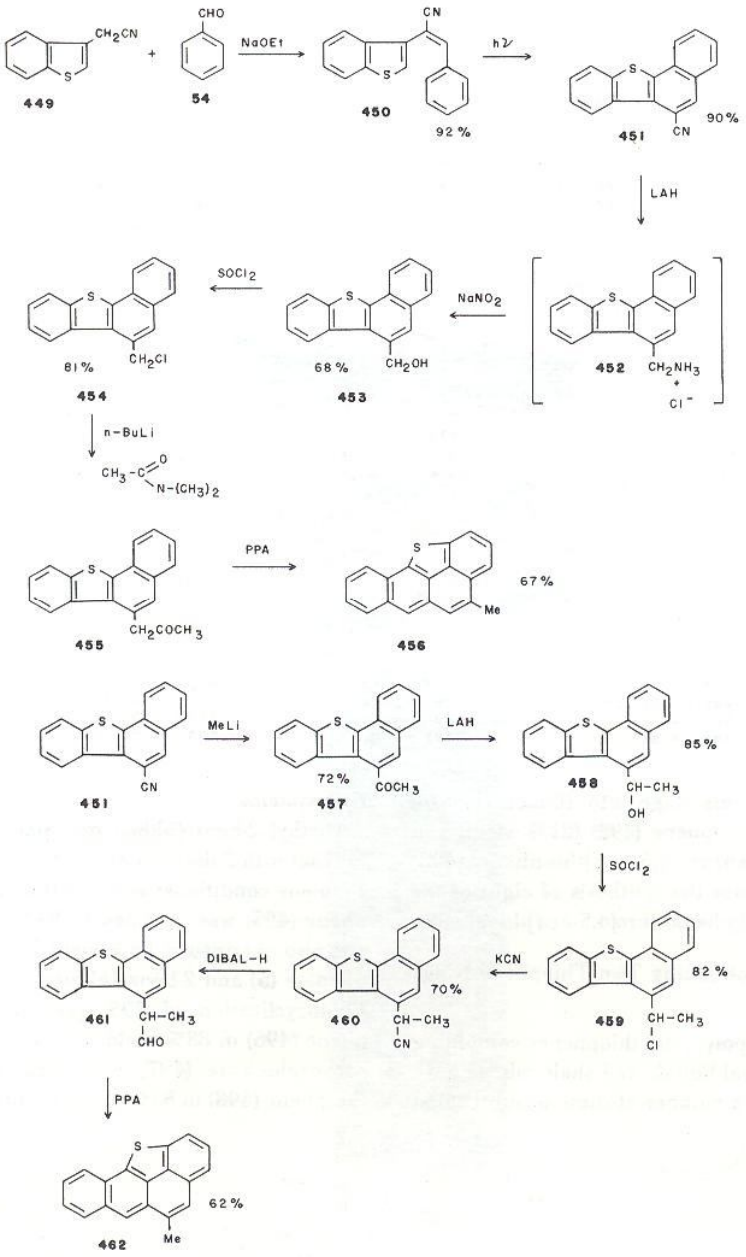

3-Cyanomethylbenzo[*b*]thiophene (**449**) when allowed to condense with *o*- (**134**), *p*- (**135**) or *m*-methylbenzaldehydes (**136**) produced the cyanoalkenes **463** (93% yield), **464** (90% yield), or **465** (94% yield). Photocyclization of **463** or **464** gave the nitriles **466** (71%) or **467** (74%) while photocyclization of **465** gave a mixture of **468** and **469** which was not separated. Reduction (LAH) of the nitriles **466**, **467** or **468** + **469** followed by acidification gave the amine hydrochlorides **470**, **471** or **472** + **473** which upon treatment with sodium nitrite and hydrochloric acid gave the alcohols **474** (69% yield), **475** (62% yield) or **476** + **477** (74% yield) which with thionyl chloride gave the corresponding chlorides **478** (82% yield), **479** (76% yield) or **480** + **481** (81% yield). Reaction of **478**, **479** or **480** + **481** with potassium cyanide gave the nitriles **482** (78% yield), **483** (62% yield) and **484** + **485** (78% yield) respectively. Reaction of **482**, **483** or **484** + **485** with DIBAL-H gave the aldehydes **486**, **487** or **488** + **489**. Cyclization of **486** or **487** with PPA produced 7-methylbenzo[2,3]phenanthro[4,5-*bcd*]thiophene (**490**) (65% yield) and 9-methylbenzo[2,3]phenanthro[4,5-*bcd*]thiophene (**491**) (62% yield) respectively. The mixture of **488** + **489** was cyclized

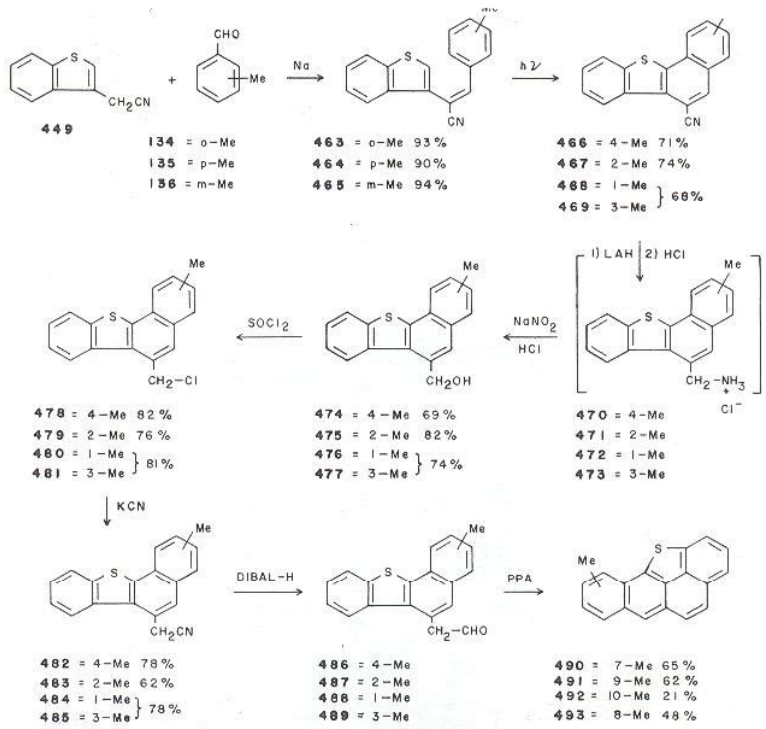

(PPA) and separated at this stage into 10-methylbenzo-[2,3]phenanthro[4,5-*bcd*]thiophene (**492**) (21% yield) and 8-methylbenzo[2,3]phenanthro[4,5-*bcd*]thiophene (**493**) (43% yield). This completes the synthesis of eight of the ten monomethylbenzo[2,3]phenanthro[4,5-*bcd*]thiophenes.

Polycyclic Thiophenes Containing Two Thiophene Rings [54].

In order to search for polycyclic thiophenes containing two thiophene rings in coal liquids and shale oils we have initiated the synthesis of a number of these unsubstituted ring systems.

Diethyl 2-benzo[*b*]thenylphosphonate (**137**) was allowed to react with 2-thiophenecarboxaldehyde (**494**) (Wadsworth-Emmons conditions) and 2-(2-thienylethenyl)benzo[*b*]thiophene (**495**) was obtained in 83% yield. The alkene **495** was also obtained in 86% yield from diethyl 2-thenylphosphonate (**5**) and 2-benzo[*b*]thiophenecarboxaldehyde (**97**). Photocyclization of **495** gave thieno[3,2-*a*]dibenzothiophene (**496**) in 88% yield. Likewise **137** and 3-thiophenecarboxaldehyde (**497**) gave 2-(3-thienylethenyl)benzo[*b*]-thiophene (**498**) in 83% yield. Compound **498** was also ob-

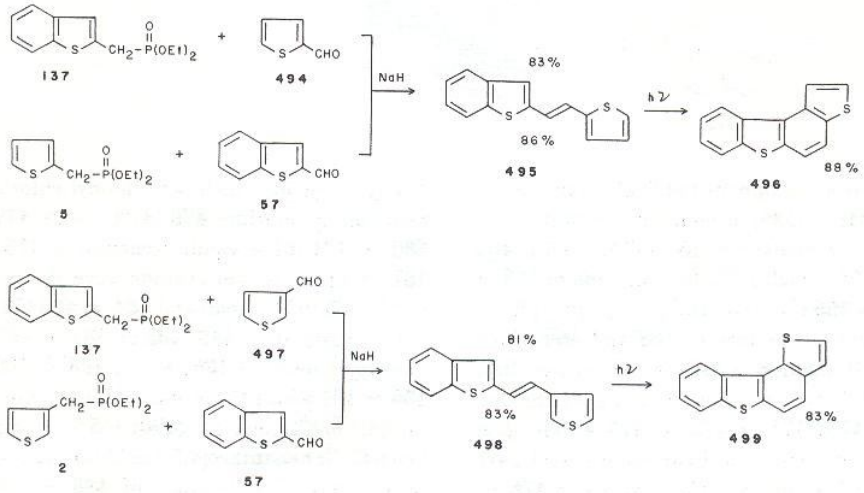

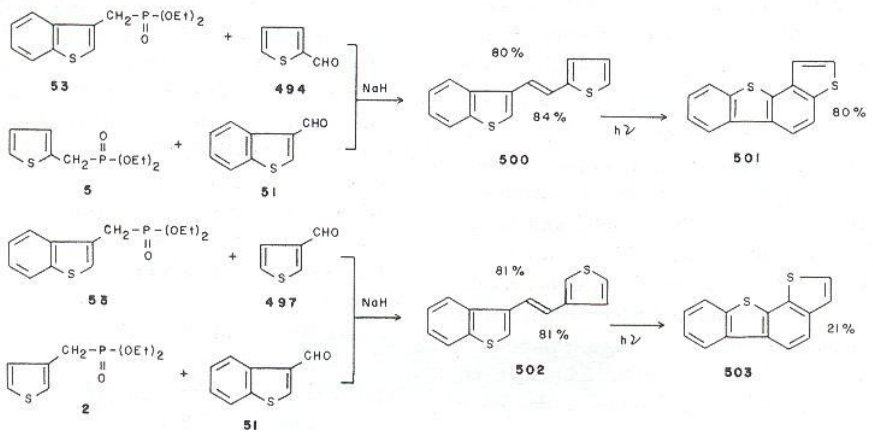

tained from **2** and **57** in 83% yield. Photocyclization of **498** produced thieno[2,3-*a*]dibenzothiophene (**499**) in 83% yield.

3-(2-Thienylethenyl)benzo[*b*]thiophene (**500**) was obtained in 80% yield from **53** and **494** and also in 84% yield from **5** and **51** both sequences *via* the Wadsworth-Emmons reaction. Photocyclization of **500** gave thieno[2,3-*c*]dibenzothiophene (**501**) in 80% yield. Likewise 3-(3-thienylethenyl)benzo[*b*]thiophene (**502**) was prepared from **53** and **497** and also from **2** and **51** both in 81% yield (Wadsworth-Emmons reaction). Photocyclization of **502** gave thieno[3,2-*c*]dibenzothiophene (**503**) in 21% yield.

Pentacyclic Thiophenes with Two Thiophene Rings [54].

2-Benzo[*b*]thiophenecarboxaldehyde (**57**) and diethyl 2-benzo[*b*]thenylphosphonate (**137**) (Wadsworth-Emmons conditions) gave 1,2-bis(2-benzo[*b*]thienyl)ethene (**504**) in 81% yield which upon cyclization gave benzo[1,2-*b*:4,3-*b*']-bisbenzo[*b*]thiophene (**505**) in 85% yield. 2-Benzo[*b*]thiophenecarboxaldehyde (**57**) and diethyl 3-benzo[*b*]thenylphosphonate (**53**) (Wadsworth-Emmons) gave 1-(2'-benzo[*b*]thienyl)-2-(3'-benzo[*b*]thienyl)ethene (**506**) (80% yield) which upon photocyclization yielded benzo[1,2-*b*:3,4-*b*']-bisbenzo[*b*]thiophene (**507**) in 84% yield. Likewise **51** and **53** gave 1,2-bis(3,3'-benzo[*b*]thienyl)ethene (**508**) (83% yield) which when photocyclized gave benzo[2,1-*b*:3,4-*b*']-bisbenzo[*b*]thiophene (**509**) in 28% yield.

Six pentacyclic thiophene ring systems containing two thiophene rings with one thiophene ring terminal have been prepared.

4-Dibenzothiophenecarboxaldehyde (**214**) was allowed to react with diethyl 2-thenylphosphonate (**5**) under Wadsworth-Emmons conditions and 1-(4-dibenzothienyl)-2-(2-thienyl)ethene (**510**) (79% yield) was obtained which upon photocyclization gave benzo[*b*]thieno[4,5-*c*]dibenzothiophene (**511**) in 75% yield. Likewise **214** and diethyl 3-then-

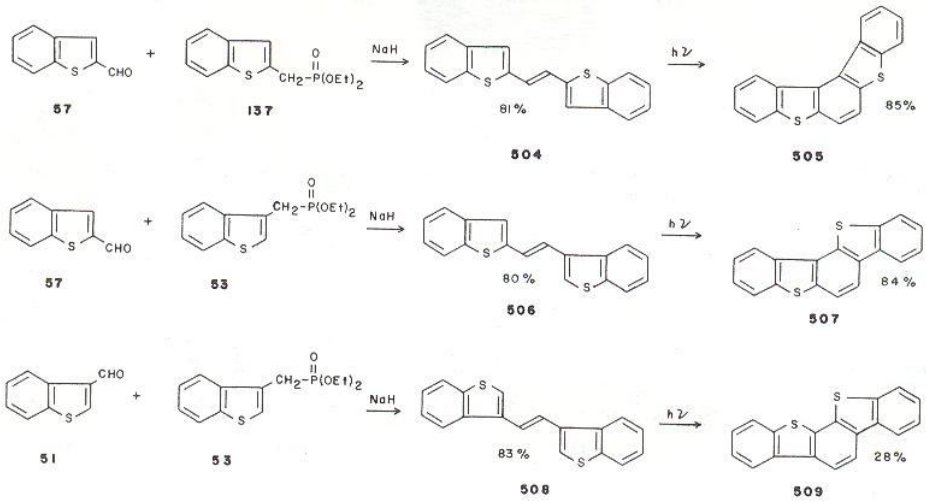

ylphosphonate (**2**) gave 1-(4-dibenzothienyl)-2-(3-thienyl)-ethene (**512**) (76% yield) which upon photocyclization gave benzo[*b*]thieno[7,6-*c*]dibenzothiophene (**513**) in 62% yield. The Wadsworth-Emmons reaction of 2-dibenzothiophenecarboxaldehyde (**211**) and **5** produced 2-(2-thienylethenyl)dibenzothiophene (**514**) which upon photocyclization gave a separable mixture consisting of benzo[*b*]thieno[4,5-*a*]dibenzothiophene (**515**) (65% yield) and benzo[*b*]thieno[5,4-*b*]dibenzothiophene (**516**) (20% yield). In like manner from **211** and **2**, 2-(3-thienylethenyl)dibenzothiophene (**517**) (68% yield) was obtained which when photocyclized gave a separable mixture of two components namely, benzo[*b*]thieno[7,6-*a*]dibenzothiophene (**518**) (57% yield) and benzo[*b*]thieno[6,7-*b*]dibenzothiophene (**519**) (19% yield).

Hexacyclic Thiophenes With Two Thiophene Rings [55].

The synthesis of seven hexacyclic thiophenes containing two thiophene rings, both internal, is described below.

Wadsworth-Emmons reaction of 2-dibenzothiophenecarboxaldehyde (**211**) with diethyl 2-benzo[*b*]thenylphosphonate (**137**) produced 1-(2-benzo[*b*]thienyl)-2-(2-dibenzothienyl)ethene (**520**) (69% yield) which upon photocyclization produced a separable mixture containing, namely, naphtho[2,1-*b*:7,6-*b*']bisbenzo[*b*]thiophene (**521**) (16% yield) and naphtho[2,1-*b*:7,8-*b*']bisbenzo[*b*]thiophene (**522**) (42% yield). Likewise **211** and diethyl 3-benzo[*b*]thenylphosphonate (**53**) gave 1-(3-benzo[*b*]thienyl)-2-(2-dibenzothienyl)ethene (**523**) (82% yield) which upon photocyclization produced a separable mixture containing, namely, naphtho[1,2-*b*:7,8-*b*']bisbenzo[*b*]thiophene (**524**) (23% yield) and naphtho[1,2-*b*:7,8-*b*']bisbenzo[*b*]thiophene (**525**) (42% yield).

1-Dibenzothiophenecarboxaldehyde (**526**) and diethyl

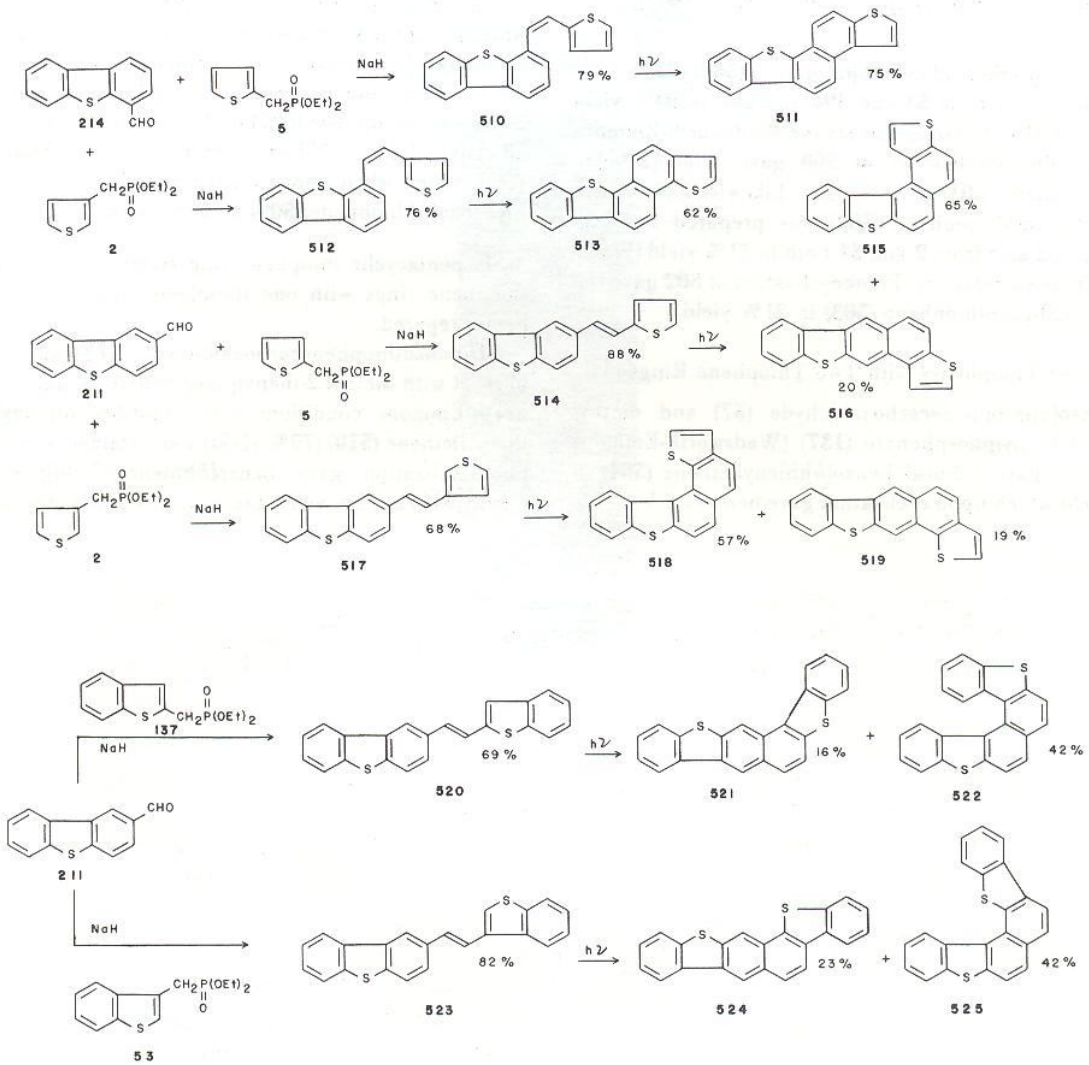

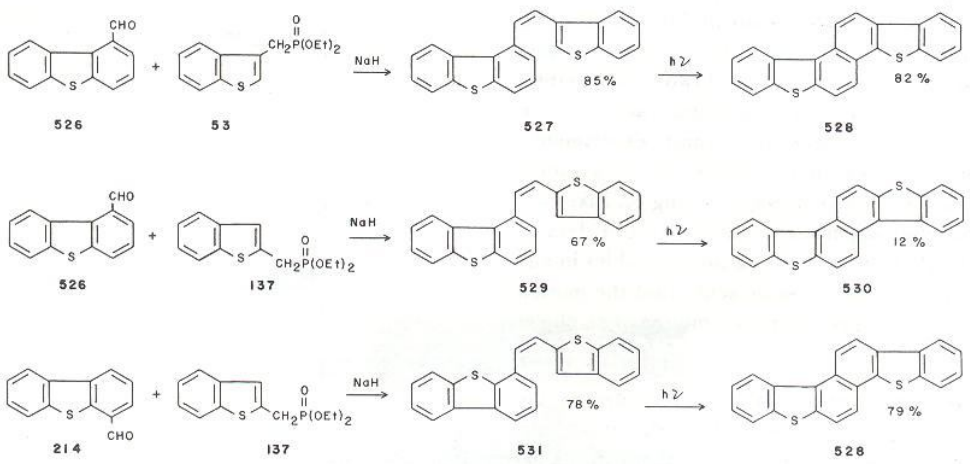

3-benzo[*b*]thenylphosphonate (**53**) produced 1-(3-benzo[*b*]-thienyl)-2-(1-dibenzothienyl)ethene (**527**) (85% yield) which upon photocyclization gave naphtho[1,2-*b*:6,5-*b'*]-bisbenzo[*b*]thiophene (**528**) in 82% yield. Likewise diethyl 2-benzo[*b*]thenylphosphonate (**137**) and **526** produced 1-(2-benzo[*b*]thienyl)-2-(1-dibenzothienyl)ethene (**529**) (67% yield) which gave upon photocyclization naphtho-[2,1-*b*:6,5-*b'*]bisbenzo[*b*]thiophene (**530**) in 12% yield. Furthermore **137** and 4-dibenzothiophenecarboxaldehyde (**214**) produced 1-(2-benzo[*b*]thienyl)-2-(4-dibenzothienyl)-ethene (**531**) (78% yield) which photocyclized into naphtho[1,2-*b*:6,5-*b'*]bisbenzo[*b*]thiophene (**528**) (79% yield).

Two-Dimensional NMR Spectroscopy. Application to the Total Assignment of the Proton and Carbon NMR Spectra of Polynuclear Aromatic Thiophenes

Introduction.

Nuclear magnetic resonance (nmr) spectroscopy, since the nearly simultaneous initial reports of the technique by Bloch [56] and Purcell [57] in 1946, has become the mainstay tool of the chemist for structure elucidation. During the intervening years since the first description of the experiment, magnetic field strengths employed have continually risen and proton observation frequencies of 300-500 MHz are now relatively routine. Techniques of data acquisition have also changed, going from continuous wave (cw) observation to time domain data acquisition and Fourier transformation data processing as a result of the pioneering work of Ernst [58,59]. Despite the improvements, however, the basic experiment remained essentially constant - intensity information was displayed as a function of a single frequency. A very significant change was however suggested in 1971 which has made a significant difference in the nature and complexity of problems which may be probed by nmr spectroscopy. Specifically, Jeener [60] suggested a series of experiments in which an evolution period would be systematically incremented across the series, the entire data matrix then subjected to not one but rather two Fourier transformations providing intensity information as a function of two frequencies rather than a single frequency.

The type of experiment suggested by Jeener [60], although not experimentally implemented until 1976 by Ernst and co-workers [61] is now referred to as two-dimensional nmr spectroscopy after the two frequency domains which were built into the experiment. Basically, two-dimensional nmr spectroscopy contrives to present intensity as a function of two discrete frequency axes, the selection of the nature of the axes as a function of the needs of the investigator which define the specific pulse sequence to be employed. Two-dimensional experiments may be subgrouped into two basic types - autocorrelated two-dimensional experiments in which the spectrum is correlated with itself *via* some fundamental parameter *e.g.* scalar coupling (J); cross-correlated two-dimensional experiments in which there may be one frequency correlated with some other fundamental parameter *e.g.* the scalar coupling constant (J) or the chemical shift (δ) of some other nuclide (*e.g.* $^{1}H/^{13}C$). Detailed treatments of the various types of two-dimensional experiments utilized in the assignment of the ^{1}H and ^{13}C-nmr spectra of the polynuclear aromatic thiophene analogs which form the basis for this reviw are presented individually in the following sections. For now, however, it is sufficient that two frequency axes are correlated with one another *via* a variety of mechanisms which ultimately result in intensity responses as a function of the frequencies.

Fundamental Considerations and Conventions of Two-Dimensional NMR Spectroscopy.

Two-dimensional nmr spectra represent substantially more than just an alternative means of data display. Rather, these experiments utilized rather formidable data matrices which are acquired in terms of two time variables rather than as a function of a single time variable as in conventional or "one-dimensional" nmr experiments. Thinking in terms of two time variables is not a simple task and there is no convenient way of doing so. Likewise, two-dimensional nmr experiments do not record data in terms of two simultaneously running time variables in any single data acquisition in the same sense that the motion picture camera does not record the net motion of an object in a single frame.

Conventional nmr experimental data recorded in the time domain is thought of in terms of the data set $S(t_2)$. Although we do not normally stop to think about it, the acquisition period is really the second defined time interval in the experiment after the end of preparation. Normally, there is also an interval, t_1, of fixed duration which is inserted between when the transmitter is turned off by the spectrometer computer and when the receiver is gated on by the computer. Since this period is constant in every acquisition, it becomes essentially transparent and serves its purpose of allowing the transmitter signal to fall to zero. Processing of the conventional Fourier transform nmr data set converts the time domain data, $S(t_2)$ to the frequency domain, $S(F_2)$, resulting in the familiar display of intensity as a function of frequency.

Making use of the additional time interval, t_1, for useful purposes can also be accomplished. As an example, consider the spin-lattice (T_1) [62] relaxation time experiments, specifically, the inversion-recovery experiment. Here, the goal of the experiment is to measure the recovery of equilibrium magnetization along the z′-axis. Since there is no means of directly measuring magnetization along the z′-axis, some alternative means of sampling this component of magnetization is necessary. Beginning with a 180°_x inverting pulse, equilibrium magnetization is rotated from the z′-axis to the -z′-axis. Accoring to the Bloch equations, this condition allows the perturbed magnetization to return to equilibrium along the z′-axis with no x′ or y′ componet to the magnetization. Hence, the 180°_x pulse produces no net signal in the receiver of the nmr spectrometer and the magnetization can be thought of as evolving with time, returning to its equilibrium state with a characteristic relaxation time constant, T_1. If after a short period of time (relative to the relaxation time constant) we apply a second pulse to the non-equilibrium system, the rotation of the magnetization which is still along the -z′-axis will be continued as a function of the flip angle of the applied pulse. In the specific case of a 90°_x pulse, as shown in Figure 1, this will produce a net rotation of the magnetization of 270° where the resultant is the equilibrium magnetization less losses due to relaxation along the z′-axis. If the receiver is gated on coincidently with the completion of pulse application, a signal is generated which, when Fourier transformed in the usual sense, will have a negative intensity. By varying the length of the period during which magnetization can return to equilibrium - evolution - we can produce a series of spectra which provide us with a sampling of the z′-magnetization as a function of the duration of the evolution period. Such data sets may be conveniently denoted $S(t_1,t_2)$ and upon Fourier transform are converted to data sets of the form $S(t_1,F_2)$, the Fourier integral operating only with respect to t_2. Thus, intensity as a function of the frequency F_2 will be a function of the evolution period, t_1. Various means of mathematically evaluating this type of intensity *vs.* time pair are available and the net result is the computation of the spin-lattice relaxation time, T_1.

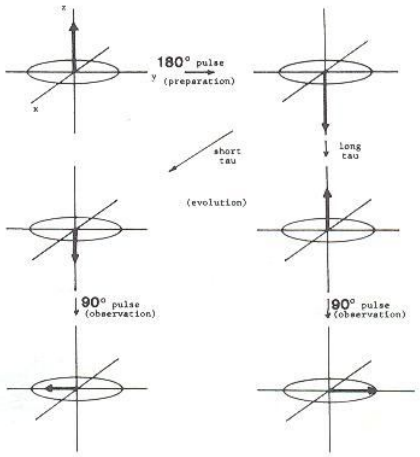

Figure 1. Spin vector diagram illustrating the effects of pulses and the duration of the evolution period in the inversion recovery spin-lattice (T_1) relaxation experiment.

By controlling the nature of the events which can occur during the evolution period, we can utilize the incrementation of the evolution period of the experiment to digitize an event which may be of experimental importance. By performing the incrementation of the evolution period in a systematic fashion, we can construct a data set which has information digitized in the t_1 time variable which is subsequently amenable to a second Fourier transformation. In the simplest sense, double Fourier transformation processing of a two-dimensional nmr data set consists of first collecting the data set $S(t_1,t_2)$ in which both time variables are appropriately digitized; subjecting the data set to the first Fourier transform which operates with respect to t_2 to give a data set which can be denoted by $S(t_1,F_2)$ followed by the second Fourier transformation which operates with respect to t_1 to give a data set of the form $S(F_1,F_2)$ in which

intensity is a function of two frequencies, F_1 and F_2. The mathemetical details of double Fourier transformation are beyond the scope of this review but have been thoroughly examined in the work of Ernst and co-workers [61] and that of Freeman and co-workers [63]. The relationship of the pulse sequenced events and the information digitized into the second frequency domain are considered in detail in the sections below devoted to the individual two-dimensional nmr experiments.

Autocorrelated *vs.* Cross-correlated Two-Dimensional Experiments.

Two-dimensional nmr experiments, in the broadest sense may be subdivided into two general categories; autocorrelated experiments in which the spectrum is correlated with itself *via* one of the fundamental spectral parameters, *e.g.* the scalar coupling constant, J, or cross-correlated experiments in which the chemical shift is correlated with either some fundamental spectral parameter such as the scalar coupling constant, J, or the chemical shift of another nuclide. In the case of the former, the utility of correlating the spectrum with itself *via* the scalar homonuclear coupling constant is quite clear, especially in the case of highly congested spectra where it would be difficult to conduct homonuclear decouplings with any degree of selectivity. Cross-correlated experiments in which the chemical shift is correlated with the scalar coupling constant, J, are also referred to as two-dimensional J-resolved or 2DJ spectra and here, the spectrum is sorted by chemical shift with the scalar coupling information segregated into the second frequency dimension thereby eliminating problems in the interpretation of the spectra which might otherwise arise from multiplet overlap. The second variant of the cross-correlated experiment in which the chemical shift of one nucleus is correlated with the chemical shift of a second is of obvious utility for spectral assignments. Both variants of the two-dimensional nmr experiment are extensively utilized in the spectral assignment of the polynuclear aromatic thiophene analogs which are discussed in detail below.

Processing Two-dimensional NMR Data Matrices.

Transformation of a two-dimensional nmr data set from the initial time domain, $S(t_1,t_2)$, to the final frequency domain (SF_1,F_2), is a relatively complex operation. In some of the newer Fourier transform spectrometers, the operation can be performed "in place" up to the limits of available computer memory and thus becomes essentially a transparent operation to the user. There are, however, some advantages inherent to having at least a fundamental understanding of the operation of the process.

Once the initial $S(t_1,t_2)$ data set has been obtained (the nature of the data contained in the matrix will be a function of the protocol employed in its' acquisition) we may embark on the processing of the data. As an example, we will utilize a data set obtained from a heteronuclear 2DJ experiment. Initially, our data will all be in time domain form and will have the appearance of the conventional free induction decay (FID). The first Fourier transformation operates on the doubly subscripted data set with respect to t_2 to provide us with intensity information as a function of frequency, F_2, in which the intensity of the response varies as a result of the incrementation of the evolution period, t_1, during the initial data collection. Thus, for an amplitude modulated 2DJ ^{13}C-nmr experiment (see below for a detailed explanation of this particular experiment) we would expect a series of traces in which a decoupled resonance has an amplitude or "intensity" which is modulated as a function of the duration of the evolution period (t_1). An example of such a series of stack plotted spectra is shown in Figure 2.

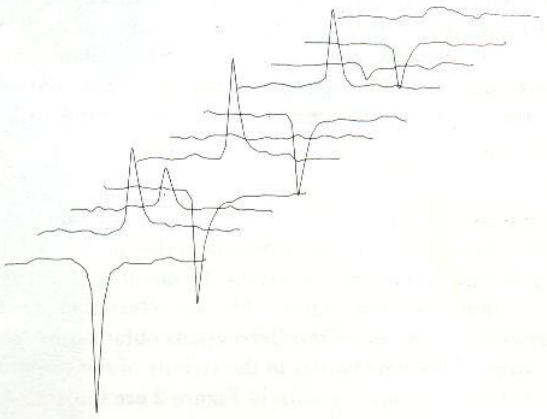

Figure 2. Stack plotted series of spectra showing the amplitude modulation of a ^{13}C resonance as a function of the duration of the evolution period.

Subsequent operations in the data processing scheme are from this point dependent upon the limitations of computer memory available to the investigator. It is useful, however, to consider the case where only limited memory is available, thus precluding the loading of the entire $S(t_1,F_2)$ data matrix into memory. Thus, it is necessary to convert the data matrix into some form which can be handled within the limitations of computer memory available. The process which accomplishes this objective is known as transposition and is shown schematically in Figure 3. Literally, transposition involves the exchange of rows and columns of the $S(t_1,F_2)$ data matrix to give a new matrix of the form $S(F_2,t_1)$. The appearance of the files contained in the newly generated $S(F_2,t_1)$ data matrix are analogous to those of the initial time domain $S(t_1,t_2)$ data. As a function of frequency, F_2, the individual files now

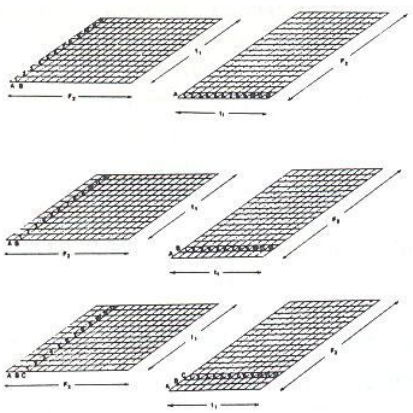

Figure 3. Schematic representation of the transposition process. Points A_1-A_{12} (typically would be points 1 through 2^n) which are contained in successive $S(t_1,F_2)$ files become the first file of the $S(F_2,t_1)$ data matrix created by the transposition algorithm. Treatment of successive points, B, C... *etc.* completes the generation of the $S(F_2,t_1)$ data matrix, providing a set of computer files which are now amenable to the second Fourier transform which operates with respect to t_1.

contain time domain information which is a function of the incremenations of the evolution period performed during the initial data accumulation. To maintain a clarity of discussion, these time domain files are referred to as interferrograms. The set of interferrograms obtained by transposition of the data matrix in the vicinity of the amplitude modulated resonance shown in Figure 2 are illustrated by Figure 4. In the specific case of the heteronuclear 2DJ experiment being employed as the basis for this discussion,

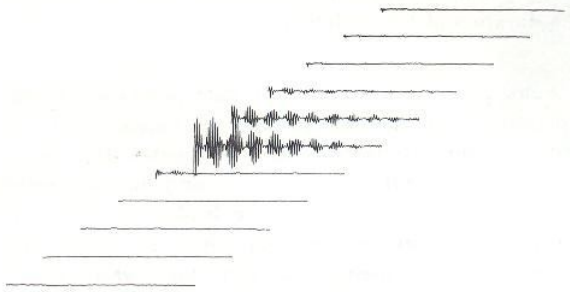

Figure 4. $S(F_2,t_1)$ interferrograms obtained by the transposition of the files (1 through 256) containing the amplitude modulated resonance shown in Figure 2.

the amplitude modulation of the resonance is a function of the heteronuclear scalar coupling constant and hence the points which constitute the resonance itself will provide intensity information while those not actually digitizing the peak will provide essentially no intensity information. Finally, Fourier transformation of the data files with respect to t_1 will provide us with the second frequency, F_1, which in this case will be coupling constant information. The second Fourier transformation of the interferrograms shown in Figure 4 produces a doublet of doublets (due to a large aromatic one bond coupling $^1J_{CH} \sim 165$ Hz and a considerably smaller three bond coupling $^3J_{CH} \sim 7$ Hz). These data are shown in Figure 5 as a "white-washed" stack plot

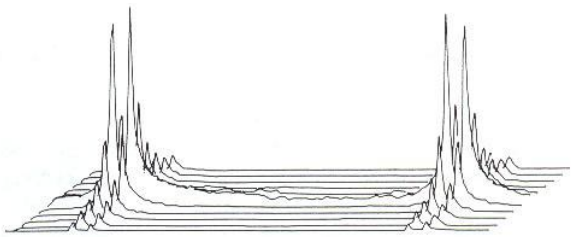

Figure 5. $S(F_2,F_1)$ result obtained by the Fourier transformation of the interferrograms ($S(F_2,F_1)$) illustrated in Figure 4. Data are presented as a white-washed stack plot showing a multiplet with a large one bond coupling, $^1J_{CH} \sim 165$ Hz and a smaller three bond coupling, $^3J_{CH} \sim 7$ Hz.

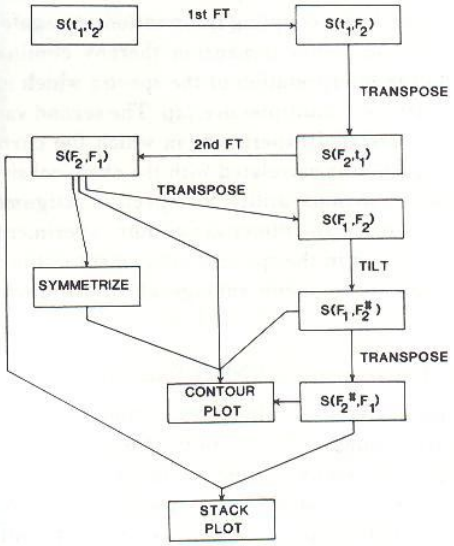

Figure 6. Flow chart illustrating the steps in the processing of a two-dimensional nmr data matrix, the steps to be utilized depending upon the experiment being performed. Not all of the steps shown will necessarily be utilized in the processing of any single experimental data set.

in which scalar coupling information is portrayed horizontally while chemical shift information is shown vertically in the plotted data. It should also be noted that the information contained in the individual traces is precisely analogous to the data which would be obtained from a heteronuclear selective excitation experiment [63-69].

Beyond the stage to which the data has been processed, $S(F_2,F_1)$, additional decisions are either possible or necessary depending upon the individual experiment being performed. A summary of the data processing and alternatives available beyond the $S(F_2,F_1)$ stage of data processing are shown in Figure 6. The utilization of the various alternative choices illustrated in the scheme will be discussed with the individual experiments discussed below.

White-Washed Stack Plot *vs.* Contour Plots.

Two-dimensional nmr spectra, since they are essentially representations of three dimensional surfaces, require somewhat more complicated presentation formats than does the conventional nmr spectrum. For the display of the entire two-dimensional nmr spectrum, basically two alternative modes of display are available: the white-washed stack plot and the contour plot. Simply, the white-washed stack plot is a means of display which utilizes the successive plotting of individual traces contained in the two-dimensional data matrix. To improve the display, an algorithm is employed which calculates when a trace in the foreground has a higher relative intensity than that of the succeeding traces. Whenever such a situation arises, the computer lifts the pen from the trace for an appropriate period of time so that no traces are overwritten as shown in Figure 5. While such displays are aesthetically pleasing, they are unfortunately rather time consuming to prepare and additionally, can become so complex that considerable information is obscured in the display.

A useful alternative to the white-washed stack plot is however available which does not take very long to prepare and which does provide excellent information access - the contour plot [70]. Contour plots are analogous to topographic maps, peaks or regions of intensity represented by a series of concentric lines or "contours". More intense spectral responses are represented by larger numbers of contour lines while weaker responses are represented by fewer. In any case, the advantage of such a display is that the user has a view of the data looking straight down on it from above.

The points illustrated above for the heteronuclear 2DJ experiment, which is the least complicated of the two-dimensional nmr experiments from a data display standpoint, clearly demonstrate the need for a usable and clear means of data presentation. From the standpoint of spectral complexity, heteronuclear 2DJ spectra are the least complicated to display which clearly demonstrates the need for the contour plot. With the exception of slices and projections, we shall utilize the contour plot exclusively in the presentation and interpretation of the nmr spectra of the polynuclear aromatic thiophene analogs which is discussed below.

Slices and Projections.

Contour plots, although extremely useful in that they provide visual access to all of the responses contained in the spectrum, suffer from a lack of familiarity - that is they do not in any sense resemble the conventional nmr spectrum that we are so accustomed to examining! This difficulty is circumvented, however, by flanking the contour plotted two-dimensional spectrum with projections [71] through the data matrix at angles of 0° and 90°. Projection of the two-dimensional $S(F_2,F_1)$ data matrix from the heteronuclear 2DJ spectrum at an angle of 0° recovers the "J-spectrum" while projection at an angle of 90° recovers the ^{1}H-decoupled ^{13}C-nmr spectrum. One useful additional projection angle is 45° when homonuclear 2DJ spectra are being examined. The utility of the 45° projection of homonuclear 2DJ spectra arises in that it produces what is effectively a broad-band proton decoupled proton spectrum in which each proton appears as a single response in the projection [72], this data having no analog in conventional spectroscopy.

Slices of two-dimensional nmr spectra are obtained simply by selecting the appropriate data matrix and then plotting the appropriate file of the matrix. The utility of spectral slices arises from the subsequent examination of line shapes, coupling constants and relative peak intensities. This utility is augmented in some cases by the fact that line widths in the second dimension are determined by T_2 and not by T_2^* [63] thereby providing somewhat better spectral resolution than can be obtained by conventional resolution enhancement techniques. For the most part, slices of two-dimensional nmr spectra will most frequently be plotted when coupling constant information or resonance intensity comparisons are to be made as for example in homo- and heteronuclear 2DJ spectra and in phase sensitive two-dimensional INADEQUATE spectra [73].

Two-Dimensional NMR Experiments - Analysis of the Pulse Sequences and the Operation of the Individual Experiments.

Heteronuclear 2DJ Spectroscopy.

Perhaps the simplest of the two-dimensional nmr experiments to understand is the heteronuclear 2DJ experiment. In the simplest case, this experiment can be conducted using only a single 90° pulse and a systematically incremented evolution (t_1) period superimposed with a decoupler gating operation. The "one-pulse 2DJ" experiment was

first described by Ernst and co-workers [74] and is shown schematically in Figure 7. As illustrated, the experiment

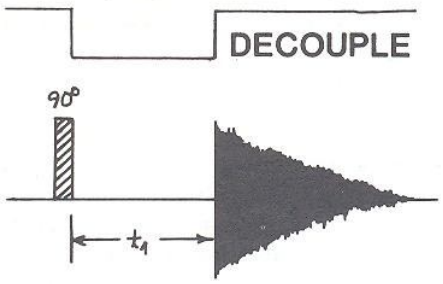

Figure 7. Pulse sequence for a "one pulse" amplitude modulated two-dimensional nmr experiment [74].

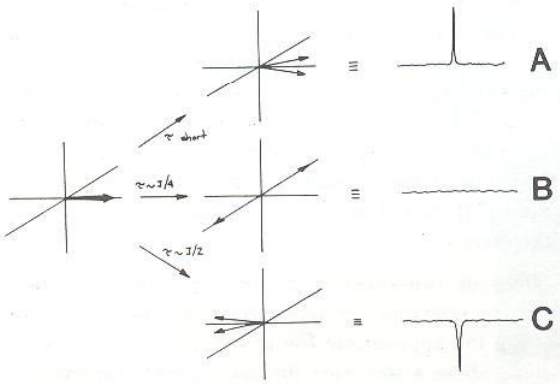

Figure 8. Spin vector diagram for the "one pulse" amplitude modulated experiment pulse sequence shown in Figure 7. Short evolution periods (sequence A) result in a slight defocusing during the evolution period and the resultant on decoupling during the acquisition period gives a resonance with a positive and nearly full intensity. Evolution periods of duration = J/4 give components of magnetization (assuming a simple doublet multiplet structure) which cancel when the decoupler is gated on (sequence B) producing no net signal in the receiver. Longer evolution periods of ~J/2 in duration (sequence C) result in a nearly refocused multiplet which produces a signal with negative and nearly full intensity on decoupling.

begins with the application of a 90° ^{13}C pulse with the decoupler gated off coincidently with the completion of pulse application. The evolution period is allowed to transpire with spins precessing under the influence of the heteronuclear spin couplings after which the decoupler is gated back on during the acquisition period.

While it may not be immediately clear why such an operation should have any utility, the explanation is reasonably straight-forward. When the decoupler is gated off, heteronuclear scalar coupling begins to defocus the precessing ^{13}C spins. This phenomenon can be illustrated even more simply if we consider the case of a ^{13}C spin which is exactly "on-resonance". Here, the 90° pulse rotates the equilibrium magnetization into the x'y' plane where the resonance would remain stationary since the offset, $\Delta\nu$, is zero. When the decoupler is gated off with the completion of pulse application, the resonance begins to defocus as a consequence of the heteronuclear spin couplings to which it is subject. This process is illustrated in Figure 8 for several arbitrarily selected evolution periods. The important point is that as a function of the evolution period duration, when the decoupler is gated back on, the resultant obtained on collapse varies from +1 (no evolution) to −1 + losses due to T_2 (at the interval J/2). When a number of such experiments are performed, the net result is an amplitude modulation of a decoupled ^{13}C resonance, the frequency of which is the heteronuclear spin-coupling characteristic of the resonance.

The problem associated with the experiment just described is that the second dimension must have the same spectral width as the decoupled spectrum which thus requires a high sampling frequency if any usable level of digitization is to be obtained. Clearly, this restraint would severely limit the utilization of the experiment. A relatively simple modification of this experiment does, however, provide an extremely usable variant, one based on eliminating chemical shift in the second dimension.

Chemical shift in the second dimension of the experiment just described may be simply eliminated by a slight modification of the decoupler gating and the insertion of a 180° refocusing pulse midway through the evolution period. The modified pulse sequence is shown in Figure 9

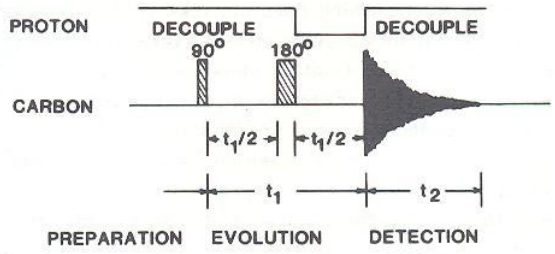

Figure 9. Amplitude modulated two-dimensional J-resolved pulse sequence. The experiment is derived from the "one pulse" amplitude modulated experiment whose pulse sequence is shown in Figure 7 and differs only in the insertion of a 180° refocusing pulse midway through the evolution period and by a slightly revised decoupler gating scheme which the decoupler is gated off only during the second half of the evolution period, $t_1/2$.

and differs from that shown in Fiugre 7 in that the decoupler is left on for the first half of the evolution period and is gated off only for the second half of the evolution period [75]. The important feature here is that as a function of the generation of a spin echo [76, 77], all chemical shift information is eliminated from the second dimension, multiplets centered about an axis $F_1 = 0$ Hz. The operation of the experiment is illustrated with the vector diagrams shown in Figure 10.

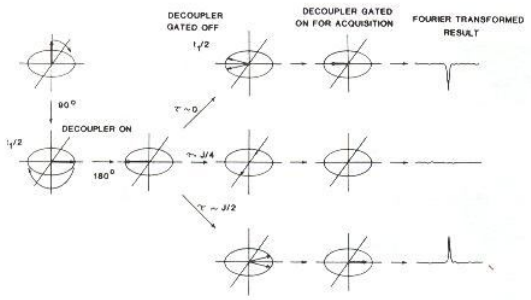

Figure 10. Spin vector diagram for the amplitude modulated two-dimensional J-resolved pulse sequence illustrated in Figure 9. Assuming the resonance used for illustration is exactly "on resonance" ($\Delta\nu = 0$ Hz), the resonance will remain stationary during the first half of the evolution period in each case. When the evolution period is relatively short, only slight defocusing will occur (sequence A) and the resultant obtained on decoupling during the acquisition period will be of negative and nearly full intensity (assuming a 180°_x pulse is employed as the refocusing pulse - signals of positive intensity may be obtained by using a 180°_y refocusing pulse). Evolution with a duration = J/4 gives components of magnetization (assuming a simple doublet) which will be colinear with the x′-axis, these subsequently canceling when the decoupler is gated back on (sequence B), thus producing no net signal. Evolution ~ J/2 in duration leads to a partial refocusing of the spin multiplet thus producing a resultant on decoupling with the opposite intensity of that obtained in sequence A.

Once again assuming the case of a resonance with $\Delta\nu = 0$, the resonance will remain stationary during the first half of the evolution peirod. When the decoupler is gated off, heteronuclear spin coupling will begin to defocus the components of the resonance which ultimately produces an amplitude modulation of the resonance as a function of the duration of the evolution period as in the previous experiment. However, since the decoupler is gated off after the application of the 180° pulse, all spins will refocus at time = t_1 thereby eliminating chemical shift effects from this phase of the experiment. The net result upon completion of data processing is a spectrum identical with that described above. It should also be noted that the coupling constants in this experiment are scaled to J/2 as a consequence of the duration ($t_1/2$) of the evolution period during which defocusing can occur [63], which may, in some circumstances, have a limiting effect on the resolution of coupling constants, especially if they are particularly small. In those cases where full coupling constants are desired, they may be obtained by a further modification of the experiment in which the decoupler is gated off coincidently with the completion of the application of the 90°_x pulse, provided that the 180° carbon pulse is coupled with a 180° proton pulse applied off the decoupler coils - this variant known as the "proton-flip" experiment [78].

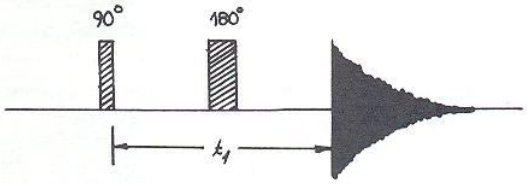

Figure 11. Homonuclear two-dimensional J-resolved pulse sequence. Since no decoupling is utilized during the experiment, the resonances ultimately recorded will be phase modulated rather than amplitude modulated. Consequences of this property of the experiment are described in the text.

With regard to data processing, the amplitude modulated or "proton-flip" heteronuclear 2DJ experiment is generally processed through the second Fourier transform to provide an $S(F_2,F_1)$ data matrix as shown in the flow chart illustrated in Figure 6. By plotting the contour plot and

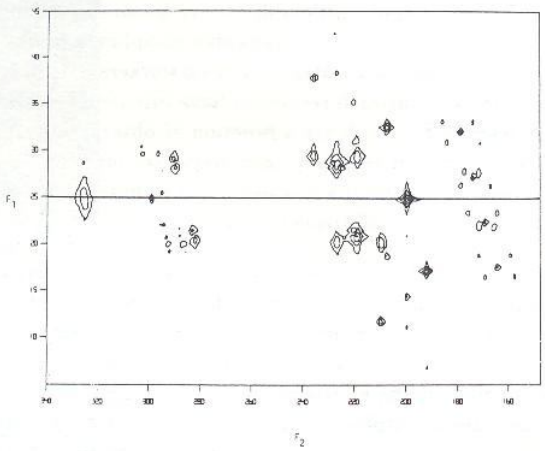

Figure 12. Contour plot of the homonuclear two-dimensional J-resolved nmr spectrum of benzo[2,3]phenanthro-[4,5-*bcd*]thiophene recorded at 200 MHz. Multiplets will be symmetric about the axis $F_1 = 0$ Hz (labeled 25 Hz in the plot). Total F_1 spectral width was ±25 Hz although only ±20 Hz is plotted in the figure shown.

appropriate projections directly or when necessary, the appropriate slices, all of the useful information contained in the spectrum can be extracted and no further manipulation of the data matrix is required.

Homonuclear 2DJ Spectroscopy.

Homonuclear variants of the 2DJ experiment described above are also based upon a spin echo pulse sequence to refocus chemical shift information in the second dimension. This pulse sequence is shown in Figure 11. Furthermore, since the decoupler cannot be employed in this sequence, the data is phase modulated rather than amplitude modulated, the net result of which is that individual multiplets are oriented at an angle of 45° in the second dimension relative to the F_2 axis as illustrated by the homonuclear 2DJ spectrum of benzo[2,3]phenanthro[4,5-*bcd*]-thiophene (**86**) shown in Figure 12.

Aside from the orientation of the individual spin multiplets in the final data matrix, there are also fundamental differences in the nature of the experiment as a consequence of the nature of the proton nmr spectrum as opposed to the carbon nmr spectrum. Specifically, proton nmr spectra are in many instances complicated by the effects of strong coupling whereas heteronuclearly coupled spectra are seldom subject to such effects [79-80]. The net result of such coupling phenomena is that the non-selective 180° refocusing pulse causes a mixing of the coherent magnetization associated with a given transition converting it into a family of magnetization components. These additional components of magnetization are sampled during the acquisition period and lead to additional responses at frequencies of the type $\frac{1}{2}(\nu_{rs} - \nu_{pq})$ which lie between the strongly coupled spins. Although such responses have long been considered to be an undesireable complication inherent to the experiment, Martin and co-workers [81] have recently shown that such responses have intensities (I) and frequencies in F_1 which are a function of observation frequency and that in addition, such responses may be used as a means of correlating coupled spins in highly congested, non-first order 2DJ spectra [82-83].

Processing of homonuclear 2DJ spectral data requires somewhat more consideration than does the heteronuclear version of the experiment. If slices are to be extracted from the two-dimensional data matrix, they clearly cannot be obtained from the matrix at the $S(F_2,F_1)$ stage of processing since the multiplets lie along a 45° axis and are thus not contained in any single file. As shown in the flow chart contained in Figure 6, the data matrix can be transposed a second time to produce an $S(F_1,F_2)$ matrix which can then be subjected to the "tilt" algorithm [84]. Tilt mathematically manipulates the data matrix, sliding files other than $F_1 = 0$ Hz, either left or right as appropriate to bring the components of the spin multiplet into a single file of the data matrix. At this stage, slices may be obtained from the tilted data matrix $S(F_1,F_2{}^*)$ by projection or alternatively, slices may be plotted by subjecting the matrix to a final transposition to give an $S(F_2{}^*,F_1)$ matrix which is now analogous to the $S(F_2,F_1)$ matrix of the amplitude modulated 2DJ experiment discussed above. For purposes of comparison, the tilted contour plot of benzo[2,3]phenanthro-[4,5-*bcd*]thiophene (**86**) is shown in Figure 13 (compare Figure 12).

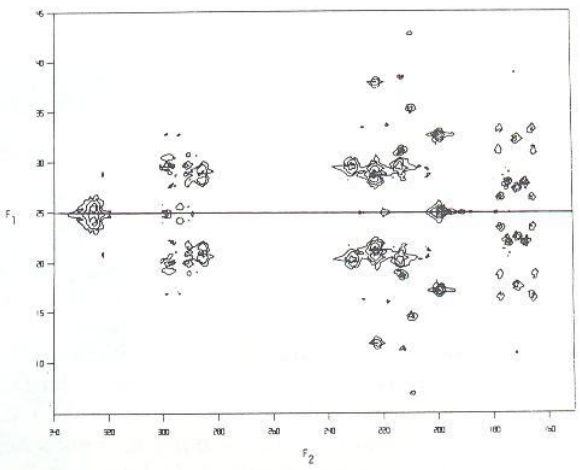

Figure 13. Contour plot of the homonuclear two-dimensional J-resolved nmr spectrum of benzo[2,3]phenanthro-[4,5-*bcd*]thiophene at 200 MHz after subjecting the data matrix to the "tilt" algorithm.

Heteronuclear Chemical Shift Correlation.

Two-dimensional heteronuclear chemical shift correlation experiments are another variant of the cross correlated experiment which, although considerably more complex than the 2DJ experiments, are extremely useful for purposes of structure elucidation or spectral assignment. Historically, numerous strategems for correlating proton and carbon chemical shifts have been employed. For example, proton chemical shifts of a molecule may be estimated by successive single frequency off-resonance decoupling (sford) experiments in which a series of spectra are obtained, each with a different proton decoupler setting [85]. Throughout this series of experiments, which can in principle be thought of as an $S(F_1,F_2)$ data set in which F_2 represents carbon chemical shifts and F_1 represents the proton decoupling frequency, by examining the changes in the heteronuclear scalar coupling it is possible to extrapolate the frequency of the directly attached proton(s) for every carbon - assuming of course that the spectrum is not too complex! Techniques of this type, although potentially useful, are both cumbersome and frequently ambiguous, particularly since they rely on the investigator's ability to

follow changes in the residually coupled components of the spin multiplets which may be an exceedingly difficult undertaking. Nonetheless, a useful point derives from the consideration of this now obviated experiment - proton and carbon chemical shifts can be correlated *via* the heteronuclear scalar coupling constant, J_{CH}.

Having established that heteronuclear chemical shift correlation may be obtained *via* the heteronuclear scalar coupling constant, it is next useful to examine the means of simultaneously correlating all coupled species in a two-dimensional nmr experiment. Ideally, we would like to obtain such a two-dimensional nmr spectrum with heteronuclear scalar coupling eliminated on both frequency axes - put another way, we would like the F_2 axis to represent the proton decoupled ^{13}C spectrum while the F_1 axis provides us with the proton spectrum showing its' characteristic

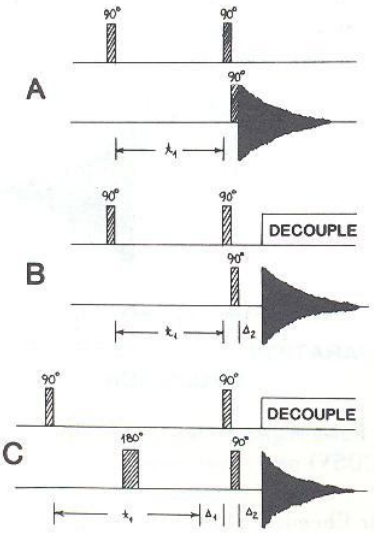

Figure 14. Pulse sequences for two-dimensional proton-carbon chemical shift correlation nmr spectroscopy: A) simplest pulse sequence which provides heteronuclear spin-coupling on both frequency axes - 90° proton pulses in this experiment are obtained by gating on the decoupler for a predetermined interval to produce the desired 90° pulse; B) modification of the pulse sequence to provide decoupling on the F_2 frequency axis - decoupling is achieved by inserting the fixed delay, Δ_2, following the 90° ^{13}C pulse which allows the components of magnetization to come back into focus thereby enabling broad band decoupling; C) modification of the pulse sequence to decouple on both the F_1 and F_2 frequency axis - the F_2 decoupling is identical to that employed in B) while decoupling of F_1 is obtained by placing a 180° refocusing pulse in the middle of the evolution period followed by a fixed delay, Δ_1, to allow for magnetization transfer which would otherwise be canceled by the 180° ^{13}C pulse.

homonuclear coupling information. While seemingly an insurmountable task, it is by no means impossible. It is useful, however to introduce features singly thus necessitating the three successively more complex pulse sequences shown in Figure 14a-c.

Beginning with the simplest of the pulse sequences, that shown in Figure 14a we first notice that pulses are to be applied to both the proton and carbon resonance frequencies. Since we will ultimately observe the ^{13}C signal, pulses applied to ^{13}C will be delivered *via* the transmitter in the usual fashion. Pulses applied to the protons of the sample will be applied *via* the decoupler coils contained in the probe which will ultimately also be used for broad-band proton decouplng in the later modifications of the pulse sequence.

The origins of the heteronuclear chemical shift correlation are to be found in the spin-population inversion experiments described some years ago by Pachler and Wessels [86] and by Sorensen and co-workers [87]. Basically, the experiment depends upon the application of a 180° pulse to the ^{13}C satellite frequencies in the proton spectrum followed by a 90° ^{13}C observation pulse. The features of this experiment are incorporated into the pulse sequence in Figure 14a almost directly. The first 90° ^{1}H pulse rotates the equilibrium magnetization into the xy-plane and each component of magnetization is labeled with its characteristic precession frequency during the evolution period (t_1) which follows. The second 90° ^{1}H pulse completes the application of the 180° net proton pulse which was applied in the spin-population inversion or transfer experiments. The transferred magnetization is then sampled by the 90° ^{13}C pulse. By successively incrementing the duration of the evolution period, all possible frequencies are sampled in the experiment and after the initial $S(t_1,F_2)$ data matrix is transposed and subjected to the second Fourier transform a two-dimensional data matrix results in which responses appear at the points of intersection of the proton and carbon resonance freuqencies. However, since there has been no decoupling applied at any point during the experiment, the spectrum projected to either frequency axis will be a doublet with the characteristic heteronuclear scalar coupling of the specie being investigated (assuming a simple AX system is being investigated for the sake of simplicity). The behavior of the ^{13}C coupled components of the proton magnetization up to the point of the application of the ^{13}C sampling pulse is shown in Figure 15. Reconsideration of the spin-population inversion experiment

quickly leads to the realization that ^{13}C transverse magnetization, when created by the 90° ^{13}C sampling pulse will consist of two anti-phase components of magnetization, these components leading to multiplets with one limb of positive intensity while the other is of equal but negative intensity as was demonstrated by Maudsley and Ernst [88].

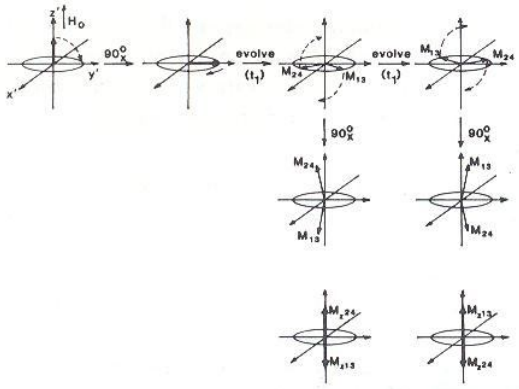

Figure 15. Spin diagrams to account for proton behavior during the evolution period in two-dimensional proton-carbon chemical shift correlation nmr spectra.

(Similar arguments can be derived for triplets and quartets which lead to responses with intensities of $-1, 0, +1$ and $-1, -1, +1, +1$ respectively.) From this argument, it should be clear that the decoupler cannot simply be switched on at the beginning of the evolution period since this would lead to the complete cancellation of the components of magnetization. This leads us to the second modification of the experiment shown by the pulse sequence in Figure 14b in which decoupling is introduced on the F_2 frequency axis.

Heteronuclear decoupling on the F_2 axis in the proton-carbon chemical shift correlation experiment can readily be inroduced by the insertion of a delay period immediately prior to the acquisition period. By allowing the duration of the delay period (Δ_2) to equal 0.3/J (this is a compromise value which is optimal for CH, CH_2 and CH_3 carbons) the antiphase components of transverse ^{13}C magnetization created by the 90° ^{13}C pulse are brought back into phase at the beginning of the evolution period. Gating the decoupler on in this sequence coincidently with the beginning of the acquisition period effectively decouples the ^{13}C resonance from the ^1H resonance, thus providing a decoupled ^{13}C spectrum on the F_2 axis. In the second dimension, however, heteronuclear scalar coupling is still present and the F_1 projection will still show a multiplet structure.

Completion of the objective, heteronuclearly decoupling both frequency axes, is now obtainable by the further modification of the pulse sequence as shown in Figure 14c. Here, midway through the evolution period a 180° carbon refocusing pulse is applied which effectively "backs out" the effects of heteronuclear coupling in what will ultimately be the F_1 dimension. Bodenhausen and Freeman in their initial approach to this problem realized that the midway position of the carbon refocusing pulse would preclude magnetization transfer and they thus used a pulse offset to $2t_1/3$ to provide a partial collapse of the heteronuclear coupling [89]. In a subsequent report, Freeman and Morris relocated the carbon refocusing pulse midway through the evolution period and added a second fixed duration delay, Δ_1, prior to the application of the second 90° proton pulse to allow magnetization transfer when the 90° proton pulse is applied [90].

The final step in the evolution of the heteronuclear chemical shift correlation pulse sequence does not alter the sequence itself but rather only the phases of the various events in the sequence. To provide the equivalent of quadrature phase detection (QPD) in both frequency domains, Bax and Morris [91] have proposed a phase cycled version of the experiment which was utilized in obtaining the spectra of the polycyclic aromatic thiophene analogs which are discussed below. As an example of the results obtained from the proton-carbon chemical shift correlation experiment, the contour plot obtained from the performance of this experiment on phenanthro[3,4-*b*]thiophene (**12**) is shown in Figure 16.

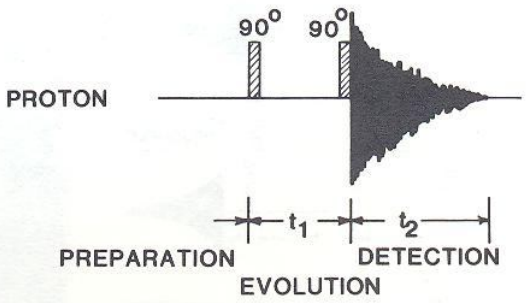

Figure 16. Pulse sequence for the two-dimensional autocorrelated (COSY) nmr experiment.

Homonuclear Chemical Shift Correlation.

The pulse sequence originally porposed by Jeener at the Ampere International Summer School in 1971 forms the basis for the contemporary homonuclear chemical shift correlation experiment which we now know as the COSY experiment. The pulse sequence, as shown in Figure 17, utilizes a pair of 90° ^1H pulses which are separated by the evolution period, t_1. As in the other experiments which were discussed above, the first 90° pulse creates transverse magnetization in the xy-plane. Each of the characteristic components of transverse magnetization created by the experiment is labeled with its' characteristic precession frequency during the evolution period. The second 90° pulse (this pulse may also be applied as a 45° pulse in some instances) transfers magnetization between the various transitions of the coupled spin system as described by Aue, Bartholdi and Ernst [61].

The benefits derived from the homonuclear chemical shift correlation experiment become obvious when the lo-

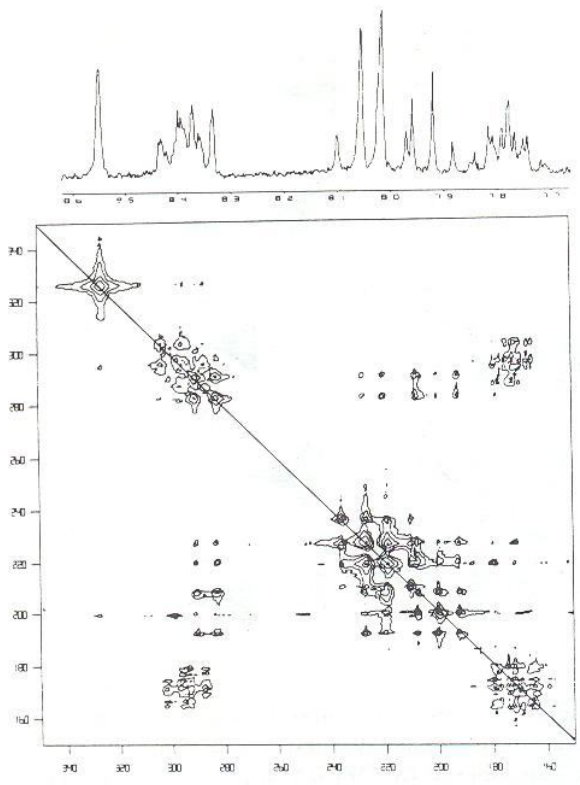

Figure 17. Contour plot of the COSY spectrum obtained for benzo[2,3]phenanthro[4,5-*bcd*]thiophene in d_6-dimethylsulfoxide at 50°. The normal spectrum resides along the diagonal and resonances which are spin coupled to one another give rise to off-diagonal responses.

cation of the information contained in the two-dimensional data matrix is considered. The exchange of magnetization between transitions of one nucleus of a coupled pair produces responses which are on or near the diagonal $F_1 = F_2$. Ultimately, the $F_1 = F_2$ diagonal contains an exact replicate of the conventional homonuclearly coupled nmr spectrum. Alternatively, transfer of magnetization between transitions for two different coupled nuclear spins leads to the formation of off-diagonal responses which serve to correlate the coupled spins in a fashion analogous to the correlation provided by homonuclearly decoupling one spin from the other in a conventional decoupling experiment. Contemporary COSY pulse sequences, from the work of Bax, Freeman and Morris [92], employ phase cycling of the second pulse in the sequence to provide the equivalent of quadrature phase detection in both frequency domains. To illustrate the presentation of information in the COSY spectrum, the contour plot obtained for benzo[2,3]phenanthro[4,5-*bcd*]thiophene (**86**) is shown in Figure 18.

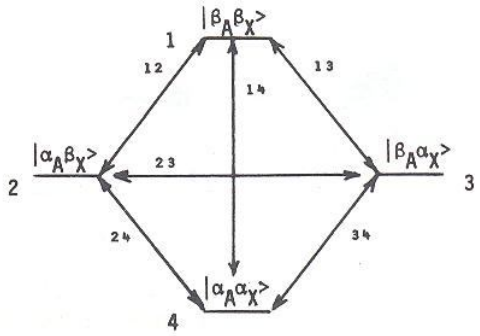

Figure 18. Energy level diagram for a simple AX spin system. The normally allowed single quantum transitions connect adjacent energy levels. The zero quantum transition connects levels 2 and 3 while the double quantum transition connects levels 1 and 4.

Two-Dimensional ^{13}C-^{13}C Double Quantum Coherence.

Double quantum coherence two-dimensional experiments are at the time of the writing of this manuscript the most complex of the two-dimensional nmr experiment yet described! In the variant of the experiment described below, the objective is to select from the molecular ensemble only those molecules which contain two ^{13}C-nuclides adjacent to one another. Such pairings may constitute either AB or AX spin systems and although we shall focus our attention only on the latter experiments have also been described which allow the exploitation of the former pairing as well [93].

Since ^{13}C is a relatively rare spin with a natural abundance of only 1.1%, the pool of molecules which contain two adjacent ^{13}C-nuclides represents only about 1 molecule in 10,000! Thus, the experiment must be designed in such a way that only the signal from the doubley labeled molecule is detected while the signal from the singly labeled molecules is rejected to avoid an insurmountable dynamic range problem. After a brief consideration of double quantum coherence, the original double quantum coherence pulse sequence and several recent modifications will be described.

Double quantum coherence is a concept alien to even those who may have some acquaintence with the concepts of two-dimensional nmr spectroscopy since we are generally accustomed to considering only single quantum coherence having been taught in our early training that double quantum transitions are forbidden. Indeed, a 90° pulse in the conventional nmr or two-dimensional nmr experiment produces only single quantum coherence which is the quantity actually observed in the nmr experiment. In the case of the simple AX spin system whose energy level diagram is shown in Figure 19, single quantum coherences

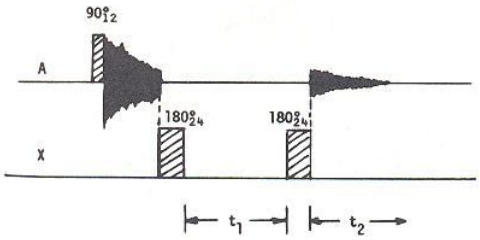

Figure 19. Pulse sequence schematic showing the effects of creating double quantum coherence between levels 1 and 4 and the reconversion of this coherence to observeable transverse magnetization. The experiment begins with selective pulse application to excite the single quantum transition connecting energy levels 1 and 2, the excited magnetization allowed to evolve causing the beginning of the free induction decay. At a point in time, t, a selective 180° pulse is applied to the transition connecting energy levels 2 and 4 thus producing double quantum coherence between energy levels 1 and 4. Upon creation of the double quantum coherence, there is no observeable transverse magnetization in this system. Finally, after a period of evolution, t_1, the evolved double quantum coherence is reconverted to observeable single quantum coherence or transverse magnetization by the application of another selective 180° pulse to the 2-4 transition. Magnetization finally created carries with it information about the evolved double quantum coherence, 1-4.

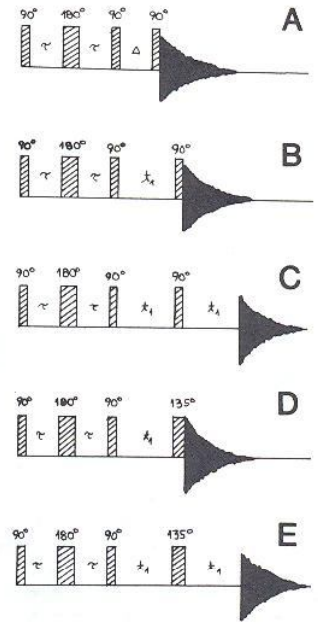

Figure 20. Pulse sequences for variants of the double quantum coherence nmr experiments: A) conventional, one-dimensional INADEQUATE pulse sequence; B) pulse sequence for the simplest two-dimensional INADEQUATE experiment, the evolution period, t_1, replacing the fixed delay of the former; C) the autocorrelated two-dimensional double quantum coherence experiment - magnetization is allowed to evolve for an additional period, t_1, following the conversion of the double quantum coherence back into observeable transverse magnetization; D) modified two-dimensional double quantum coherence pulse sequence utilizing a 135° read pulse to provide additional sensitivity; E) autocorrelated two-dimensional double quantum coherence pulse sequence incorporating a 135° read pulse to improve sensitivity.

are those which link adjacent energy levels. Those linking non-adjacent energy levels 2 to 3 and 1 to 4 are zero and double quantum transitions respectively. Although double quantum transitions cannot be directly observed in the nmr experiment they can, however, be studied when the spin system is suitably prepared provided that the double quantum coherence is converted back into and detected as single quantum coherence. The concept is shown schematically in Figure 20. Single quantum coherence is first created, is converted to double quantum coherence and allowed to evolve for a period of time, and is then converted back into and detected as single quantum coherence.

Illustration of how double quantum coherence may be created is available to us from the energy level diagram for the AX spin system shown in Figure 19. Consider the application of a selective 90° pulse to one of the A transitions of the AX energy level diagram. The application of such a pulse creates a non-equilibrium condition for the spin system. If after some period of time we then apply a selective 180° pulse to the related X-transition (for example transition 24 if transition 12 was initially chosen for the application of the selective 90° pulse), the 180° pulse causes a transfer of coherence from transition 12 to transition 14, a double quantum transition! It is important to note that no signal will be detectable in the receiver as a result of this event and the application of the 180° pulse corresponds to the point of interruption in the free induction decay shown in Figure 20. During the period of time following its creation, the coherence represented by transition 14 evolves. The state of the evolved double quantum coherence can be detected by the selective application of a second 180° pulse to transition 24 which converts the double quantum coherence back into detectable single quantum coherence between levels 1 and 2 which may then be detected in the receiver. The reconversion of double quantum coherence to single quantum coherence corresponds to the point of resumption of the free induction decay

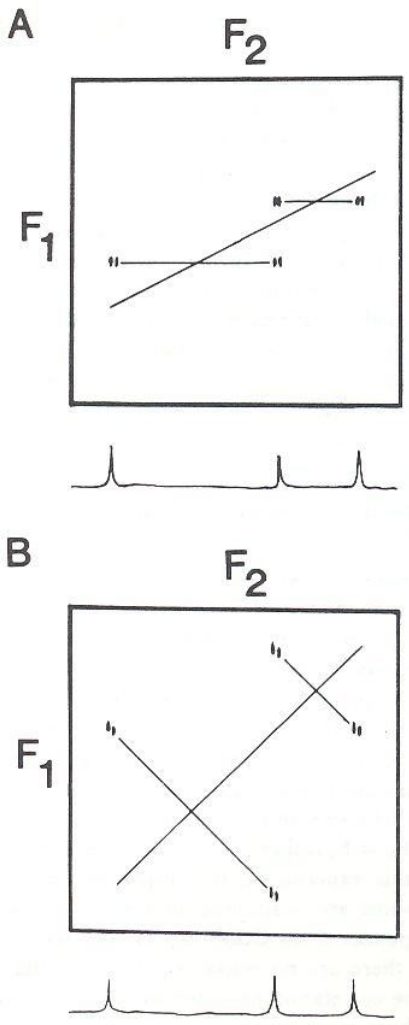

Figure 21. Schematic presentation of data interpretation in the two different variants of the double quantum coherence experiments: A) conventional two-dimensional double quantum coherence experiments (see pulse sequences in Figures 21b and 21d) correlate about a diagonal $F_1 = 2F_2$; B) autocorrelated two-dimensional double quantum coherence experiments contain data which correlates about the diagonal $F_1 = F_2$ analogous to the COSY experiment.

shown in Figure 20. Although the utility of the sequence of events which have just been described may still not be apparent, the phase of the finally detected single quantum coherence is a function of the angular frequency of the double quantum coherence and the period of time, t_1, during which it was allowed to evolve. In the specific case of the experiment which we shall utilize in the eventual assignment of the ^{13}C-nmr spectra discussed below, the double quantum frequency is the algebraic sum of the offsets of the two coupled ^{13}C resonances from the carrier frequency, the double quantum frequency ultimately determined as a consequence of the systematic variation of the duration of the evolution period and a double Fourier transformation.

1. One Dimensional Double Quantum Coherence - The INADEQUATE Experiment.

The simplest version of the double quantum coherence experiments is the one-dimensional variant which has been labeled with the acronym INADEQUATE by Freeman and co-workers [94,95]. The pulse sequence is shown in Figure 21a and contains a $90^\circ_x - \tau - 180^\circ_y - \tau - 90^\circ_x$ segment which creates the double quantum coherence accompanied only by longitudinal magnetization along the $-z$ axis (where the interval τ is a function of the $^1J_{CC}$ coupling, typically $\frac{1}{4}J_{CC}$). The double quantum coherence is then reconverted into detectable single quantum coherence with a 90° "read" pulse after a short, fixed delay, Δ.

Ideally, only the longitudinal magnetization along the $-z$ axis and the double quantum coherence would be created in the sequence above, but unfortunately we do not live in an ideal world. Pulse imperfections, inaccurate phase settings and the like all impinge on the experiment and lead to the formation of residual single quantum coherences in addition to the desired double quantum coherence. By cycling the phase of the receiver phase in a four step $+x, +y, -x, -y$ sequence accompanied by countercycling of the receiver phase $(+x, -y, -x, +y)$, cancellation of the undesired single qunatum coherence as well as the undesired longitudinal magnetization is obtained as soon as the four step cycle is completed. While in principle this cycle should be sufficient in and of itself, typically more complex phase cycles are routinely employed, the most common being a 128 step phase cycle which provides excellent cancellation of all unwanted components of magnetization.

Although a number of papers exploiting the one-dimensional INADEQUATE experiment have appeared in the literature [96-98], this experiment suffers the same fate as the proton-coupled ^{13}C experiment when applied to large molecules. Specifically, the spectrum becomes so congested with responses that it becomes intractable. To circumvent the difficulties inherent to the one-dimensional experiment, the INADEQUATE pulse sequence has been extended to two-dimensions as described in the succeeding sections.

2. Basic Two-Dimensional Double Quantum Coherence.

Extending the INADEQUATE pulse sequence from a one to a two-dimensional experiment is a relatively simple one requiring only that the fixed delay, Δ, be replaced by

a systematically incremented evolution period, t_1. This modification of the pulse sequence is shown in Figure 21b [99-101]. The double quantum coherence is created as in the previous experiment but is then allowed to evolve for the period t_1. Again, the 90° "read" pulse converts the double quantum coherence back into detectable single quantum coherence which is then recorded during the acquisition period, t_2.

Experimentally, an AX ^{13}C-^{13}C spin system produces, as expected, a pair of doublets which are symmetrically disposed about an axis $F_1 = 2F_2$. Usefully, the double quantum frequency (F_1) is equivalent to the algebraic sum of the offset frequencies of the coupled spins relative to the carrier or transmitter frequency. In most cases, the double quantum frequency will be unique and will thus all the unequivocal assignment of the coupled resonances.

The utilization of the two-dimensional analog of the INADEQUATE experiment provided by the pulse sequence shown in Figure 21b is shown schematically in Figure 22a. Coupled resonances are denoted by the dashed lines connecting the various AX doublets and all that is necessary for an unequivocal assignment to be made of all correlated resonances would be the unequivocal assignment of any one of the resonances. Typically, a starting point for the assignment will be provided from one of the other two-dimensional nmr experiments, from a heteronuclear coupling constant or from a relaxation time. It must also be remembered that if the molecule contains any pair(s) of resonances which constitute a ^{13}C-^{13}C AB spin system that these systems will leave "holes" in the connectivity provided by the experiment and that allowances must be made for such situations. Although this eventuality may limit the utilization of the experiment to the assemblage of non-contiguous structural fragments, the experiment is still exceedingly useful and in many cases may provide the only means available to the investigator of making an unequivocal assignment.

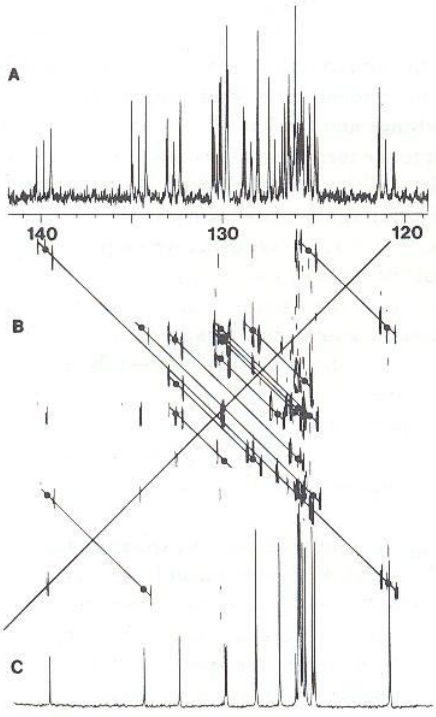

Figure 22. Autocorrelated two-dimensional double quantum coherence experiment performed on phenanthro-[3,4-*b*]thiophene (**12**) [109]. The data are presented as a four level contour plot of the $S(F_1,F_2)$ data matrix which consisted of 256 × 4K data points (B) with a projection of the two-dimensional data matrix above (A) and the conventional ^1H-decoupled ^{13}C-nmr spectrum (C) below.

3. Autocorrelated Two-Dimensional Double Quantum Coherence.

While the basic two-dimensional double quantum coherence experiment just described is exceedingly useful in its' own right, work by Turner has been directed at the further evolution of the experiment [102-103]. Specifically, the pulse sequence developed by Turner is shown in Figure 21c. Here the double quantum coherence is converted back to single quantum coherence as in the conventional experiment but acquisition is delayed for an additional period also with a duration of t_1 making the correlation axis $F_1 = F_2$ rather than $F_1 = 2F_2$ as shown in Figure 22b. In this experiment, the responses which correlate coupled spins are positioned analogously to the off-diagonal responses of the COSY experiment described above although there are no responses along the diagonal. Although the correlation provided by this experiment is, to these authors, more conveniently interpreted than the conventional double quantum coherence two-dimensional experiment represented by the pulse sequence shown in Figure 21b, it is not without a price. Specifically, the second phase of the evolution, while beneficial in the reorientation of the spectral data in the matrix, is also responsible for a loss in signal-to-noise due to the decay of components of the magnetization as was discussed by Bax and Mareci [104]. As will be shown in the following two sections, however, these losses may be satisfactorily overcome by still further modifications of the pulse sequence.

4. Two-Dimensional Double Quantum Coherence with a Modified "Read" Pulse.

Because of the inherent insensitivity of the double quantum coherence experiment under even the best of circumstances, Mareci and Freeman [101] have studied the response obtained by varying the flip angle of the "read" pulse. Thus, Mareci and Freeman have shown that up to a 30% enhancement in signal response may be obtained

when a 120° "read" pulse is utilized in place of the conventional 90° "read" pulse. (Conversely a similar enhancement in sensitivity may also be obtained by using a 60° "read" pulse if the echo component of magnetization is detected rather than the antiecho component which is detected when the 120° pulse is utilized.) Mareci and Freeman have further shown that a somewhat better discrimination between the echo and antiecho components of magnetization may be obtained with either a 45° or a 135° pulse with only small losses in sensitivity relative to the 60° and 120° pulses. Detection of the antiecho component being preferable, Mareci and Freeman [101] thus recommend the utilization of a 135° read pulse as shown by Figure 21d.

5. Autocorrelated Two-Dimensional Double Quantum Coherence with a Modified "Read" Pulse.

The final modification of the double quantum coherence reported to date incorporates the autocorrelated sequence of Turner [102,103] with the modified "read" pulse recommended by Mareci and Freeman [101] just described. Using the pulse sequence shown in Figure 21e which employs a 135° "read" pulse we have recently described the assignment of the ^{13}C-nmr spectrum of phenanthro[3,4-*b*]thiophene (**12**) [105]. A related report by Turner which differed only in that it employed a 120° "read" pulse [106] has led to the successful assignment of the ^{13}C-nmr spectrum of the antibiotic tylosin. To illustrate the correlation of coupled resonance obtained using this technique, the autocorrelated double quantum coherence spectrum of phenanthro[3,4-*b*]thiophene (**12**) is shown in Figure 23.

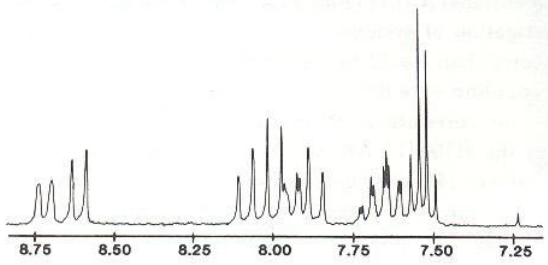

Figure 23. Conventional ^{1}H-nmr spectrum of phenanthro[1,2-*b*]thiophene (**4**) in deuteriochloroform at 200 MHz.

Concerted Application of Two-Dimensional NMR Spectroscopy in the Total Assignment of the Proton and Carbon NMR Spectra of Polynuclear Aromatic Thiophenes

Having presented the fundamentals of two-dimensional nmr spectroscopy in the preceeding segments of this review, it is appropriate to direct the focus of attention to the actual problem of assigning the proton and carbon nmr spectra of polynuclear aromatic thiophenes whose synthesis is described above. One of the problems inherent in the assignment of the proton and carbon nmr spectra of these interesting molecules is the severely congested nature of their spectra. Although the proton nmr spectra would be expected to be highly congested because of the limited range of proton chemical shifts, the carbon nmr spectrum might not *a priori* be expected to exhibit the same degree of congestion. however, as is quite common with alternate polynuclear aromatic hydrocarbons, the chemical shift range is generally limited to about 6-9 ppm [107-108]. For specific examples, the most congested member of the phenanthro[*b*]thiophene family is the phenanthro[9,10-*b*]thiophene, with the protonated carbons resolved at 25.2 MHz but compressed into a "window" only 5.5 ppm wide. The "least" congested member of the series has the protonated carbon resonances in a "window" only about 8 ppm wide [109]. With spectra this congested, the empirical calculation of ^{13}C-nmr chemical shifts is of relatively little utility, clearly underscoring the need for an alternative means of making unequivocal assignments of the resonances. It is at this point that the utility of two-dimensional nmr experiments for making assignments in these systems becomes obvious. When utilized in a concerted fashion, the difficulties inherent in the use of "classical" techniques are obviated.

Assignment Strategies.

Various assignment strategies may be devised which will effectively lead to total assignments of the proton and carbon nmr spectra of these interesting molecules. Although strategies will vary when other chemical classes are

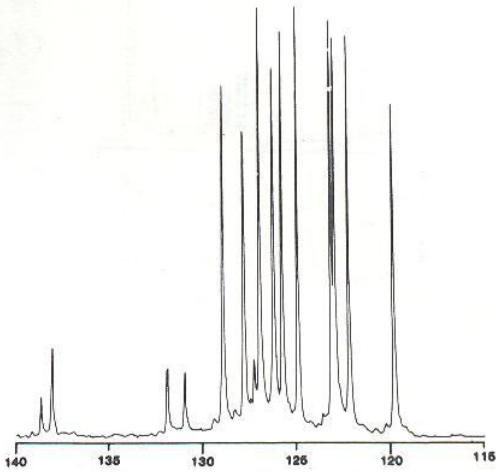

Figure 24. The ^{1}H-decoupled ^{13}C-nmr spectrum of phenanthro[1,2-*b*]thiophene (**4**) in deuteriochloroform. Resonances due to quaternary carbons exhibit lower intensities due to incomplete relaxation during the interpulse delay chosen for this experiment.

considered, a reasonably uniform approach may be employed in the investigation of the polynuclear aromatic thiophene systems. First, one dimensional ^{1}H- and ^{13}C-nmr spectra will routinely be obtained. While the former may vary considerably, the latter will characteristically have a highly congested protonated carbon region which will nominally be only 6-8 ppm in width. Clearly, the congestion of the ^{13}C-nmr spectrum will largely preclude any strong reliance on calculated chemical shifts until a very substantial data base has been generated. Thus, whenever possible, preliminary resonance assignment should be made in the proton spectrum first. For example, in the case of phenanthro[1,2-*b*]thiophene (**4**) [110] whose 200 MHz ^{1}H-nmr spectrum is shown in Figure 24, the two resonances (nominally "doublets") furthest downfield will clearly be attributable as the protons in the "bay" region, H9 and H10. Additionally, the resonance at $\delta = 8.72$, which is the

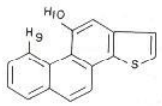

4

broader of the two, may be tentatively assigned as H9, the broadening due to the more extensive coupling of H9 relative to H10. Within the carbon spectra, in contrast, it may not be possible to make any tentative assignments other than possibly the quaternary carbons. As an example, the quaternary carbon resonance observed at $\delta = 137.83$ in

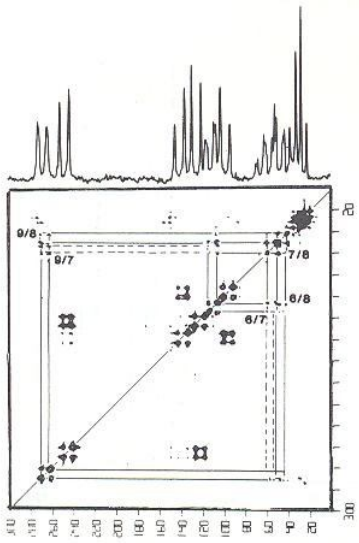

Figure 25. Contour plot of the COSY spectrum of phenanthro[1,2-*b*]thiophene (**4**): A) correlations of resonances of the H6-H9 four spin ABMX spin system; B) correlations of the resonances of the H10-H11 AX spin system.

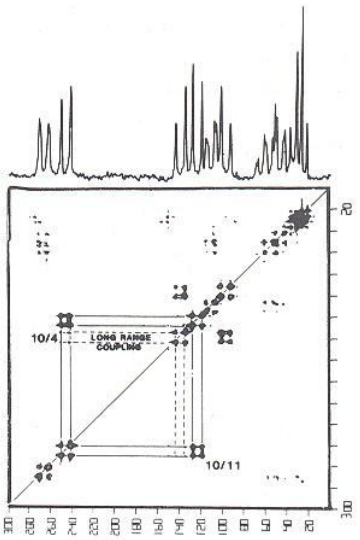

the ^{1}H-decoupled ^{13}C-nmr spectrum of phenanthro[1,2-*b*]-thiophene (**4**) (Figure 25) may be reasonably assigned as C3a based upon a knowledge of the assigned resonances of benzo[*b*]thiophene [111-112] and of phenanthrene [113].

Proceeding with the development of assignment strategies, the next logical step is the subgrouping of the proton resonances into component subsystems. Traditionally, this would have been done using homonuclear decoupling. However, in molecules possessing highly congested ^{1}H spectra, this approach may be expected to lead to ambiguous results. In contrast, autocorrelated homonuclear two-dimensional (COSY) nmr experiments [61,92] allow the investigation of systems with considerably more congested spectra than would be amenable to study if homonuclear decoupling were the only technique available. As an example, the correlations of resonances for the H6-H9 ABMX and the H10-H11 AB spin systems of phenanthro[1,2-*b*]-thiophene (**4**) are shown in Figure 26.

Once the proton spectrum has been subgrouped, it is reasonable to proceed with assignments in the carbon spectrum. Resonances which may be unequivocally assigned from either chemical shift considerations or coupling behavior lead directly to protonated carbon resonance assignments through the agency of the two-dimensional proton-carbon chemical shift correlation experiment [88-91]. Generally, this is the most convenient means of making the largest number of assignments. Whenever necessary, additional assignment criteria can sometimes be provided by heteronuclear spin-coupling ($^{1}J_{CH}$ or $^{3}J_{CH}$) coupling constants or spin-lattice (T_1) relaxation times if the molecule has an axis of anisotropic reorientation. In those cases where protonated carbons remain to be assigned, it will be necessary to resort to means of unequivocally assigning

the protons beyond merely subgrouping them or alternatively, they may be assignable by ^{13}C-^{13}C two-dimensional double quantum coherence (2DDQC) experiments [99-101]. Regardless, it should be possible to obtain unequivocal assignments of all of the proton and carbon resonances contained in the spectra of polynuclear aromatic thiophenes.

Phenanthro[1,2-*b*]thiophene.

The assignment of the ^{1}H- and ^{13}C-nmr spectra of phenanthro[1,2-*b*]thiophene (**4**) follows directly from the strategy described above, the one dimensional spectra shown in Figures 24 and 25 respectively. Based upon a consideration of the chemical shifts expected for the corresponding proton of phenanthrene in the "bay" region [114], the H9 and H10 resonances may be utilized as a starting point for the proton assignments, the former being discriminated from the latter on the basis of additional couplings. Thus, H9 was assigned to the "doublet" observed at $\delta = 8.72$ while the H10 resonance was assigned to the resonance at $\delta = 8.61$. From the assignments of H9 and H10, the identification of the balance of the resonances in the two spin systems containing these resonances is readily accomplished from the COSY spectrum as shown in Figure 26. Additionally, the observation of a long range five bond epi-zig-

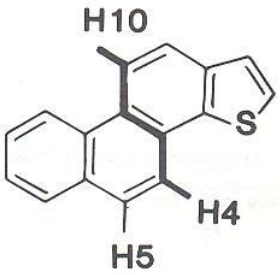

Figure 26. Long range epi zig-zag coupling between H10 and H5 in phenanthro[1,2-*b*]thiophene which was utilized to identify and orient the assignments of the H4-H5 AB spin system.

zag coupling between H10 and H5 which has been observed in the case of considerable numbers of related compounds [115] provides an assignment for H5 and thus the accompanying H4 resonance of that AB spin system as shown in Figure 27. At this point, there remains only the H1-H2 AB spin system to be assigned and there is no method for accomplishing this task from any of the available proton nmr experiments, two-dimensional or otherwise. Also, while the component resonances of the H6-H9 ABMX spin system have been identified from the COSY spectrum, the H7 and H8 resonances cannot be unequivocally assigned from the COSY spectrum alone.

Having assigned a number of the proton resonances of **4** from the COSY spectrum and chemical shift considerations, more complex experiments must be utilized if further assignments are to be made. Based upon the similarity of **4** to the steroid nucleus which is known to reorient

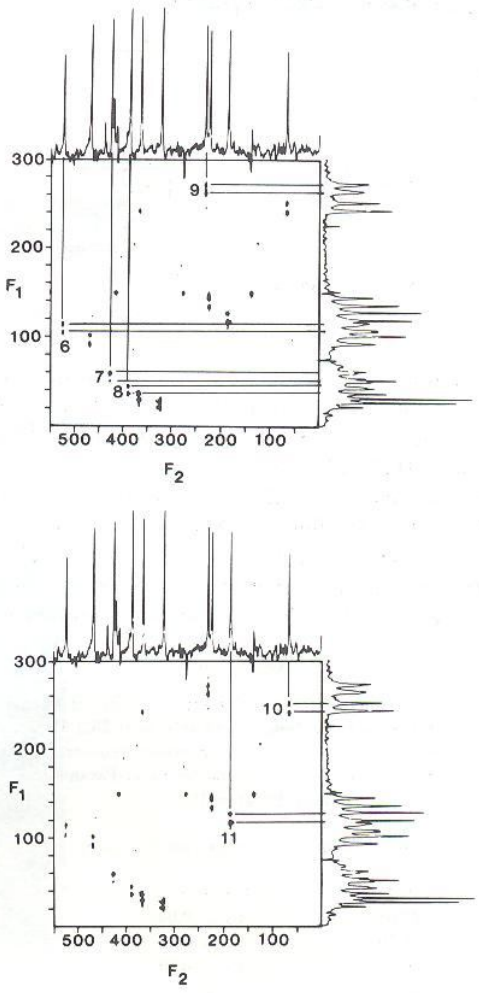

Figure 27. Proton-carbon two-dimensional chemical shift correlation spectra of phenanthro[1,2-*b*]thiophene: A) correlation of the proton and carbon resonances of the H6-H9 ABMX system; B) correlation of the proton and carbon resonances of the H10-H11 AX spin system; C) correlation of the proton and carbon resonances of the H4-H5 AB system.

anisotropically, it is reasonable to assume that the identities of one of the carbons of the H1/C1-H2/C2 pair will be identified from relaxation times as will either H7/C7 or H8/C8. Further, since an independent means of identifying C2 is available on the basis of the one bond heteronuclear coupling constant, $^{1}J_{CH}$, which is larger at this posi-

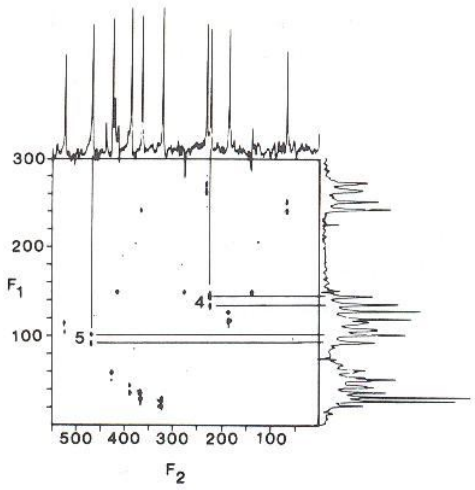

tion of thiophene than would be a normal aromatic carbon one bond coupling constant [113,116], it will be possible to determine the precise alignment of the axis of anisotropic reorientation [117,118], thus providing an unequivocal assignment for either C7 or C8. With this objective, the spin-lattice (T_1) relaxation times for **4** were measured using an inversion-recovery experiment [119-121], the results obtained shown in Table I. As expected, two resonances exhibited shorter relaxation times: 2.4 sec for the resonance at

Table I

Protonated Carbon Spin-lattice (T_1) Relaxation Times for Phenanthro-[1,2-*b*]thiophene (**4**) in Deuteriochloroform at 25.2 MHz. Relaxation data was obtained using the inversion-recovery experiment, the resultant data reduced using the Three-Parameter Fitting Program [121]

chemical shift (δ)	relaxation time (sec)
128.74	3.3 ± 0.06
127.63	3.3 ± 0.04
126.79	3.6 ± 0.02
126.04	2.4 ± 0.04
125.59	2.5 ± 0.03
124.75	3.1 ± 0.03
122.94	3.4 ± 0.04
122.76	3.2 ± 0.06
122.02	3.5 ± 0.05
119.67	3.3 ± 0.07

126.04 ppm and 2.5 sec for the resonance at 125.59 ppm as opposed to an average relaxation time of approximately 3.4 sec. Following the measurement of the relaxation times, an amplitude modulated ^{13}C two-dimensional J-resolved spectrum [78] of **4** was obtained, providing one bond coupling constants for all of the protonated carbon resonances. From this experiment, the resonance at 125.59 ppm was observed to have a one bond coupling of 184.4 Hz consistent with the C2 resonance of thiophene [116], thus unequivocally assigning this resonance as C2 of phenanthro[1,2-*b*]thiophene (**4**). The balance of the one bond coupling constants were unremarkable and are shown in Table II. Having assigned the C2 resonance, the axis of anisotropic reorientation was oriented relative to the

Table II

One-bond Heteronuclear Spin-coupling Constants Observed for Phenanthro[1,2-*b*]thiophene (**4**) in Deuteriochloroform

chemical shift (δ)	$^1J_{CH}$
128.74	157.6
127.63	160.6
126.79	159.4
126.04	161.0
125.59	184.4
124.75	168.8
122.94	154.9
122.76	159.6
122.02	162.2
119.67	158.8

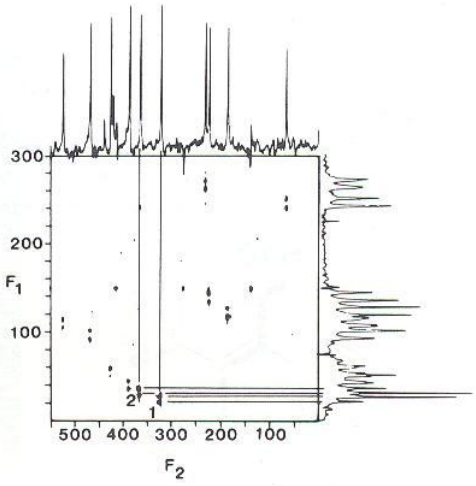

Figure 28. Two-dimensional proton-carbon chemical shift correlation for the assignment of the C1/H1 and C2/H2 resonance pairs. Since the C2 resonance can be assigned on the basis of the independently measured one bond coupling ($^1J_{CH}$ = 184.4 Hz), the C2 resonance may be assigned directly, providing the assignment for the H2 resonance. From the COSY spectrum, the H1 resonance may then be assigned along with the C1 resonance from the proton-carbon chemical shift correlation experiment.

C2-H2 bond vector and those of the already assigned C4-H4, C5-H5, C9-H9 and C10-H10 bond vectors according to the method of Platzner [117], providing the identity of the resonance at 126.04 ppm as C8.

Having made assignments for sufficient key resonances of the proton spectrum of phenanthro[1,2-*b*]thiophene (**4**), a two-dimensional proton-carbon chemical shift correlation spectrum was next obtained. From the proton assign-

ments, the ^{13}C assignments follow directly as shown for the H4-H5, H10-H11 AB and the H6-H9 ABMX spin systems in Figures 28a-c. In the case of the H1-H2 AB spin system, however, neither of the protons could be assigned, requiring that the information contained in the contour plot of the proton-carbon experiment be used in reverse. Thus, it follows that from the assigned C2 resonance at 125.59 ppm that the H2 resonance may be assigned as the doublet at 7.55 ppm, the H1 resonance, of necessity, assigned as the resonance at 7.51 ppm thereby providing the assignment of C1 to the resonance at 124.74 ppm as shown in Figure 29. All of the proton and protonated carbon resonance assignments are collected in Table III, as are the calculated chemical shifts for the carbon resonances and the deviation ($\Delta\delta$) for purposes of illustration.

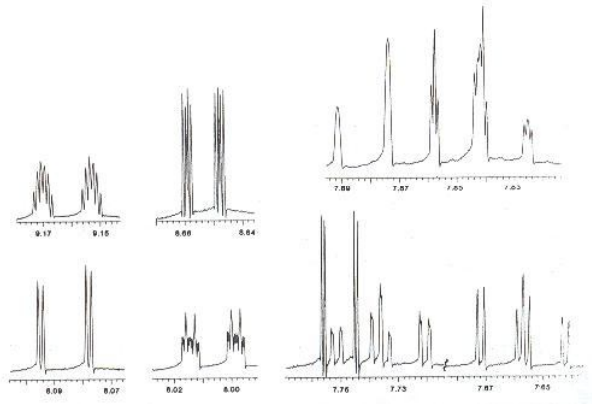

Figure 29. Resolution enhanced 500 MHz ^1H-nmr spectrum of phenanthro[3,4-*b*]thiophene in deuteriochloroform.

Table III

Proton and Protonated Carbon Resonance Assignments of Phenanthro[1,2-*b*]thiophene (**4**) in Deuteriochloroform at 200 and 50 MHz Respectively

Position	δ ^1H	Observed	δ ^{13}C Calcd.	$\Delta\delta$
1	7.51	124.74	124.0	+0.7
2	7.55	125.59	126.4	−0.8
4	8.09	122.76	126.9	−4.1
5	7.87	127.63	126.9	+0.7
6	7.94	128.74	128.5	+0.2
7	7.66	126.78	126.5	+0.3
8	7.62	126.03	126.5	−0.5
9	8.72	122.94	122.6	+0.3
10	8.61	119.67	118.3	+1.4
11	8.06	121.02	121.7	+0.3

Remaining to be assigned at this point are the quaternary carbon resonances of **4**. With the exception of the C3a resonance which may be reliably assigned on the basis of chemical shift considerations from benzo[*b*]thiophene [111-112] to the resonance at 137.83 ppm, the balance cannot be reliably assigned solely from chemical shift considerations. These resonances were partially assigned from the two-dimensional INADEQUATE experiment [99,100] whose pulse sequence is shown in Figure 21b above. Because of the relatively long relaxation times exhibited by the quaternary carbons, only four of the six resonances gave sufficient signal intensity in the 2DDQC experiment to allow their unequivocal assignment. The assigned resonances and the remaining pair of possibly permuted resonances are given in Table IV. Although more efficient 2DDQC experiments have become available since the work on the phenanthro[1,2-*b*]thiophene (**4**) system was originally conducted [110], no effort has been made to assign these resonances through a repetition of the 2DDQC study. More profitably, we have have instead directed our attention toward the assignment of additional members of this interesting family of compounds with the intent that it will eventually be possible to assign the C3b/C9b pair from chemical shift considerations once a sufficient body of reliably assigned spectra has been obtained.

Table IV

Quaternary Carbon Resonance Assignments of Phenanthro[1,2-*b*]thiophene Made by ^{13}C-^{13}C Two-dimensional Double Quantum Coherence

Position	Observed	δ ^{13}C Calcd.	$\Delta\delta$
3a	137.83 [a]	139.8	−2.0
3b	127.08	126.1	+1.0
5a	131.67 [a]	132.0	−0.3
9a	127.08 [a]	130.3	−3.2
9b	130.73	126.1	+4.6
11a	138.83 [a]	137.7	+1.1

[a] Assignments of these resonances were made *via* the 2DDQC experiment. The remaining resonance assignments could not be made from the spectrum due to inadequate signal to noise.

Phenanthro[3,4-*b*]thiophene.

Continuing from the phenanthro[1,2-*b*]thiophene (**4**) system, which was selected as a model starting point because of the availability of significant quantities of material, we next directed our attention to the assignment of the proton and carbon nmr spectra of phenanthro[3,4-*b*]thiophene (**12**) [105]. Specifically, phenanthro[3,4-*b*]thiophene (**12**) is a much more interesting compound in that it has been shown to be a reasonably potent mutagen [14], thereby making the assignment of the spectra useful for the eventual structure elucidation of oxidized metabolites. As in the assignment of phenanthro[1,2-*b*]thiophene (**4**) just

discussed above, it was useful to begin our study of phenanthro[3,4-*b*]thiophene (**12**) with the acquisition of a high field proton spectrum. However, before discussing the spectrum itself, it is useful to begin by developing an initial hypothesis for the types of spin systems which the molecule might contain.

Examining the structure of phenanthro[3,4-*b*]thiophene (**12**) it is immediately apparent that the molecule will be comprised of four discrete spin systems, several with the possibility of being long range coupled to one another. Clearly, the H4-H5 and H6-H7 spin systems would be AB in nature. The two remaining spin systems offer some more interesting possibilities because of the large bay region formed by the molecule which is flanked by H1 and H11. Thus, we expected that the H1-H2 spin system, rather than being an AB system as in the case of phenanthro[1,2-*b*]thiophene (**4**) [110], would instead by an AX spin system because of the position of H1 in the bay region. Similarly, we expected the H8-H11 four spin system to be at a minimum, an ABMX spin system or possibly an ABXY system. Thus, when the one-dimensional proton spectrum of **12** was obtained, we have several initial points of entry into the assignment of the spectrum.

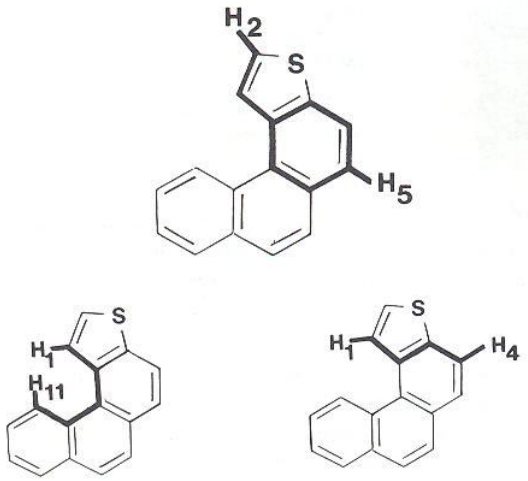

Figure 30. Long range coupling pathways identified in the ^{1}H-nmr spectrum of phenanthro[3,4-*b*]thiophene based on homonuclear decouplings and COSY spin connectivities.

The ^{1}H-nmr spectrum of phenanthro[3,4-*b*]thiophene (**12**) was first obtained at 500 MHz and is shown in Figure 30 in a number of segments to permit the detail of the multiplets to show readily. Rather surprisingly, a number of very interesting long range couplings were observed in this spectrum, allowing the unequivocal assignment of all of the proton resonances directly. Perhaps the most interesting of the long range couplings was that observed between the H1 and H11 resonances of 0.55 Hz which is unusually large for a six bond coupling [115]. In addition, the H1 resonance was also coupled to H4 *via* a five bond epi-zig-zag pathway (0.90 Hz) which is more typical. Both of these compound pathways are shown in Figure 31. Other noteworthy couplings were that between H2 and H7 *via* six or seven bonds [110,122,123] (0.55 Hz); H10 to H6 *via* a seven bond extended epi-zig-zag pathway (0.24 Hz) and finally a four bond peri coupling between H8 and H7 (0.62 Hz).

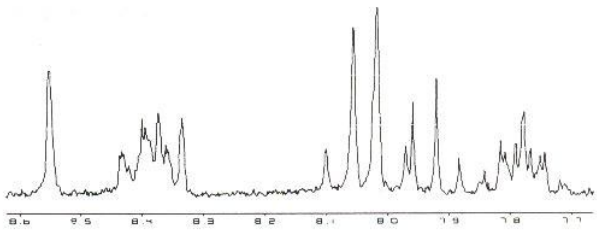

Figure 31. Conventional ^{1}H-nmr spectrum of benzo-[2,3]phenanthro[4,5-*bcd*]thiophene recorded at 200 MHz in d_6-dimethylsulfoxide at 50°.

Confirmation of the assignments made for **12** from the high resolution 500 MHz spectrum was confirmed by the two-dimensional COSY spectrum which was recorded at both 500 and 300 MHz for reasons which will be discussed in more detail below. Having made the proton resonance assignments, a two-dimensional proton carbon chemical shift correlation experiment was next performed and is shown in Figure 16. Interestingly, when the concentration of phenanthro[3,4-*b*]thiophene (**12**) was increased to minimize data acquisition times, a noticable shift in the position of some of the proton resonances occurred, necessitating the recollection of a 300 MHz COSY spectrum to reconfirm the assignments of the shifted resonances. This observation highlights the necessity of obtaining all spectra, whenever possible, at identical concentrations. In those specific cases where it is necessary to conduct some experiments at higher concentrations, care must be excercised to insure that permutations of the assignment do not occur as a function of the altered concentration. Although assignments for all of the protonated carbons could be made with a reasonable level of confidence from the two-dimensional proton-carbon chemical shift correlation experiment after the recollection of the 300 MHz COSY spectrum, we were interested in insuring the accuracy of these assignments. To accomplish this and to assign the quaternary carbon resonances of **12**, an autocorrelated two-dimensional double quantum coherence spectrum [102,103] of **12** was obtained using the pulse sequence shown in Figure 21e with the observed pulse increased to

135° from the normal 90° to provide additional sensitivity [101,105,106].

From the autocorrelated 2DDQC spectrum of phenanthro[3,4-*b*]thiophene (**12**) which is shown in Figure 22, assignments of all of the quaternary carbon resonances were developed. Assignments are made in this experiment in a fashion analogous to that utilized in the COSY experiment. Responses are symmetrically disposed about a diagonal (Figure 22b) $F_1 = F_2$ rather than the $F_1 = 2F_2$ (Figure 22a) in the older 2D-INADEQUATE experiment [99-100]. Resonances coupled to one another are thus correlated *via* the lines drawn perpendicular to the diagonal as shown in Figure 22b. Thus, with the exception of those pairs of carbon resonances which are AB in nature rather than AX, assignments of virtually all possible carbon-carbon pairings were obtained for phenanthro[3,4-*b*]thiophene (**12**) leading to a totally unequivocal assignment of its carbon spectrum, the assignments of all of the protons and their coupling constants which were discussed above and the carbon resonances given in Tables V and VI respectively.

Having completed the total assignment of the proton and carbon nmr spectra of phenanthro[3,4-*b*]thiophene (**12**) [105], it was suggested by a referee for the manuscript that we also investigate the tertiary structure of the molecule. Thus, NOE measurements were made within the groupings of H10-H11-H1 and H2-H1-H11 when H11 and H1 respectively were irradiated. Assuming standard geometries for the phenanthrene and thiophene portions of the molecule, it was possible to measure the H1-H11 interatomic distance from the NOE data obtained. Based upon the NOE measurements, the distance between H1 and H11 was determined to be 1.99 Å. Assuming a planar configuration for the molecule, the H1-H11 interatomic distance would be a scant 1.3 Å thus confirming that the molecule would undergo a helical distortion to provided sufficient separation between H1 and H11. Although phenanthro-[3,4-*b*]thiophene (**12**) has not been examined crystallographically there are a number of structurally related helical systems which exhibit very similar intra-atomic distances: benzo[*c*]phenanthrene at 2.04 Å [124]; trithia(5)heterohelicene at 2.06 Å [125], suggesting that the nmr determined tertiary structure of phenanthro[3,4-*b*]thiophene (**12**) has a high probability of being correct. Furthermore, since the helical distortion of systems such as phenanthro[3,4-*b*]thiophene (**12**) is accompanied by deformations in the carbon-carbon bond lengths in the "bay" region of the molecule, this could in some way help to account for the differences in mutagenicity observed for some of these systems.

Benzo[2,3]phenanthro[4,5-*bcd*]thiophene.

Having completed the assignments of the nmr spectra of two members of the phenanthro[*b*]thiophene series, we next turned our attention to a more complex system, benzo[2,3]phenanthro[4,5-*bcd*]thiophene (**86**). Our interest

Table V

^{1}H Chemical Shifts and Coupling Constants of Phenanthro[3,4-*b*]thiophene (**12**) in Deuteriochloroform at 500 MHz

Position	Spin Label	^{1}H	$^3J_{HH}$ (*ortho*)	$^4J_{HH}$ (*meta* or *peri*)	$^5J_{HH}$ (*para*, *epi*, long range	$^6J_{HH}$ long range	$^7J_{HH}$ long range
H1	X	8.653	$^3J_{H_1H_2}$ = 5.62	—	$^5J_{H_1H_4}$ = 0.90 [a]	$^6J_{H_1H_{11}}$ = 0.55	—
H2	A	7.750	$^3J_{H_2H_1}$ = 5.61	—	—	—	$^7J_{H_2H_5}$ = 0.55
H4	A	8.086	$^3J_{H_4H_5}$ = 8.45	—	$^5J_{H_4H_1}$ = 0.88 [a]	—	—
H5	B	7.849	$^3J_{H_5H_4}$ = 8.37	$^4J_{H_5H_6}$ = 0.52 [b]	—	—	$^7J_{H_5H_2}$ = 0.52
H6	A	7.883	$^3J_{H_6H_7}$ = 8.62	no other couplings resolved			
H7	B	7.834	$^3J_{H_7H_6}$ = 8.64	$^4J_{H_7H_8}$ = 0.62	—	—	—
H8	M	8.006	$^3J_{H_8H_9}$ = 7.89	$^4J_{H_8H_{10}}$ = 1.55	$^5J_{H_8H_{11}}$ = 0.67	—	—
—	—	—	—	$^4J_{H_8H_7}$ = 0.67	$^5J_{H_8H_6}$ = 0.22 [c]	—	—
H9	B	7.656	$^3J_{H_9H_8}$ = 7.90	$^4J_{H_9H_{11}}$ = 1.18	—	—	—
—	—	—	$^3J_{H_9H_{10}}$ = 6.91	—	—	—	—
H10	A	7.736	$^3J_{H_{10}H_9}$ = 6.92	$^4J_{H_{10}H_8}$ = 1.57	—	—	$^7J_{H_{10}H_6}$ = 0.24 [d]
—	—	—	$^3J_{H_{10}H_{11}}$ = 8.49	—	—	—	—
H11	X	9.161	$^3J_{H_{11}H_{10}}$ = 8.50	$^4J_{H_{11}H_9}$ = 1.27	$^5J_{H_{11}H_8}$ = 0.63	$^6J_{H_{11}H_1}$ = 0.63 [a]	—

[a] Confirmed by homonuclear decoupling. [b] The corresponding coupling for the H6 resonance was unresolved. Typical peri couplings in coumarin based systems range from 0.35-0.40 Hz (M. W. Jarvis and A. G. Moritz, *Aust. J. Chem.*, **21**, 2445 (1968)); peri couplings in a variety of polycyclic aromatic hydrocarbons ranged from 0.20-0.50 Hz; K. D. Bartle, D. W. Jones and R. S. Matthews, *Rev. Pure Appl. Chem.*, **19**, 191 (1969)), which are in excellent agreement with the 0.52 Hz coupling observed in the case at hand. [c] The corresponding coupling for the H6 resonance was unresolved. Analogous five bond couplings in coumarin based systems ranged from 0.30-0.45 Hz (M. W. Jarviz and A. G. Moritz, *Aust. J. Chem.*, **21**, 2445 (1968)); the corresponding $J_{1,7}$ coupling of naphthalene is reported as 0.21 Hz (M. W. Jarvis and A. J. Moritz, *Aust. J. Chem.*, **24**, 89 (1971)), which is in excellent agreement with the observed coupling of **1**. [d] The corresponding coupling for the H6 resonance was unresolved. The corresponding $J_{2,6}$ coupling in naphthalene was observed to be 0.28 Hz (M. W. Jarvis and A. G. Moritz, *Aust. J. Chem.*, **24**, 89 (1971)), which agrees quite well with the observed coupling of 0.24 Hz between H10 and H6 in **1**.

Table VI

Calculated *vs.* Observed ^{13}C-nmr Chemical Shifts of Phenanthro-[3,4-*b*]thiophene (**12**) in Deuteriochloroform at 75 MHz

Position	Calcd. [a]	δ ^{13}C Observed	$\Delta\delta$
1	127.2	125.42	−1.8
2	125.4	126.11	+0.7
3a	137.8	140.56	+2.8
4	120.5	121.29	+0.8
5	124.3	125.56	+1.3
5a	127.7	130.86	+3.2
6	126.9	127.30	+0.4
7	126.9	126.31	−0.6
7a	132.0	133.38	+1.4
8	128.5	128.68	+0.2
9	126.5	125.92	−0.6
10	126.5	126.20	−0.3
11	122.6	126.24	+3.6
11a	130.3	130.78	+0.5
11b	125.5	126.94	+1.4
11c	133.8	135.31	+1.5

[a] ^{13}C-nmr chemical shifts of **1** were calculated by incrementing the known chemical shifts of phenanthrene for the [3,4-*b*] ring fusion of the thiophene ring to the phenanthrene nucleus. Chemical shift additivities for this type of ring fusion were derived by calculating differences between the observed chemical shifts of benzo[*b*]thiophene [P. Geneste, J.-L. Olive, S. N. Ung, M. E. A. El Faghi, J. W. Easton, H. Bierbeck and J. K. Saunders, *J. Org. Chem.*, **44**, 2887 (1979)] and benzene.

in this system, as with the preceeding system, derives from the high mutagenicity exhibited by these compounds [14].

Thus far, only the ^{1}H-nmr spectrum of benzo[2,3]phenanthro[4,5-*bcd*]thiophene (**86**) has been studied [82,126], assignments for the ^{13}C-nmr spectrum remaining to be made. Based upon the structure of the molecule, several initial expectations for the subgrouping of the resonances in the ^{1}H-nmr spectrum arise. First, the H6 resonance would be expected to appear as a "singlet", complicated only by long range couplings. The adjacent H7-H10 four spin system would be expected to resonate either as an AB-MX or as an ABXY spin system as do the analogous four spin systems of phenanthro[1,2-*b*]thiophene [110] and phenanthro[3,4-*b*]thiophene [105]. The H1-H3 spin system, based upon the observed ^{1}H-nmr spectrum for phenanthro[4,5-*bcd*]thiophene (**302**) [46] was expected to appear as an ABX spin system. Finally, the H4-H5 spin system was expected to appear as an AB spin system. In support of these contentions, the 200 MHz ^{1}H-nmr spectrum of **86** is shown in Figure 32 and contains a "singlet" resonating at 8.549 ppm which can be attributed to H6, a cluster of resonances between 8.45-8.30 ppm which integrates for three protons which may be ascribed to H3, H7 and H10 and several complex clusters of resonances upfield which integrated for the balance of the six protons contained in the spectrum.

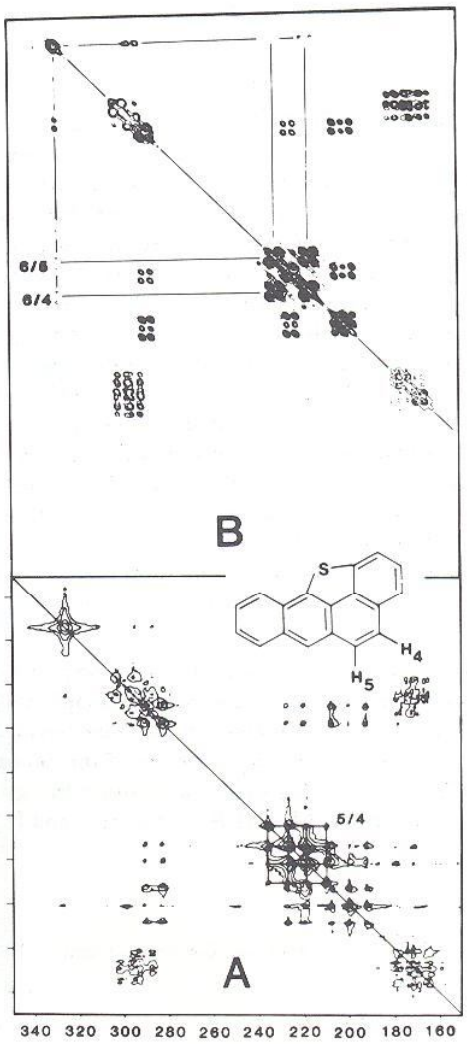

Figure 32. COSY spectrum of benzo[2,3]phenanthro-[4,5-*bcd*]thiophene in d_6-dimethylsulfoxide at 50°: A) spectrum obtained at 200 MHz showing connectivities of the H4 and H5 resonances; B) spectrum obtained at 400 MHz showing long range couplings of H4 and H5 to the H6 resonance *via* five and four bonds respectively.

Having established criteria for subgrouping the proton resonances into their component spin systems, an autocorrelated two-dimensional ^{1}H-nmr (COSY) spectrum was next obtained (see Figure 18 above). As expected, the singlet furthest downfield which was initially attributed to H6 was correctly assigned, this resonance exhibiting only long range couplings. Specifically, the 400 MHz COSY spectrum of **86** (Figure 33) shows the H6 resonance to be long

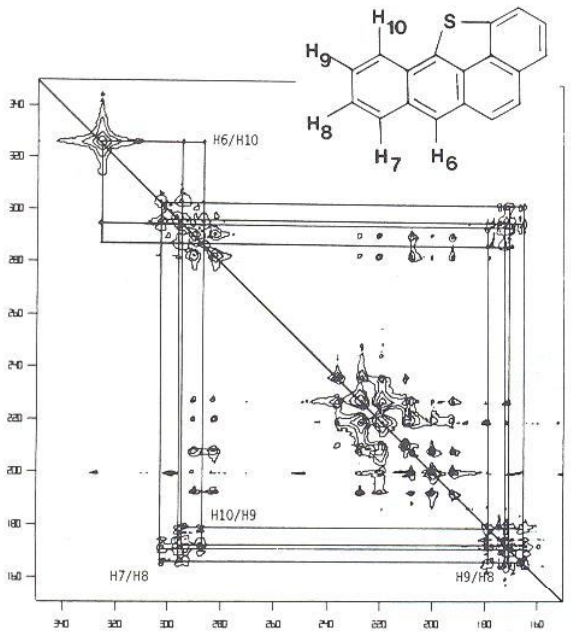

Figure 33. COSY spectrum of benzo[2,3]phenanthro-[4,5-*bcd*]thiophene recorded at 200 MHz in d_6-dimethylsulfoxide at 50° showing the coupling of H6-H10 and the connectivities of the H7-H10 ABXY spin system.

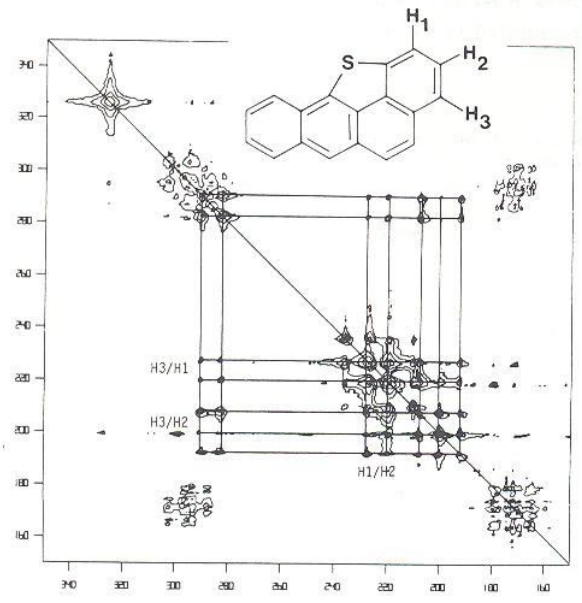

Figure 34. Connectivities of the H1-H3 ABX spin system at 200 MHz.

range coupled to a total of three other resonances one of which was ultimately assigned as H10 (coupled *via* $^5J_{HH}$, epi zig-zag), the other two ultimately assigned as H4 and H5 at 8.072 and 7.999 ppm respectively. From the connectivity between H6 and H10, the COSY spectrum can be utilized to assign the balance of the resonances in the four spin system which, as shown in Figure 34, ultimately identifies the resonance at 8.409 ppm as H10 and the two resonances furthest upfield as H8 and H9 which resonated at 7.757 and 7.808 ppm respectively. With these assignments made, only the three spin ABX and two spin AB groups of resonances remain to be assigned. Usefully, the H2 resonance would be expected to appear as either a doublet of doublets or as an apparent triplet due to equivalent vicinal couplings to H1 and H3. In either case, such a multiplet would have a unique appearance in the COSY spectrum - either a 4 × 4 cluster or a 3 × 3 cluster of responses astride the diagonal. Thus, the 3 × 3 cluster of responses on the diagonal resonating at 7.925 ppm may be readily assigned as H2. Usefully, this apparent "triplet" will also produce readily discernable off-diagonal responses with a 2 × 3 grouping. Thus, as shown in Figure 35, H2 is coupled to the H3 resonance at 8.353 ppm and to the H1 resonance at 8.039 ppm. Additionally, H1 and H3 are also

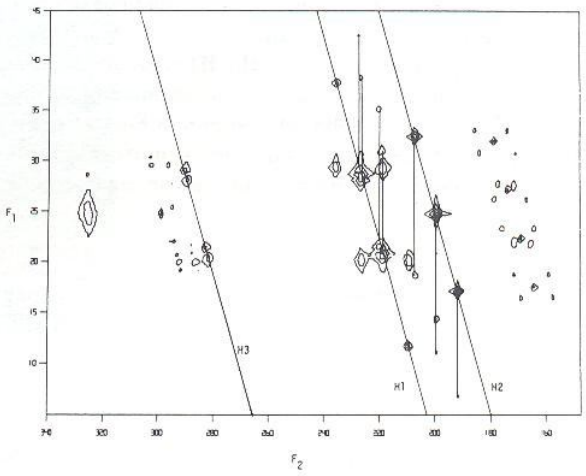

Figure 35. 200 MHz homonuclear J-resolved two-dimensional spectrum of benzo[2,3]phenanthro[4,5-*bcd*]thiophene showing the three resonances of the ABX spin system along the diagonals, with responses due to strong coupling between the A and B component spins indicated by solid vertical lines.

shown to be coupled to one another *via* off-diagonal responses. Finally, there remains to be assigned the H4-H5 AB spin system. Interestingly, the center two responses of the H4-H5 AB spin system, at 200 MHz, exhibited intensi-

ties which were disproportionately large, this clearly due to the location of the H1 resonance, once all of the resonance assignments are known. Additionally, the location of H1 can also be readily determined from the 400 MHz COSY spectrum shown in Figure 33. However, quite frequently, individuals studying a particular molecule will not have access to higher field spectrometers or will not be benefited by resorting to a higher field strength. Thus, it becomes necessary to have alternative means of making assignments. By resorting to the two-dimensional homonuclear J-resolved spectrum (see Figure 12), the location of the H1 resonance and its spin-couplings may be unequivocally obtained as described below.

One of the advantages inherent to the homonuclear two-dimensional J-resolved spectrum is the T_2 determined line widths in the second dimension (as opposed to T_2^* in the conventional spectrum) [63]. Additionally, resonances with different chemical shifts are sorted from one another. Thus, the three resonances of the H1-H3 ABX spin system are readily located on the diagonals shown in Figure 36.

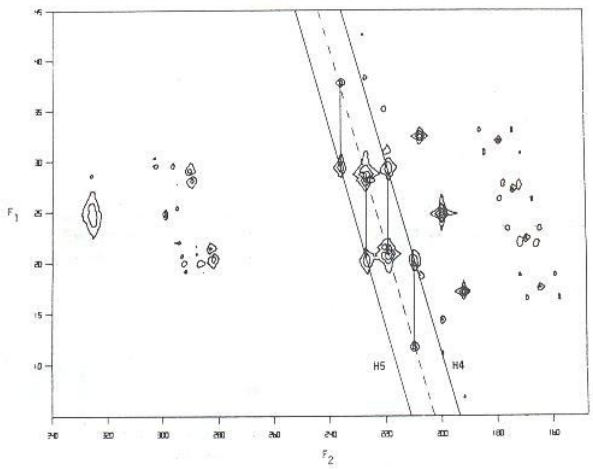

Figure 36. 200 MHz homonuclear J-resolved two-dimensional spectrum of benzo[2,3]phenanthro[4,5-*bcd*]thiophene showing the resonances of the H4-H5 AB spin system (solid diagonal lines) and the H1 resonance of the ABX spin system on the dashed diagonal line. Responses due to strong coupling between the H4-H5 AB spins are shown by solid vertical lines and these responses reside exactly on the dashed diagonal line containing the H1 resonance.

While homonuclear two-dimensional J-resolved spectra are complicated by responses due to strong coupling [79-83], these responses may also be used to correlate coupled resonances [82,83]. Thus, the strong coupling responses between the H2 and H3 resonances of the ABX spin system serve to unequivocally locate the H1 resonance (dashed line) between the two diagonals corresponding to the H4 and H5 resonances (solid lines) shown in Figure 36. Finally, once the H1 resonance has been unequivocally located, the assignments for H4 and H5 may be made on the basis of the long range coupling constants for these resonances obtained from the homonuclear two-dimensional J-resolved spectrum. Chemical shifts for all of the ^{1}H-resonances of **86** and their respective spin coupling constants are collected in Table VII.

Table VII

Chemical Shift Assignments and Homonuclear Spin-Coupling Constants of Benzo[2,3]phenanthro[3,4-*bcd*]thiophene (**86**) in Hexadeuteriodimethylsulfoxide

Position	Spin Label	δ ^{1}H	$^3J_{HH}$ (*ortho*)	$^4J_{HH}$ (*meta*)	$^5J_{HH}$ (*para*, or long range interring)	$^7J_{HH}$
H1	A	8.039	$^3J_{H_1H_2}$ = 7.78	$^4J_{H_1H_2}$ = 1.22	—	—
H2	B	7.925	$^3J_{H_2H_1}$ = 7.78	—	—	—
			$^3J_{H_2H_3}$ = 7.78	—	—	—
H3	X	8.353	$^3J_{H_3H_2}$ = 7.74	$^4J_{H_3H_1}$ = 1.21	$^5J_{H_3H_5}$ = 0.43	—
H4	A	8.072	$^3J_{H_4H_5}$ = 9.14	—	$^5J_{H_4H_6}$ [a]	—
H5	B	7.999	$^3J_{H_5H_4}$ = 9.14	$^4J_{H_5H_6}$ = 0.44	$^5J_{H_5H_3}$ = 0.44	—
H6	—	8.549	—	$^4J_{H_6H_5}$ = 0.44	$^5J_{H_6H_{10}}$ = 0.95	—
					$^5J_{H_6H_4}$ [a]	
H7	Y	8.409	$^3J_{H_7H_8}$ = 9.75	$^4J_{H_7H_9}$ = 2.13 $^5J_{H_7H_{10}}$ = 0.63	—	
H8	B	7.757	$^3J_{H_8H_7}$ = 9.89	$^4J_{H_8H_{10}}$ = 1.73	$^5J_{H_7H_{10}}$ = 0.63	—
			$^3J_{H_8H_9}$ = 6.86			
H9	A	7.808	$^3J_{H_9H_8}$ = 6.84	$^4J_{H_1H_2}$ = 2.13	—	—
			$^3J_{H_9H_{10}}$ = 9.72	—	—	—
H10	X	8.379	$^3J_{H_{10}H_9}$ = 9.61	$^4J_{H_{10}H_8}$ = 1.79	$^5J_{H_{10}H_7}$ = 0.52	—
					$^5J_{H_{10}H_6}$ = 0.93	—

[a] The existence of this coupling was shown by the 400 MHz COSY spectrum (Figure 33B) but was not resolved.

Summary.

Clearly, from the applications of two-dimensional nmr techniques which have been shown with the three molecules discussed in this segment of the presentation, the future is very bright indeed for the utilization of two-dimensional nmr spectroscopy in the study of complex heterocyclic systems. Ultimately, we may expect to see other experiments developed and applied to the study of heterocyclic systems. Along these lines, work is going on in my laboratories and those of several of my co-authors directed toward the assignment of the nmr spectra of even more complex heterocyclic systems. The results of these studies will be forthcoming.

Acknowledgement.

This work was supported by funds from the U. S. Department of Energy, Office of Health and Environmental Research, Contract No. DE-AC02-79EV10237 to R. N. C. and M. L. L. and also from the Robert E. Welch Foundation thorugh Grant Nos. E-792 and E-183 to G. E. M., M. R. W. and M. J. M.

[1] To whom inquiries should be addressed at the Department of Chemistry, University of South Florida, Tampa, FL 33620 USA.

[2] Present address: Facilty of Pharmaceutical Sciences, Nagasaki University, 1-14 Bunkyo-machi, Nagasaki, 852, Japan.

[3] Present address: Medicinal Chemistry Division, Central Drug Research Institute, Lucknow-226001, India.

[4] Present address: Faculty of Pharmaceutical Sciences, Meijo University, Nagoya, Japan.

[5] Present address: Faculty of Liberal Arts, Nagasaki University, Nagasaki 852, Japan.

[6] Present address: Department of Physiology, College of Medicine, University of South Florida, Tampa, FL 33620.

[7] "Symposium of Coal Liquification", ACS Publications, Vol 27, No. 3-4, 1982.

[8] *Chem. Eng. News*, Aug. 9, 1982, p 21.

[9] M. L. Lee, C. Willey, R. N. Castle and C. M. White, "Polycyclic Aromatic Hydrocarbons: Chemistry and Biological Effects", A. Bjørseth and A. J. Dennis, eds, Battelle Press, Columbus, Ohio, 1980, p 59-73.

[10] M. Iwao, M. L. Lee and R. N. Castle, *J. Heterocyclic Chem.*, **17**, 1259 (1980).

[11] W. S. Wadsworth and W. D. Emmons, *J. Am. Chem. Soc.*, **83**, 1733 (1961).

[12] J. Szmuszkovicz and E. J. Modest, *J. Am. Chem. Soc.*, **72**, 571 (1950).

[13] P. Cagniant and G. Kirsch, *C. R. Acad. Sci. Paris, Ser. C*, **281**, 393 (1975).

[14] R. A. Pelroy, D. L. Stewart, Y. Tominaga, M. Iwao, R. N. Castle and M. L. Lee, *Mutat. Res.*, **117**, 31 (1983).

[15] B. D. Tilak and V. K. Dikshit, *Proc. Indian Acad. Sci., Sect A*, 78 (1951).

[16] H. Wynberg, H. van Driel, R. M. Kellogg and J. Buter, *J. Am. Chem. Soc.*, **89**, 3487 (1967).

[17] Y. Tominaga, M. L. Lee and R. N. Castle, *J. Heterocyclic Chem.*, **18**, 967 (1981).

[18] P. Faller, *C. R. Acad. Sci. Paris, Ser. C*, **267**, 543 (1968).

[19] F. Mayer, A. Mombour, W. Lassman, W. Werner, P. Landmann and E. Schneider, *Am. Chem.* **488**, 259 (1931).

[20] W. Davies, Q. N. Porter and J. R. Wilmshurst, *J. Chem. Soc.*, 3366 (1957).

[21] E. Campaigne and S. W. Osborne, *J. Heterocyclic Chem.*, **5**, 655 (1968).

[22] K. Rabindran and B. D. Tilak, *Proc. Indian Acad. Sci.*, **37A**, 557 (1953).

[23] R. Pratap, Y. Tominaga, M. L. Lee and R. N. Castle, *J. Heterocyclic Chem.*, **18**, 973 (1981).

[24] J. W. Cook, C. L. Hewett and I. Hieger, *J. Chem. Soc.*, 395 (1933).

[25] A. Streitwieser, Jr., R. G. Lawler and D. Schwaab, *J. Org. Chem.*, **30**, 1470 (1965).

[26] L. J. Pandya and B. D. Tilak, *Chem. Ind.*, 981 (1958).

[27] Y. Tominaga, M. L. Lee and R. N. Castle, *J. Heterocyclic Chem.*, **18**, 977 (1981).

[28] R. D. Thompson, M. Iwao, M. L. Lee and R. N. Castle, *J. Heterocyclic Chem.*, **18**, 981 (1981).

[29] W. Karcher, A. Nelen, R. Depaus, J. van Eijk, P. Glaude and J. Jacob, "Chemical Analysis and Biological Fate: Polynuclear Aromatic Hydrocarbons", M. Cooke and A. J. Dennis, eds, Battelle Press, Columbus, OH, 1981, pp 317-327.

[30] T. McFall, G. M. Booth, M. L. Lee, Y. Tominaga, R. Pratap, M. Tedjamulia and R. N. Castle, *Mutat. Res.*, **135**, 97 (1984).

[31] R. Pratap, M. L. Lee and R. N. Castle, *J. Heterocyclic Chem.*, **18**, 1457 (1981).

[32] D. N. Nicolaides, *Synthesis*, 675 (1976).

[33] R. Pratap, R. N. Castle and M. L. Lee, *J. Heterocyclic Chem.*, **19**, 439 (1982).

[34] Y. Tominaga, R. N. Castle and M. L. Lee, *J. Heterocyclic Chem.*, **19**, 1125 (1982).

[35] Y. Tominaga, R. Pratap, R.N. Castle and M. L. Lee, *J. Heterocyclic Chem.*, **19**, 859 (1982).

[36] R. Pratap, M. L. Lee and R. N. Castle, *J. Heterocyclic Chem.*, **19**, 219 (1982).

[37] M. L. Tedjamulia, Y. Tominaga, R. N. Castle and M. L. Lee, *J. Heterocyclic Chem.*, **20**, 861 (1983).

[38] W. Davies and Q. N. Porter, *J. Chem. Soc.*, 459 (1957).

[39] A. Croisy, P. Jacquignon and F. Perin, *J. Chem. Soc., Chem. Commun.*, 106 (1975).

[40] G. N. Pillai, T. S. Murthy and B. D. Tilak, *Indian J. Chem.*, **1**, 112 (1963).

[41] D. D. Gverdtsiteli and V. P. Litvinov, *Soobshch. Akad. Nauk Gruz. SSR*, **59**, 333 (1970); *Chem. Abstr.*, **74**, 87729u (1971).

[42] M. L. Tedjamulia, Y. Tominaga, R. N. Castle and M. L. Lee, *J. Heterocyclic Chem.*, **20**, 1143 (1983).

[43] W. Wilputte and R. H. Martin, *Bull. Chim. Soc. Belg.*, **65**, 874 (1956).

[44] K. Rabindran and B. D. Tilak, *Proc. Indian Acad. Sci. Sect. A*, **38**, 271 (1958).

[45] K. Clarke, D. N. Gregory and R. M. Scrowston, *J. Chem. Soc., Perkin Trans. I*, 2956 (1973).

[46] M. L. Tedjamulia, Y. Tominaga, R. N. Castle and M. L. Lee, *J. Heterocyclic Chem.*, **20**, 1149 (1983).

[47] C. Willey, M. Iwao, R. N. Castle and M. L. Lee, *Anal. Chem.*, **53**, 400 (1981).

[48] L. H. Klemm and W. Hsin, *J. Heterocyclic Chem.*, **13**, 1245 (1976).

[49] L. H. Klemm, D. R. McCoy and D. R. Olson, *J. Heterocyclic Chem.* **7**, 1347 (1970).

[50] M. L. Tedjamulia, Y. Tominaga, R. N. Castle and M. L. Lee, *J. Heterocyclic Chem.*, **20**, 1485 (1983).

[51] Y. Tominaga, M. L. Tedjamulia, R. N. Castle and M. L. Lee, *J. Heterocyclic Chem.*, **20**, 487 (1983).

[52] R. Pratap, Y. Tominaga, R. N. Castle and M. L. Lee, *J. Heterocyclic Chem.*, **19**, 865 (1982).

[53] M. Sugiura, M. L. Tedjamulia, Y. Tominaga, R. N. Castle and M. L. Lee, *J. Heterocyclic Chem.*, **20**, 1453 (1983).

[54] H. Kudo, M. L. Tedjamulia, R. N. Castle and M. L. Lee, *J. Heterocyclic Chem.*, **21**, 185 (1984).

[55] M. L. Tedjamulia, H. Kudo, R. N. Castle and M. L. Lee, *J. Heterocyclic Chem.*, **21**, 321 (1984).

[56] F. Bloch, *Phys. Rev.*, **70**, 460 (1946); F. Bloch, W. W. Hansen and M. Packard, *Phys. Rev.*, **69**, 127 (1946).

[57] E. M. Purcell, H. C. Torrey and R. V. Pound, *Phys. Rev.*, **69**, 37 (1946).

[58] R. R. Ernst, *Adv. Magn. Reson.*, **2**, 1 (1966).

[59] R. R. Ernst, and W. A. Anderson, *Rev. Sci. Instr.*, **37**, 93 (1966).
[60] J. Jeener, Ampere International Summer School, Basko Polje, Yugoslavia, 1971.
[61] W. P. Aue, E. Bartholdi and R. R. Ernst, *J. Chem. Phys.*, **64**, 2229 (1976).
[62] F. W. Wehrli, "Organic Structure Assignments Using ^{13}C Spin-Relaxation Data", in "Topics in Carbon-13 NMR Spectroscopy", Vol 2, G. C. Levy, ed, Wiley-Interscience, NY, 1976, pp 343-391; F. W. Wehrli and T. Wirthlin, "Nuclear Spin-Relaxation", "Interpretation of Carbon-13 NMR Spectra", Heyden, NY, 1976.
[63] G. Bodenhausen, R. Freeman, R. Niedermeyer and D. L. Turner, *J. Magn. Reson.*, **26**, 133 (1977).
[64] G. Bodenhausen, R. Freeman and G. A. Morris, *J. Magn. Reson.*, **23**, 171 (1976).
[65] G. A. Morris and R. Freeman, *J. Magn. Reson.*, **29**, 433 (1978).
[66] G. E. Martin, *J. Heterocyclic Chem.*, **15**, 1539 (1978).
[67] J. C. Turley and G. E. Martin, *Spectros. Letters*, **11**, 681 (1978).
[68] O. M. Sejiny and G. E. Martin, *J. Heterocyclic Chem.*, **17**, 1741 (1980).
[69] S. R. Caldwell, G. E. Martin, S. H. Simonsen, R. R. Inners and M. R. Willcott, III, *J. Heterocyclic Chem.*, **18**, 479 (1981).
[70] A. Kumar, D. Welti and R. R. Ernst, *Naturwissenschaften*, **62**, 34 (1975).
[71] S. Brownstein, *J. Magn. Reson.*, **42**, 150 (1981).
[72] W. P. Aue, J. Karhan and R. R. Ernst, *J. Chem. Phys.*, **64**, 4226 (1976).
[73] A. Bax, R. Freeman and S. P. Kempsell, *J. Magn. Reson.*, **41**, 349 (1980).
[74] L. Müller, A. Kumar and R. R. Ernst, *J. Chem. Phys.*, **63**, 5490 (1976).
[75] G. Bodenhausen, R. Freeman and D. L. Turner, *J. Chem. Phys.*, **65**, 839 (1976).
[76] E. L. Hahn, *Phys. Rev.*, **80**, 580 (1950).
[77] E. L. Hahn and D. F. Maxwell, *Phys. Rev.*, **88**, 1070 (1952).
[78] G. Bodenhausen, R. Freeman, R. Niedermeyer and D. L. Turner, *J. Magn. Reson.*, **24**, 291 (1976).
[79] A. Kumar, *J. Magn. Reson.*, **30**, 227 (1978).
[80] G. Bodenhausen, R. Freeman, G. A. Morris and D. L. Turner, *J. Magn. Reson.*, **31**, 75 (1978).
[81] G. E. Martin, R. T. Gampe, Jr., J. J. Ford, M. R. Willcott, III, M. Morgan, A. L. Ternay, Jr., C. O. Okafor and K. Smith, *J. Heterocyclic Chem.*, **20**, 1063 (1983).
[82] M. J. Musmar, R. T. Gampe, Jr., G. E. Martin, W. J. Layton, S. L. Smith, R. D. Thompson, M. Iwao, M. L. Lee and R. N. Castle, *J. Heterocyclic Chem.*, **21**, 225 (1984).
[83] E. L. Ezell, R. P. Thummel and G. E. Martin, *J. Heterocyclic Chem.*, **21**, 817 (1984).
[84] L. D. Hall and S. Sukumar, *J. Magn. Reson.*, **38**, 555 (1980).
[85] B. Birdsall, N. J. M. Birdsall and J. Feeney, *J. Chem. Soc., Chem. Commun.*, 316 (1972).
[86] K. G. R. Pachler and P. L. Wessels, *J. Magn. Reson.*, **12**, 337 (1973).
[87] S. Sorenson, R. S. Hansen and H. Jakobsen, *J. Magn. Reson.*, **14**, 243 (1974).
[88] A. A. Maudsley and R. R. Ernst, *Chem. Phys. Letters*, **50**, 368 (1977).
[89] G. Bodenhausen and R. Freeman, *J. Magn. Reson.*, **28**, 471 (1977).
[90] R. Freeman and G. A. Morris, *J. Chem. Soc., Chem. Commun.*, 684 (1978).
[91] A. Bax and G. A. Morris, *J. Magn. Reson.*, **42**, 501 (1981).
[92] A. Bax, R. Freeman and G. A. Morris, *J. Magn. Reson.*, **42**, 164 (1981).
[93] A. Bax and R. Freeman, *J. Magn. Reson.*, **41**, 507 (1980).
[94] A. Bax, R. Freeman and S. P. Kempsell, *J. Am. Chem. Soc.*, **102**, 4849 (1980).
[95] A. Bax, R. Freeman and S. P. Kempsell, *J. Magn. Reson.*, **41**, 349 (1980).
[96] R. Freeman, T. Frenkiel and M. B. Rubin, *J. Am. Chem. Soc.*, **104**, 5545 (1982).
[97] A. C. Pinto, M. L. A. Gonçalves, R. B. Filho, A. Neszmelyi and G. Lukacs, *J. Chem. Soc., Chem. Commun.*, 293 (1982).
[98] J. Buddrus, H. Bauer, H. Gotthardt and R. Jung, *Angew. Chem., Int. Ed. Engl.*, **22**, 548 (1983).
[99] A. Bax, R. Freeman, T. A. Frenkiel and M. H. Levitt, *J. Magn. Reson.*, **43**, 478 (1981).
[100] A. Bax, R. Freeman and T. A. Frenkiel, *J. Am Chem. Soc.*, **103**, 2102 (1981).
[101] T. H. Mareci and R. Freeman, *J. Magn. Reson.*, **48**, 158 (1982).
[102] D. L. Turner, *Mol. Phys.*, **44**, 1051 (1981).
[103] D. L. Turner, *J. Magn. Reson.*, **49**, 175 (1982).
[104] A. Bax and T. H. Mareci, *J. Magn. Reson.*, **53**, 360 (1983).
[105] M. J. Musmar, M. R. Willcott, III, G. E. Martin, R. T. Gampe, Jr., M. Iwao, M. L. Lee, R. E. Hurd, L. F. Johnson and R. N. Castle, *J. Heterocyclic Chem.*, **20**, 1661 (1983).
[106] D. L. Turner, *J. Magn. Reson.*, **53**, 259 (1983).
[107] G. E. Maciel, "Substituent Effects on ^{13}C Chemical Shifts", "Topics in Carbon-13 NMR Spectroscopy", Vol 1, G. C. Levy, ed, Wiley-Interscience, NY, 1974, pp 53-77.
[108] A. B. Strong, D. Ikenberry and D. M. Grant, *J. Magn. Reson.*, **9**, 145 (1973).
[109] R. T. Gampe, Jr., G. E. Martin, M. L. Lee and R. N. Castle, unpublished data.
[110] G. E. Martin, S. L. Smith, W. J. Layton, M. R. Willcott, III, M. Iwao, M. L. Lee and R. N. Castle, *J. Heterocyclic Chem.*, **20**, 1367 (1983).
[111] P. Geneste, J.-L. Olive, S. N. Ung, M. El Amoudi El Faghi , J. W. Easton, H. Beierbeck and J. K. Saunders, *J. Org. Chem.*, **44**, 2887 (1979).
[112] J. D. Memory and N. K. Wilson, "NMR of Aromatic Compounds", Wiley-Interscience, NY, 9182, p 96; references contained therein.
[113] P. E. Hansen, *Org. Magn. Reson.*, **12**, 109 (1979).
[114] P. M. G. Bavin, K. D. Bartle and J. A. S. Smith, *Tetrahedron*, **21**, 1087 (1965); N. Jonathan, S. Gordon and B. P. Dailey, *J. Chem. Phys.*, **36**, 2443 (1962); R. H. Martin, N. Defay, F. Geerts-Evrard and S. Delavarenne, *Tetrahedron*, **20**, 1073 (1964).
[115] K. D. Bartle, D. W. Jones and R. S. Matthews, *Rev. Pure Appl. Chem.*, **19**, 191 (1969).
[116] F. J. Weigert and J. D. Roberts, *J. Am. Chem. Soc.*, **90**, 3543 (1968).
[117] N. Platzner, *Org. Magn. Reson.*, **11**, 350 (1978).,
[118] M. Jay and G. E. Martin, *J. Heterocyclic Chem.*, **19**, 241 (1982).
[119] R. L. Vold, J. S. Waugh, M. P. Klein and D. E. Phelps, *J. Chem. Phys.*, **48**, 3831 (1968).
[120] R. Freeman and H. D. W. Hill, *J. Chem. Phys.*, **51**, 3140 (1969).
[121] J. G. Kowalewski, G. C. Levy, L. F. Johnson and L. Palmer, *J. Magn. Reson.*, **26**, 533 (1977).
[122] I. M. Al-Najjar, H. B. Amin and S. S. Al-Showiman, *J. Chem. Soc. Pak.*, **4**, 155 (1982).
[123] K. Takahashi, T. Kanda, F. Shoji and Y. Matsuki, *Bull. Chem. Soc. Japan*, **38**, 508 (1965).
[124] F. L. Hirshfeld, S. Sandler and G. M. T. Schmidt, *J. Chem. Soc.*, 2108 (1963).
[125] M. Konno, Y. Saito, K. Yamada and H. Kawazura, *Acta Cryst.*, **B36**, 1680 (1980).
[126] W. Karcher, R. J. Fordham, A. Nelen, R. Depaus, J. Dubois and P. Glaüde, "Molecular Spectra of Polycyclic Aromatic Hydrocarbons", Mobile Source Emissions Including Polynuclear Aromatic Hydrocarbons, D. Roüdia, ed, Reidel Publ., Dordrecht, The Netherlands, in press.